2016

Enhanced Oil Recovery from a Low Pressure Tight Oil Reservoir in Ordos Basin

Han, Jiabei

UNIVERSITY OF CALGARY

Enhanced Oil Recovery from a Low Pressure Tight Oil Reservoir in Ordos Basin

by

Jiabei Han

A THESIS

SUBMITTED TO THE FACULTY OF GRADUATE STUDIES

IN PARTIAL FULFILMENT OF THE REQUIREMENTS FOR THE

DEGREE OF MASTER OF SCIENCE

GRADUATE PROGRAM IN CHEMICAL AND PETROLEUM ENGINEERING

CALGARY, ALBERTA

JUNE, 2016

Abstract

As one of the biggest sedimentary basins in China, abundant oil reserves exist in the Ordos Basin. Compared with Bakken formation, the pressure of the study area is quite low, which may results in inefficient primary recovery.

The primary recovery in the study area has been studied through simulation. The results indicate that primary recovery is not efficient in such a low pressure reservoir. Water or gas should be injected to enhance the oil recovery. Compared with water, gas is more suitable for improving the oil recovery from the study area. Among all gases investigated, CH_4 and separator gas are a better choice. The effects of heterogeneity have also been studied by reservoir simulation. As reservoir heterogeneity increases, oil recovery will decrease. However, gas injection can still highly improve the oil recovery. A geological model has been built to predict the gas injection performance in case studies.

Acknowledgements

I would like to express my utmost gratitude and thankfulness to my supervisor, Dr. Zhangxing (John) Chen, for his helpful guidance and immense support during my studies at the University of Calgary.

My gratitude also goes to the examination members, Dr. Ayodeji Aderopo Jeje and Dr. Christopher Clarkson. Thanks for their valuable suggestions.

I would also like to thank the members in the Reservoir Simulation Group and the sponsors of the Group.

Table of Contents

List of Tables

List of Figures and Illustrations

Nomenclature

CCE	constant composition expansion
EOS	equation of state
FCM	first contact miscible
GOR	gas oil ratio, m^3/m^3
h	reservoir thickness, md
IFT	interfacial tension, mN/m
k	rock permeability, md
LGR	local grid refinement
MCM	multiple contact miscible
MMP	minimum miscible pressure
OOIP	original oil in place
PV	pore volume
RF	recovery factor, %
SRV	stimulated reservoir volume
SIS	sequential indicator simulation
SGS	sequential Gaussian simulation
u_c	critical flow rate, ml/min
μ_0	oil viscosity, mPa·s
μ_g	gas viscosity, mPa·s
ρ_0	oil density, lb/ft^3
ρ_g	gas density, lb/ft^3
φ	rock porosity, %

Chapter One: INTRODUCTION

1.1 Literature Review

Tight oil recovery, which profits from the development of horizontal drilling and multi-stage fracturing technologies, has drawn attention and has gradually become a crucial fuel source in the last decades. After considerable improvements in the exploration of the Bakken formation in 2000 and the Eagle Ford formation in 2008 (EIA, 2013), the tight oil project in Monterey also gained enormous increase. Production grew rapidly and reached approximately $9{,}690\times10^4$t by the end of 2012 (EIA, 2013)

Tight oil resources in China are abundant and are distributed externally in sedimentary basins including the Ordos basin, Junggar basin, Sichuan basin and Songliao basin (Du, et al., 2014).

1.1.1 Concept of Tight Oil

With the continuous development of oil and gas, conventional oil resources, which can be easily produced with ordinary drilling and completion technologies like vertical drilling technologies, gradually decrease. To satisfy the increasing demand for energy, the development of tight oil resources has an enormous potential (Pang, et al., 2012).

Currently, there is no consolidated definition for tight oil. The Canadian Society for Unconventional Resources (CSUR) has defined tight oil as an unconventional oil resource that is found in low permeability and low porosity reservoirs (CSUR, 2014). It cannot be economically developed without horizontal drilling and hydraulic fracturing. Figure 1.1 shows the reservoir classification criteria from CSUR (CSUR, 2014).

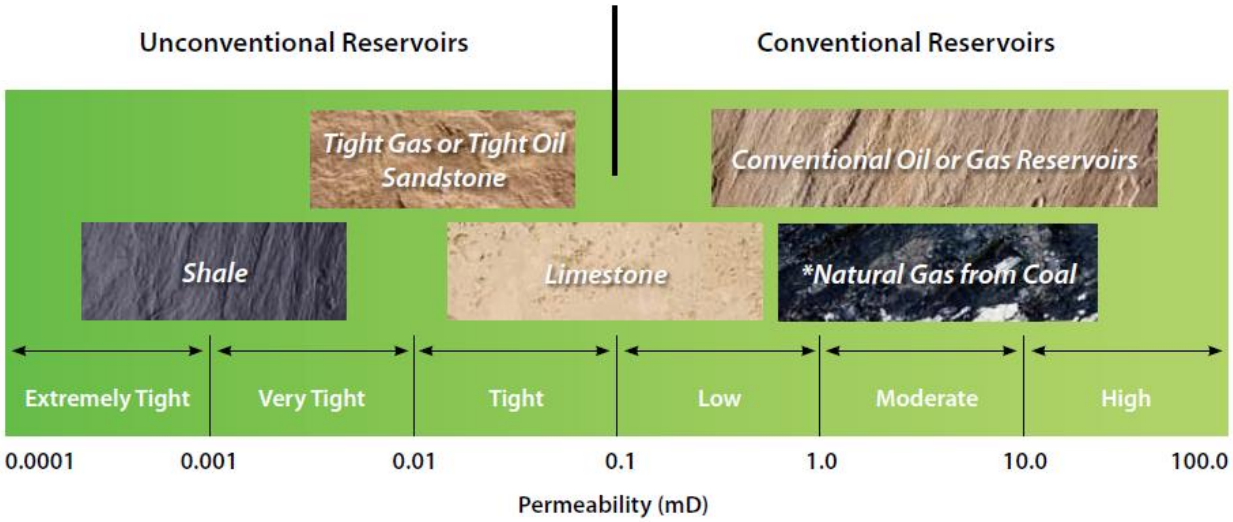

Figure 1.1 Reservoir Classification (CSUR, 2014)

Clarkson and Pedersen has divided unconventional (tight) light oil (ULO) into three categories, including halo oil, tight oil and shale oil (Clarkson and Pedersen, 2011). For halo oil, the reservoir permeability is relatively high compared with other two categories, and is greater than 0.1md; the oil has migrated from the source to the reservoir; and the reservoirs are comprised of clastics or carbonates. For tight oil, the reservoir permeability is lower than 0.1md; the source is different from the reservoir; and the reservoirs are comprised of clastics or carbonate. For shale oil, the reservoir permeability is very low (<0.1md); the source and the reservoir are the same or finely interbeded; and organic matter content is high (Clarkson and Pedersen, 2011).

Jia defined tight oil as petroleum accumulations that are buried in tight sandstone and carbonate rock, interbedded with or adjacent to source rocks. These oil accumulations are usually absorbed by formation rocks or present at the dissociative state and have not migrated through long distances (Jia et al., 2012).

Using reconstruction nanometer-CT and field-emission scanning electron microscope technologies, Zou et al. observed nanoscale pore throats, which are less than 1μm, in tight oil reservoirs (Zou, et al., 2012). Zou et al. considered that a critical pore throat size for tight oil reservoirs should be 45nm, and the critical permeability should be equal to or less than 0.1md. He also stated that in such a nano scale pore throat, the immense attraction between fluid molecules and solid surfaces drastically increases the fluid percolation resistance (Zou, et al., 2012)

Based on the tight oil development in the Ordos basin, Yang et al. defined tight oil as unconventional oil sources which are reserved in formations with permeability equal to or lower than 0.1md (Yang, et al., 2013). In the Ordos basin, economic development for tight oil formations with permeability greater than 0.03md has already been achieved (Yang et al., 2013)

1.1.2 Development of Tight Oil

1.1.2.1 Well Types

The reservoir properties of tight oil are very poor, and its permeability is less than 0.1md (Jia et al., 2012). When developed with vertical wells (without hydraulic fracture), the fluid flow near a wellbore is a radial flow and the percolation resistance is relatively high. For the development of thin reservoir formations, their production is quite small. As horizontal wells can effectively increase a contact area of a wellbore and a reservoir, change a flow form and decrease the percolation resistance, such wells are used for tight oil recovery. To increase individual well production, the corresponding reservoir stimulation should be applied (Pang, et al., 2012).

The net pay thickness of the Bakken formation is about 23m (Meissner et al., 1991); to maximize the primary recovery, horizontal wells and multi-stage hydraulic fractures have been implemented. The initial oil production is high, thus enabling a rapid return on investment.

The facies of the Ordos Basin are composed primarily of turbidite sandstone, resulting in a thick formation and well sand body connectivity (Chen, et al., 2013). Horizontal wells and hydraulic fractures are usually used to ensure well production. At the same time, water is injected to maintain production energy.

1.1.2.2 Development Technologies

In the Bakken formation, horizontal well drilling and hydraulic fracturing technologies have been applied since 2000. At the end of 2011, the number of production wells was 3,273 (the horizontal wells stood at 3,098) and the oil production was $1{,}838\times10^4$t per year. The production rate of horizontal wells with hydraulic fractures was 17t/day. This is 1.4 times greater than the production rate of horizontal wells without hydraulic fractures, and 2.8 times that of vertical wells (Dou et al., 2012). The length of horizontal wells in the Bakken formation is relatively long, mainly from 1,600m and 3,200m, and the maximum length is 6,090m. The initial distance between two wells is 1,100m, and the distance between two wells after infill drilling is about 500m. A 1,600m horizontal well has seen the stage number of hydraulic fractures increased from 10 in 2008 to between 15 to 20 in 2011. A 3220m horizontal well has seen the stage number of hydraulic fractures increased from 10 in 2008 to between 20 to 40 in 2011. The maximum number of stages of hydraulic fractures was up to 47. The distance between hydraulic fractures has been decreased from 120-170m to 75-100m. The initial production rate was 50-160t/day (Wu et al., 2011). After

a span of four month, the production rate dropped to 30%-60% of the initial production rate. The production was 1×10^4t-1.5×10^4t in the first year and 0.5×10^4t-1×10^4t in the second year. The initial production rate in the Bakken formation was quite high but is declining rapidly (Lin et al., 2011).

1.1.3 Water Injection

For the development of a conventional reservoir, water injection is the simplest and the most economical way to improve oil recovery. Even in a low permeability reservoir found in the Ordos basin, water injection can be used to establish an effective displacement system and crucial for economic development.

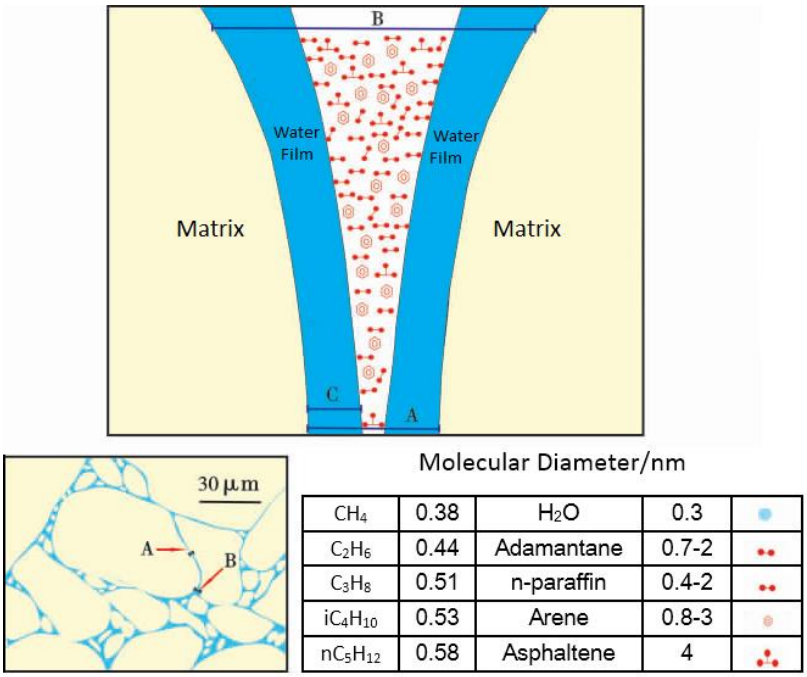

Figure 1.2 Critical pore and throat diameters of tight sandstone of Yanchang Formation in Ordos Basin (Yang, et al., 2013)

When reservoir permeability is equal to or less than 0.3md, the pore size is minuscule and mainly in nano scale (Figure 1.2). The diameter of the hydrocarbon molecules in oil is 0.3-4nm. Thus, the

hydrocarbon molecules can move in a nano scale pore throat. The average thickness of a water film attached on the surface of the matrix is 43nm. Consequently, water has a difficulty flowing in such a minuscule pore throat. The critical pore throat diameter should be greater than 90nm to remedy this situation.

1.1.4 Gas Injection

The gas injection process includes miscible, immiscible and near-miscible gas injections. When two or more different fluids are mixed in any proportion and there is no phase interface between these fluids, the phenomenon is called miscible (Green and Willhite, 1998). Theoretically, with a miscible gas injection, the residual oil of a swept area decreases to zero. The miscible gas injection can be divided into first contact miscible (FCM) and multiple contact miscible (MCM). The FCM gas injection means that the phase interface will immediately disappear, and the miscibility will be formed when the injected gas comes into contact with the reservoir oil. The MCM gas injection process is not as easy as the FCM, as the miscible between the injected gas and reservoir oil is formed after repeated contacts between the gas and oil. As gas continuously moves into the reservoir, under the effect of the interphase mass transfer between the injected gas and reservoir oil, a transition zone will be formed. The composition of the transition zone will gradually change so that the interface between the gas and transition zone and the interface between the oil and transition zone will disappear and the miscibility will be established (Green and Willhite, 1998). The MCM can also be divided into vaporizing and condensing (Figures 1.3 and 1.4). Vaporizing is also known as the forward contact miscibility because during the multiple times of contact between gas and oil, except for gas solutions in oil, the light components in the oil will also spread into gas. The gas will gradually be enriched, and miscibility will be formed at the gas front

(Hutchinson et al., 1961). Condensing is also known as the backward contact miscibility. During the condensing drive, a rich gas, which contains intermediate components like C_2-C_6, will be injected into a reservoir. With repeated contact between the gas and oil, the intermediate components in the rich gas will condensate into the oil. The oil will be enriched until miscibility is formed (Hutchinson et al., 1961).

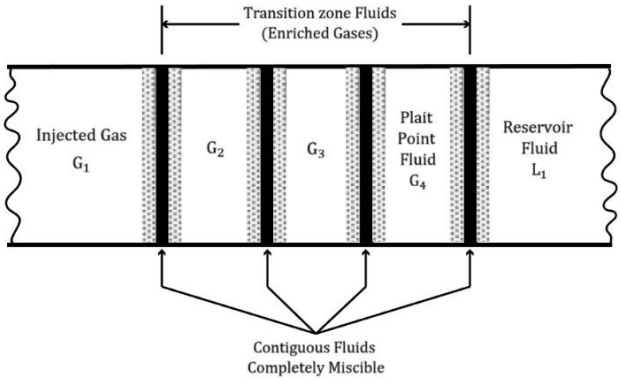

Figure 1.3 Relative positions of the fluids of the vaporizing drive process in a porous medium (C.A. Hutchinson et al., 1961)

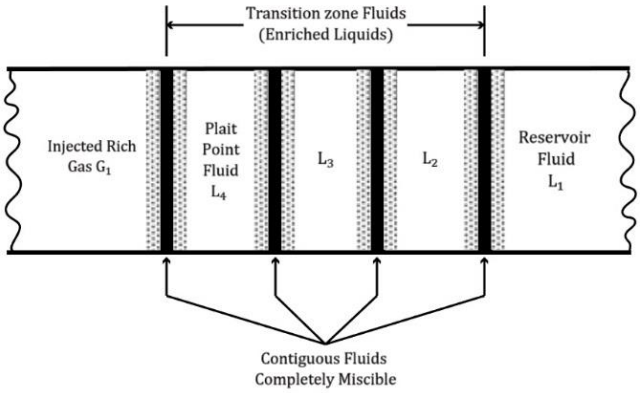

Figure 1.4 Relative positions of the fluids of the condensing drive process in a porous medium (C.A. Hutchinson et al., 1961)

In 1986, Zick observed that under the effect of both vaporizing and condensing, the interfacial tension (IFT) between gas and oil can decrease to a very low value. After injecting a 1.2

hydrocarbon pore volume of gas, the oil recovery can achieve 95% or even higher (Zick, 1986). The strict miscibility, however, has not been formed, and this phenomenon is considered to be near miscibility. In practice, most of the miscible projects in oil fields are under near-miscible conditions (Thomas, et al., 1994). The strict miscibility and zero IFT is not necessary for oilfield development. Near-miscibility with low IFT can achieve competitive oil recovery (Thomas et al., 1994). Thus, near-miscibility may be a better choice for oilfield development.

Gas injection has three benefits (Li and Zhou, 2002). First, when miscibility or near-miscibility is formed, the IFT between the injected gas and reservoir oil will decrease to zero or a small value, as will the residual oil of the gas swept area. Second, since the gas viscosity and molecular diameter is minuscule, gas can easily spread into a nano scale pore throat in tight oil reservoirs and achieve well displacement. Third, gas can be dissolved in oil to reduce oil viscosity and swell oil. Overall, gas injection can improve production energy.

Theoretically, gas injection is more beneficial for light oil reservoirs (Taber et al., 1997) and a nano scale pore throat size can help to reduce the minimum miscible pressure of CO_2 and CH_4 (Teklu et al., 2014). Consequently, gas can be an effective substitution of water for enhancing oil recovery in tight oil reservoirs.

1.2 Reservoir Characteristics of Study Area

1.2.1 Geologic Background

The Ordos basin, a cratonic basin with a complex basement, is located at the junction of the stable region of eastern China and the mobile zone of western China (Figure 1.5).

The Ordos basin features a monoclinal structure, being higher in the north and lower in the south and being higher in the east and lower in the west (Chen, et al., 2006). Its slope gradient is gentle, with a dip angle of about 0.5 degree. The Ordos basin can be divided into six tectonic units which include the northern Yimeng uplift, the western margin thrust belts, the western Tianhuan depressions, the North Shaanxi slope in the middle, the southern Weibei uplift and the eastern Jin West Flexure belt (Chen, et al., 2006). The study area is located in the North Shaanxi slope and next to the Tianhuan depressions.

In the Ordos basin, the Upper Triassic Yanchang formation is the primary source rock and oil reservoir. Based on the study of the sedimentary cycle, paleontology and lithology etc., the Yanchang formation is divided into five members and ten formations (Figure 1.6). Chang 7 is the interval of interest in this study.

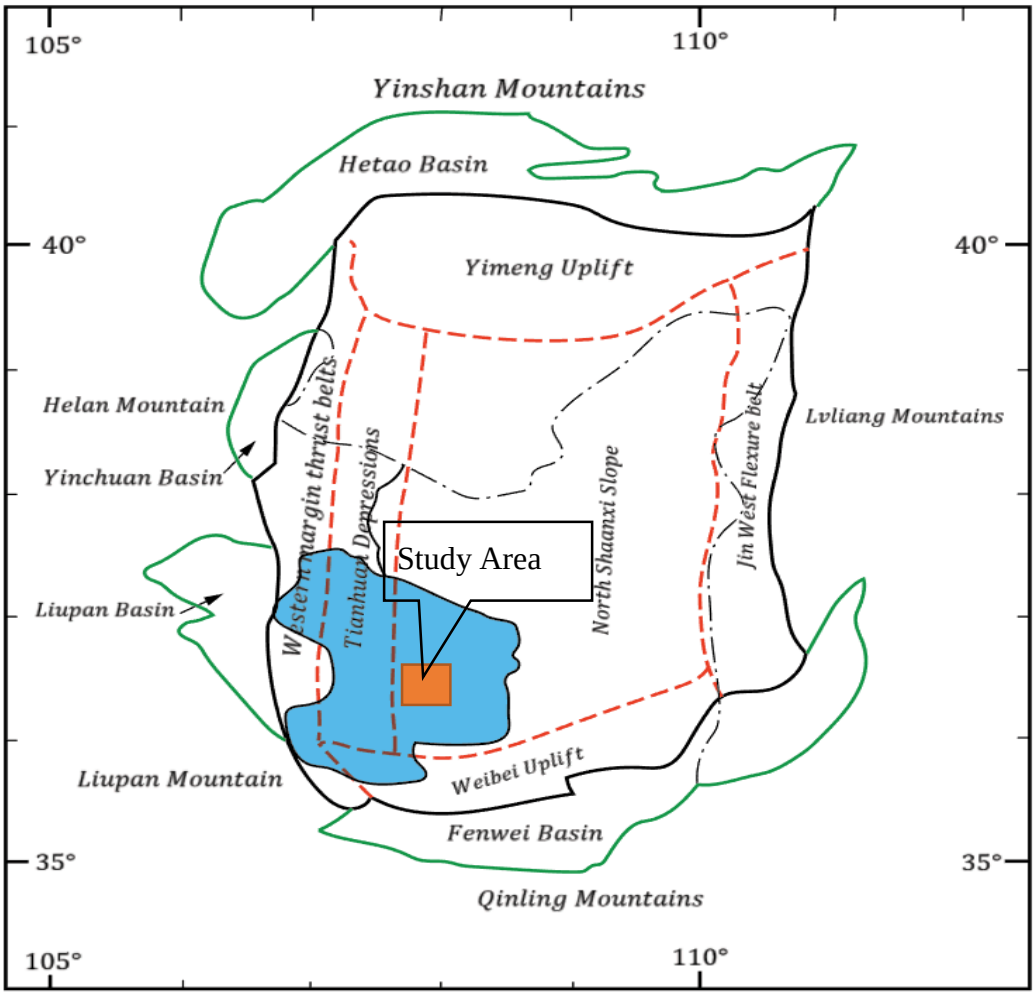

Figure 1.5 Location of study area (Gao et al., 2013)

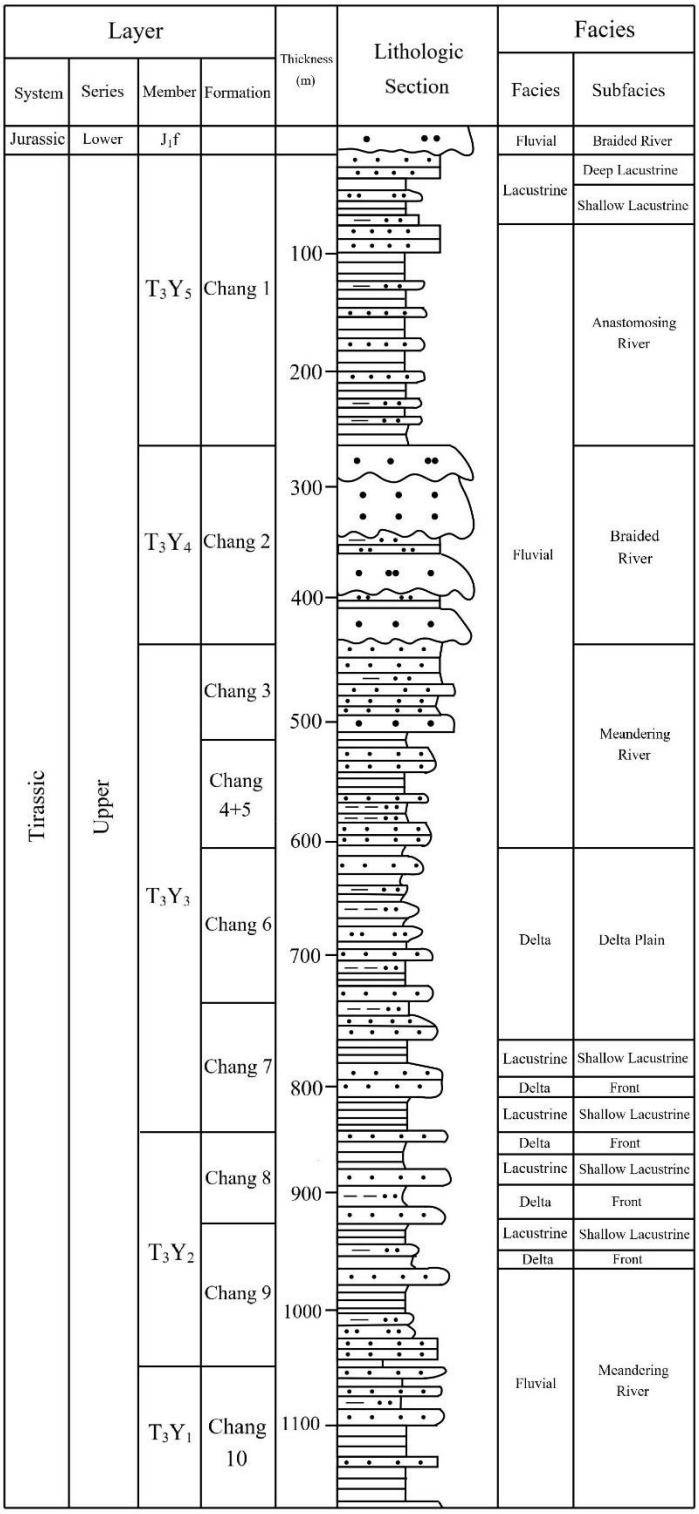

Figure 1.6 Stratigraphic section of Yanchang Formation (Chen et al., 2006)

The thickness of T_3Y_3 of the Yanchang formation is 300-350m, and comprises Chang 7, Chang 6 and Chang 4+5 intervals. The sand thickness of T_3Y_3 gradually thins out from north to south. The content of fine-grained silt is less from south to north. T_3Y_3 shows an interbed of sand and shale. At the south of the Ordos basin, the top and the bottom of T_3Y_3 are comprised of a thick layer of dark mudstone (Zhao, et al., 2014).

The oil shale and carbonaceous shale at the bottom of the Chang 7 interval in T_3Y_3 are thick and show high resistance. At the middle and the top of the Chang 7 interval are thick sandstones, which belong to the deep lacustrine of turbidity sediment. The oil reservoir, with a lithologic deposit formation, is directly connected with source rocks. Tectonics have a lesser effect on oil trap than do lithofacies variations and reservoir properties (Zhao, et al., 2014).

The Chang 7 interval is tight, and its reservoir properties are very poor. Its porosity is between 7.6%-12.4%, and the average porosity is 11.1%. Its permeability is between 0.01-0.03md, and the average is 0.22md. In some areas of the Chang 7 interval, the porosity and permeability are relatively high. The reservoir grain size is mainly fine-grained, with an average content of fine sandstone being 78%. The content of interstitial materials is relatively high, with an average of 15%, and the main content of interstitial materials is illite, at about 90%.

1.2.2 Rock-fluid Properties

1.2.2.1 Crude Oil Properties

According to the PVT data of oil in the Chang 7 interval, viscosity is 0.578mPa·s; the density is 0.717g/cm^3; the gas oil ratio (GOR) is 101.4m^3/m^3; the saturation pressure is 9.563 MPa (Table 1.1).

Table 1.1 PVT data of oil of Chang 7 interval in study area

Formation	Chang 7
Reservoir Temperature/℃	64.75
Saturation Pressure/Mpa	9.563
Oil Density/g/cm3	0.717
Oil Viscosity/mPa·s	0.578
Gas Oil Ratio/m3/m3	101.4
Formation Volume Factor	1.3357

1.2.2.2 Solution Gas Properties

The critical pressure of the solution gas in the Chang 7 interval is 4.282 MPa; the critical temperature is 6.8℃; the relative density 1.07. The content of C_1 in the solution gas is 39%; C_2 is 2.2%; C_3 is 14.2%. The overall hydrocarbon content is 73.7%. There is no hazardous gas such as H_2S and CO, in the solution gas (Table 1.2).

Table 1.2 Composition of the solution gas of Chang 7 in study area

Formation	Composition of the solution gas/%										
	C_1	C_2	C_3	iC_4	nC_4	C_{5+}	H_z	CO_2	N_2	Air	Total Hydrocarbon
Chang 7	39.0	12.2	14.2	1.2	3.4	3.7	23.2	3.1	0	0	73.7

1.2.3 Reservoir Sensitivity

1.2.3.1 Clay Mineral Composition

In the study area, clay mineral occupies 13% to 14% of the total rock grains. The main composition of clay in the Chang 7 interval is illite and chlorite, and the content is 58.6% and 23.7%, respectively. The secondary composition is kaolinite, at about 15% (Table 1.3). The content of illite/semectite is quite low, standing at only 2.7%.

Table 1.3 X-ray diffraction analysis of clay mineral composition in the study area

Formation	Content of clay mineral/%			
	Illite	Illite/semectite	Kaolinite	Chlorite
Chang 7	58.6	2.7	15.0	23.8

1.2.3.2 Sensitivity Experiment

A sensitivity experiment reveals that the formation exhibits weak water sensitivity, weak-no velocity sensitivity, weak acid sensitivity, and medium salinity sensitivity. Water injection is favorable (Table 1.4).

Table 1.4 Sensitivity Experiment in the study area

Formation	Sensitivity				
	Water-sensitivity	Velocity sensitivity	Acid-sensitivity	Salinity-sensitivity	Alkali sensitivity
Chang 7	Weak	Weak-no	Weak	Medium	/

1.2.4 Water Seepage Characteristics

Based on an analysis of experiment data of water flooding in the study area, the oil recovery factor (RF) before water breakthrough was 25%. The RF at 95% of water cut is 42.9%, and the injected water at this time is 1.15 pore volume (PV). The RF at 98% of water cut is 45.1% and the injected water at this stage is 1.8PV. After injected 8.4PV of water, the cumulative RF is 48.7%. The experiment indicated that after injecting 2PV of water, subsequent water injection has no significant effect on enhanced oil recovery.

Table 1.5 Experiment data of water flooding in the study area

Formation	Chang 7	RF at 95% water cut/%	42.9
Sample number	2	Injected water at 95% water cut/PV	1.15
Permeability/md	0.23	Oil recovery at 98% water cut/%	45.1
Porosity/%	13.4	Injected water at 98 water cut/ PV	1.79
Pressure difference/Mpa	20.0	Cumulative RF/%	48.7
RF before water breakthrough/%	25.0	Cumulative injected water/PV	8.4

1.2.5 Reservoir Heterogeneity

Reservoir heterogeneity describes the variation of lithology, reservoir properties, oil saturation and connectivity of sand bodies in both the horizontal and vertical directions. Reservoir heterogeneity includes inter-layer heterogeneity, inner-layer heterogeneity, and horizons heterogeneity.

1.2.5.1 Inter-Layer Heterogeneity

Inter-layer heterogeneity is caused by interbedding formations and differences of permeability and porosity between sand bodies. In the study area, the inter-layer heterogeneity is relatively high.

1.2.5.2 Inner-Layer Heterogeneity

Inner-layer heterogeneity in a single sand body refers to the factors that can affect and control the flow and distribution of reservoir fluids. These factors include grain-size variation, bedding structure, permeability variation, permeability anisotropy, and in-layer interbeds. In the study area, the inner-layer heterogeneity is relatively high. The variation coefficient of permeability is greater than 0.5.

1.2.5.3 Horizon Heterogeneity

Horizon heterogeneity is highly correlated with the distribution of sedimentary microfacies and sand bodies. For a higher content of shale, the reservoir properties are relatively poor, and the permeability and porosity are relatively low.

1.2.6 Reservoir type

1.2.6.1 Formation Depth, Pressure, and Temperature

Based on the data from the exploratory and development wells, the average depth of the Chang 7 interval in the study area is 1960-1991m.

As the formation depth increases, the pressure and temperature will increase as well. According to the pressure measurement data, the initial pressure of the Chang 7 interval is 16.4-16.8MPa, the pressure gradient is 0.84 and the formation temperature is 64.73-64.76℃ (Table 1.6).

Table 1.6 Data of pressure measurement in the study area

Formation	Depth/m	Initial Pressure/Mpa	Pressure Gradient/Mpa/10^2m	Temperature/℃
Chang 7	1970	16.5	0.84	64.75

1.2.6.2 Oil Trap and Reservoir type

The Chang 7 interval sedimentary is controlled by gravity flow and the reservoir sand bodies are extensively distributed. Lithology mainly controls the distribution of a reservoir. Sandstone reservoirs with high permeability are usually sealed and covered by mudstones at the side direction or overlapped. According to well logging, no edge and bottom water appear in the Chang 7 interval. The saturation pressure and GOR are relatively high. The main driving energy is solution gas driving.

1.3 Development Prospect of Tight Oil in Ordos Basin

As an unconventional oil resource, tight oil has become an important part of world energy development. America, Canada, and Australia have already achieved viable commercial development. The tight oil resource in the Ordos basin is abundant. At the end of 2012, the explored tight oil reserve is 1.643 billion tons, which is 53.43% of the total explored reserve in this basin (Jingli Yao et al., 2013).

Horizontal drilling and hydraulic fracturing can significantly increase a contact area between a well and a reservoir and are indispensable technologies for the successful development of tight oil reservoirs. The Ordos basin has characteristics similar to those found in other typical tight oil

reservoirs (Table 1.7). Horizontal drilling and hydraulic fracturing should be suitable to the Ordos Basin.

Table 1.7 shows that the formation depth of the Ordos basin is shallow and the maturity of organic matter is high. The shallowness indicates that the initial reservoir pressure is low, which is a disadvantage to the development of tight oil in the region. The initial pressure of the Bakken formation is 36.5MPa (Pramudito, 2008), whereas the initial pressure of the Ordos basin is 16.5Mpa, only half that of the Bakken formation. Even with horizontal drilling and hydraulic fracturing technologies, primary recovery will be still uneconomical.

The high maturity of organic matter indicates the high GOR and light oil under the reservoir condition. The lighter the oil, the more appropriate for using gas injection for reservoir development (Taber, 1997).

The tight oil reservoir properties in the Ordos Basin are poor; the permeability is equal to, or less than 0.03md and the initial reservoir pressure is quite low. For such tight oil reservoirs, there are no precedents of effective development. Thus, in this study, based on reservoir simulation and a slim tube experiment, enhanced oil recovery through water injection and gas injection (including CO_2, CH_4 and separator gas) have been analyzed and compared.

Table 1.7 Comparison of Characteristics between Various Tight Oil Reservoirs (Zou, et al., 2012; Yang, et al., 2013)

Formation	Reservoir				API	Depth/m	Pressure Gradient/Mpa/10^2m
	Lithology	h/m	φ/%	k/md			
Yanchang, Ordos Basin	Siltstone	20-80	2-12	0.001-0.1	33-45	1000-2600	0.75-0.85
Jurassic, Sichuan Basin	Siltstone, shell limestone	10-60	0.2-7.0	0.0001-0.21	31-55	2000-5200	1.23-1.72
Bakken, Williston Basin	Dolomitic-argilaceous siltstone	5-55	5-13	0.01-0.1	39-43	2593-3203	1.35-1.58
Eagle Ford, Western Gulf Basin	marlstone	30-90	2-12	＜0.01	31-41	2500-4267	1.35-1.8

*h stands for thickness, φ stands for porosity and k stands for permeability

1.4 Study Objectives

The primary aim of this study is to find an effective way to enhance the oil recovery from the low-pressure reservoir in the Ordos basin. The specific objectives are proposed as follows:

1. Based on the analysis of the geologic characteristics and simulation study, the reservoir characteristics and the results of primary recovery in the study area have been investigated.
2. Based on a slim tube experiment, the MMP of CH_4 and CO_2 for the reservoir oil in the study area has been determined.
3. A reservoir simulation study has been conducted to investigate and compare the performance of water and gas (including CO_2, CH_4, and separator gas) injection.
4. Based on the simulation study, the effect of heterogeneity has been studied.
5. A simulation study has been conducted to predict the oil production in 20 years.

1.5 Organization of Thesis

This thesis consists of seven chapters, described as follows:

Chapter Two includes the comparison of geological characteristics and PVT data between the study area and the Bakken formation. The properties of a basic simulation model, such as permeability, porosity, and rock-fluid properties, are described and the performance of the primary recovery is investigated. The necessity for the second and third recovery is stated.

Chapter Three summarizes the procedure and the results of a slim tube experiment. Through the slim tube experiment, the minimum miscible pressure (MMP) of CH_4 and CO_2 is determined. The MMP of the separator gas is determined through CMG WINPROP calculations.

Chapter Four presents the simulation results of the water and gas (includes CH_4, CO_2 and separator gas) injection. The performance is compared through the analysis of the swept area, pressure distribution, and viscosity variation.

Chapter Five investigates the effect of reservoir heterogeneity through the use of the geostatistical method and simulation.

Chapter Six describes the geological model of the study area. Based on the geological model, the production of the study area in 20 years is predicted.

Chapter Two: EVALUATION OF PRIMARY RECOVERY

2.1 Comparison of the Study Area with Bakken Formation

As the Bakken formation has been economically developed, the area in this study is compared with the Bakken formation to investigate whether its development method can be adopted.

2.1.1 Geological Characteristics

According to Table 2.1, the Bakken formation is comprised of marine facies and limestone lithology; the study area is composed of lacustrine facies and silt-sandstone. Thus, the reservoir heterogeneity of the study area is higher than that of the Bakken formation.

The reservoir depth of the Bakken formation is greater than 2,500m, and the pressure gradient is higher than 1.35MPa/10^2m. The reservoir depth of the study area is about 2,100m and the pressure gradient is as low as 0.75MPa/10^2m. The initial reservoir pressure of the study area is much lower than that of the Bakken Formation. Other properties, such as permeability and porosity, are similar.

Table 2.1 Comparison of Reservoir Properties between Bakken and Yanchang Formation (Zou, et al., 2012; Yang, et al., 2013)

Formation		Bakken, Williston Basin	Yanchang, Ordos Basin
Area/10^4km^2		7	8-10
Source Rock	Lithology	Marin shale	Lacustrine shale
	Thickness/m	5-12	20-110
	TOC/%	10-14	2-20
	R_o/%	0.6-0.9	0.7-1.1
Reservoir	Lithology	Dolomitic-argilaceous siltstone	Silt-sandstone
	Thickness/m	5-55	20-80
	Porosity/%	5-13	2-12
	Permeability/md	0.01-0.1	0.001-0.1
Oil Density/g/cm^3		0.81-0.83	0.8-0.86
Formation Depth/m		2500-3500	2100
Pressure Gradient/Mpa/10^2m		1.35-1.58	0.75-0.85
OOIP/10^8t		566	35.5-40.6

2.1.2 PVT Data

According to Table 2.2, the gas-oil ratio (GOR) in the study area is around 100m^3/m^3, and the difference between the reservoir pressure and the saturation pressure is 7MPa. The GOR in the Bakken formation, however, is 145m^3/m^3, and the difference between the reservoir pressure and

saturation pressure is 25MPa. Thus, the GOR of the study area is lower than that of the Bakken formation, which means lower elastic energy.

The results show that for formations like the Bakken formation, the driving energy is sufficient, and the primary recovery is relatively high; for formations like the Yanchang, the primary recovery may be undesirable.

Table 2.2 Comparison of PVT Data between Bakken and Yanchang Formation (Zou, et al., 2012; Yang, et al., 2013)

Formation	Initial Pressure/Mpa	Saturation Pressure/Mpa	GOR/m^3/m^3	Oil Viscosity/mPa·s
Yanchang, Ordos, Basin	16.5	9.56	101.4	0.58
Bakken, Williston Basin	36.5	11.56	145	0.46

2.2 Evaluation of Primary Recovery through Reservoir Simulation

Based on a former analysis, the primary recovery of the Yanchang formation may be undesirable. Consequently, reservoir simulation is used to investigate the performance of the primary recovery in the study area.

2.2.1 Simulation Model

2.2.1.1 Equation of State (EOS) Model

The reservoir fluid composition and PVT properties vary for different reservoirs. Capturing the fluid properties accurately is significant for reservoir simulation. In this study, the reservoir fluid

was collected from a well, with the fluid's molar fraction composition shown in Figure 2.1. PVT tests, such as a separator test and a constant composition expansion experiment (CCE), were performed; the results are listed in Tables 2.3 and 2.4. Table 2.5 presents the data of oil viscosity.

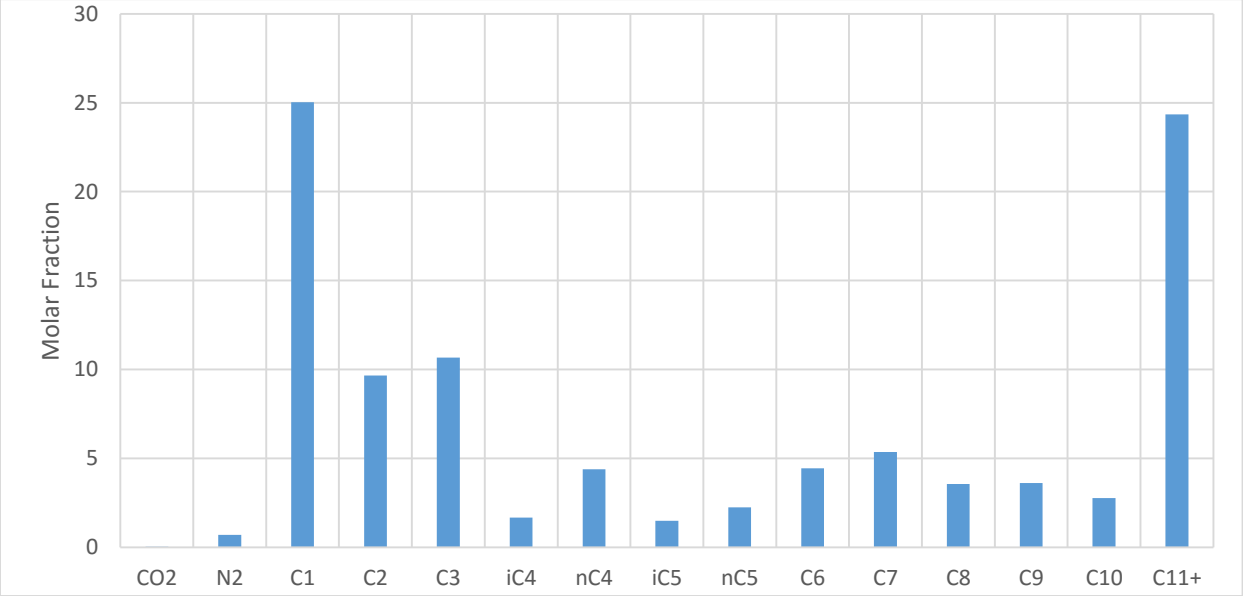

Figure 2.1 Reservoir fluid composition of the study area.

Table 2.3 Separator Test

Saturation Pressure/Kpa	Ratio/m^3/m^3	Formation Volume Factor	API
9563	101.4	1.3503	39.64

Table 2.4 Constant Composition Expansion @ 64.75℃

Pressure/MPa	Relative Volume	Y-Function	Oil Density/g/cm^3
16.500	0.9891		0.7170
14.532	0.9920		0.7149
12.550	0.9950		0.7128
11.487	0.9967		0.7116
10.505	0.9983		0.7104
9.563	1.0000		0.7092
9.482	1.0025	3.362	
9.335	1.0085	2.854	
9.197	1.0144	2.729	
8.938	1.0263	2.622	
8.482	0.0502	2.510	
7.865	1.0889	2.396	
7.319	1.1307	2.314	
6.685	1.1904	2.228	
5.935	1.2799	2.147	
5.201	1.3993	2.060	
4.650	1.5188	1.993	
4.218	1.6382	1.939	

Table 2.5 Oil Viscosity @64.75 ℃

Pressure/MPa	Oil Viscosity/mPa·s
16.500	0.578
15.510	0.567
14.521	0.557
13.530	0.547
12.541	0.538
11.550	0.528
10.562	0.519
9.563	0.510

Because too many components significantly increase the simulation time, in this study, 15 components were lumped into 7 components. CO_2, CH_4 and a separator gas are potential injection gases, and the primary compositions of the separator gas are CH_4, C_2H_6, and C_3H_8. Thus, CO_2, CH_4, C_2H_6, and C_3H_8 are not lumped with other components, but left as a single component. The molar fraction of the lumped composition is shown in Figure 2.2.

The Peng-Robinson EOS describes the characteristics of the reservoir fluid in the study area. Experiments such as a separator test and a constant composition expansion experiment (CCE) are used for accurate EOS tuning. A satisfactory match between the EOS regression and experiment data is obtained, with the results presented in Figures 2.3-2.5 and Table 2.6.

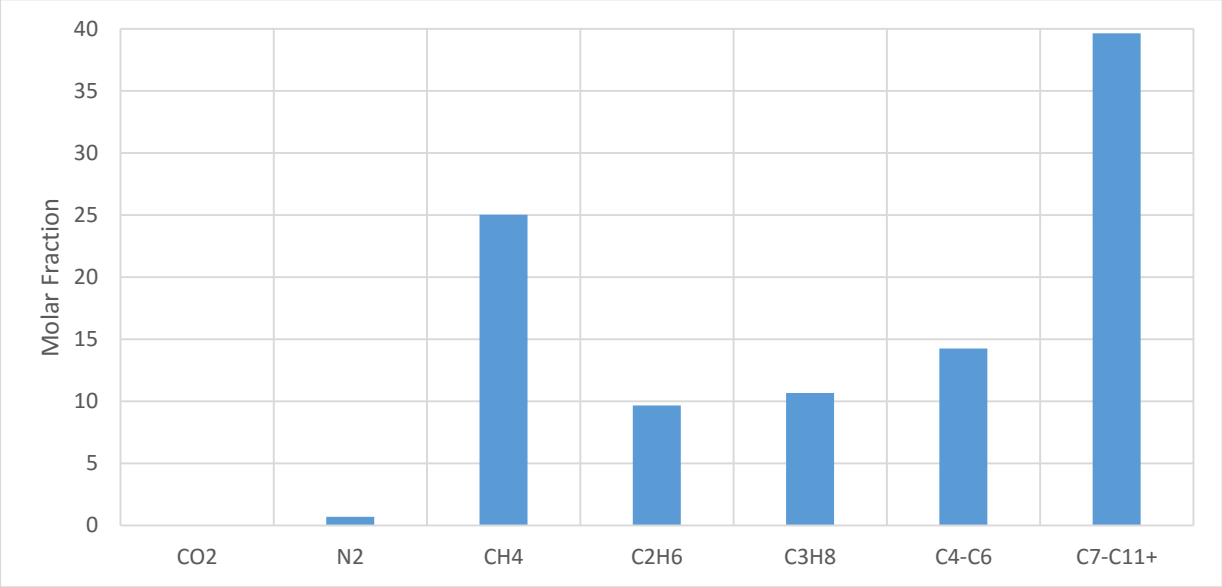

Figure 2.2 Lumped reservoir fluid components in the study area

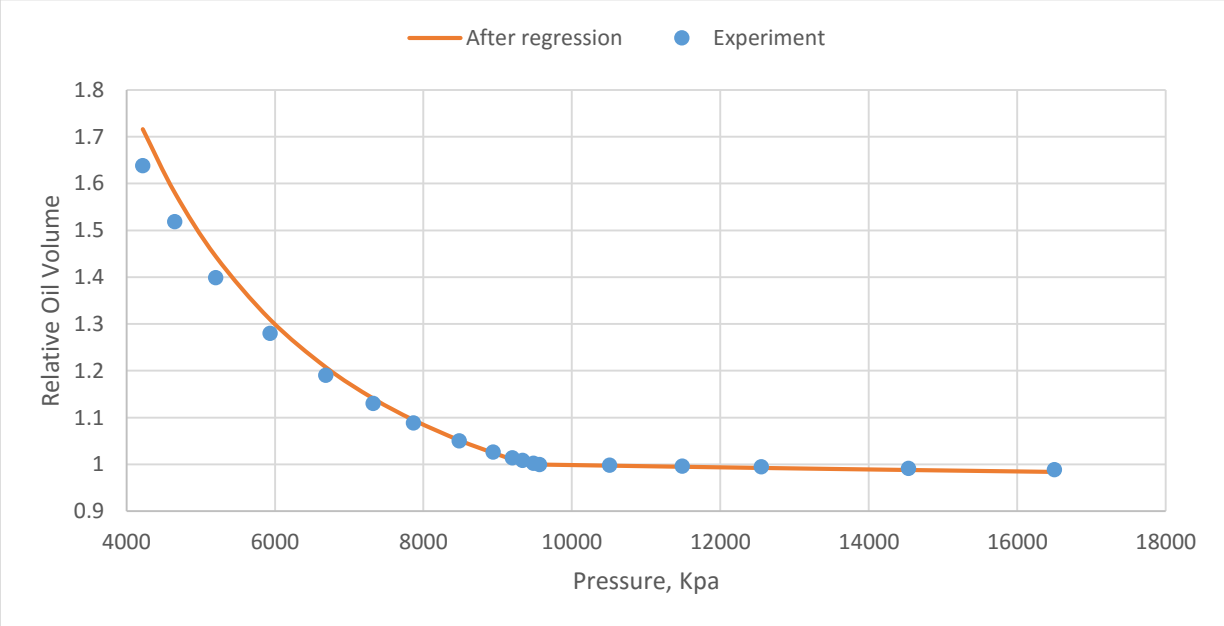

Figure 2.3 Matched results of relative oil volume.

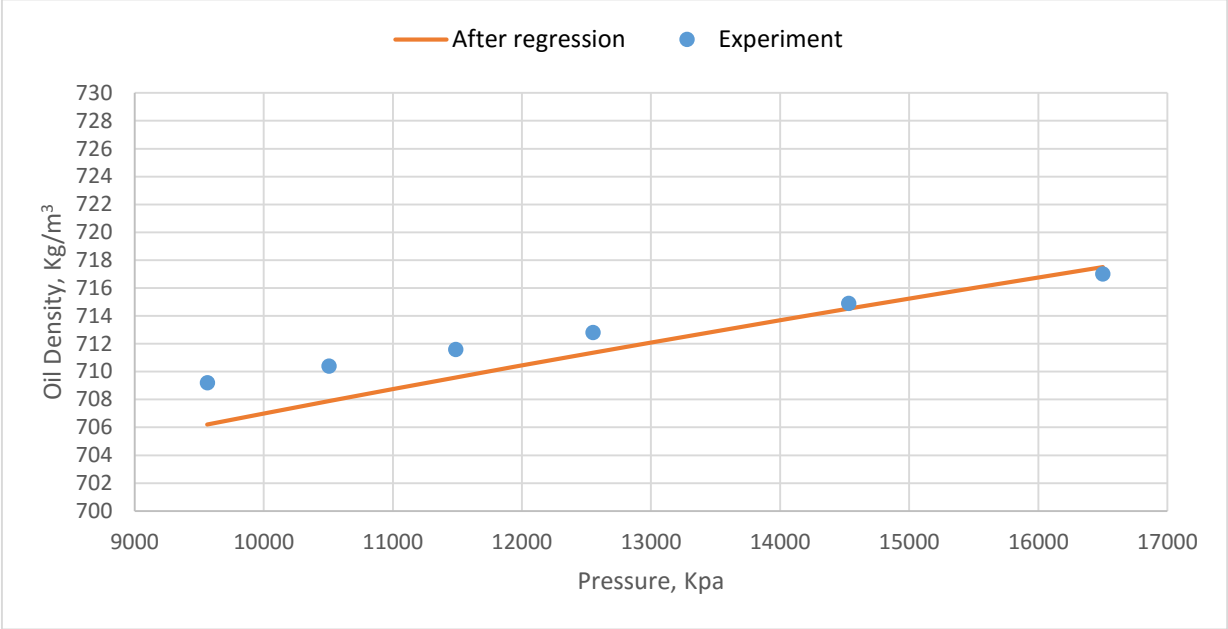

Figure 2.4 Matched results of oil density.

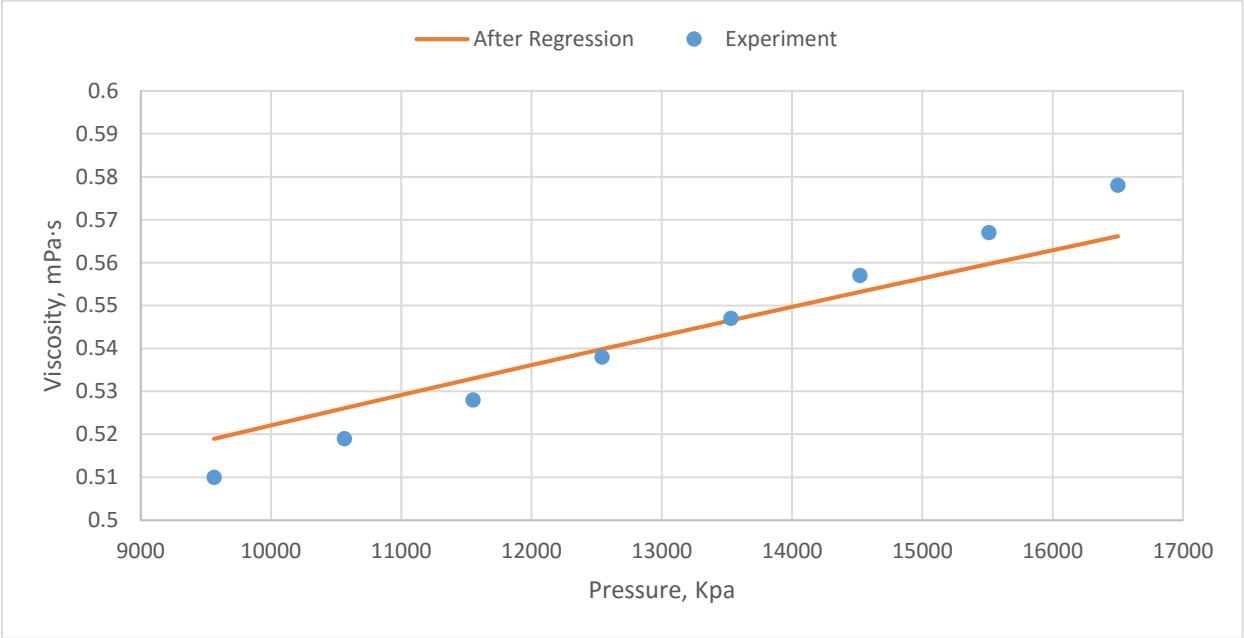

Figure 2.5 Matched results of oil viscosity.

Table 2.6 Matched results between EOS regression and separator test

	Saturation Pressure/Kpa	GOR/m^3/m^3	Formation Volume Factor	API
Experiment	9563	101.4	1.3503	39.64
EOS	9419	100.6	1.3726	39.64

2.2.1.2 Static Model

In this study, CMG GEM is used for reservoir simulation. Three models (Model 1, Model 2 and Model 3) were built to investigate the performance of the primary recovery. All three models have the same grid and blocks. The modeled volume is 1,500m in length (I-direction) by 810m in width (J-direction) by 41.5m in thickness (K-direction), and 100 (I-direction) × 54 (J-direction) × 9 (K-direction) grid blocks are used. The grid block size in the I-direction and J-direction is 15m.

Two horizontal production wells are placed in layer 7 (Figure 2.6) and the maximum bottom hole pressure of the wells is 7,650Kpa, which is lower than the saturation pressure of the study area. Along the wells' distance, 11 transverse hydraulic fractures are placed and a stimulated reservoir volume (SRV) is defined around the fractures (Figure 2.7). The permeability of the SRV is twice that of the reservoir permeability. The local grid refinement (LGR) is used for the hydraulic fractures. The conductivity of the hydraulic fractures is defined by the following equation:

$$k_f \times w_f = k_f' \times \Delta f \tag{2-1}$$

where $k_f \times w_f$ is the product of fracture permeability and width and $k_f' \times \Delta f$ is the corresponding product in the simulation model. In this study, the width of the hydraulic fractures is defined to 0.5m and the permeability is 20md, which gives 10md-m of fracture conductivity.

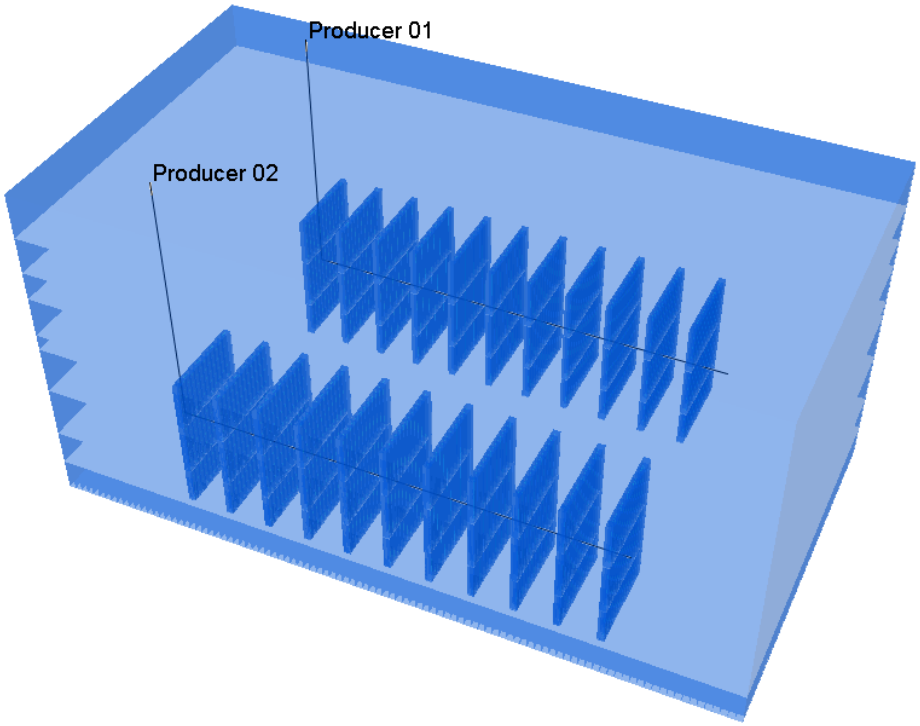

Figure 2.6 Simulation model

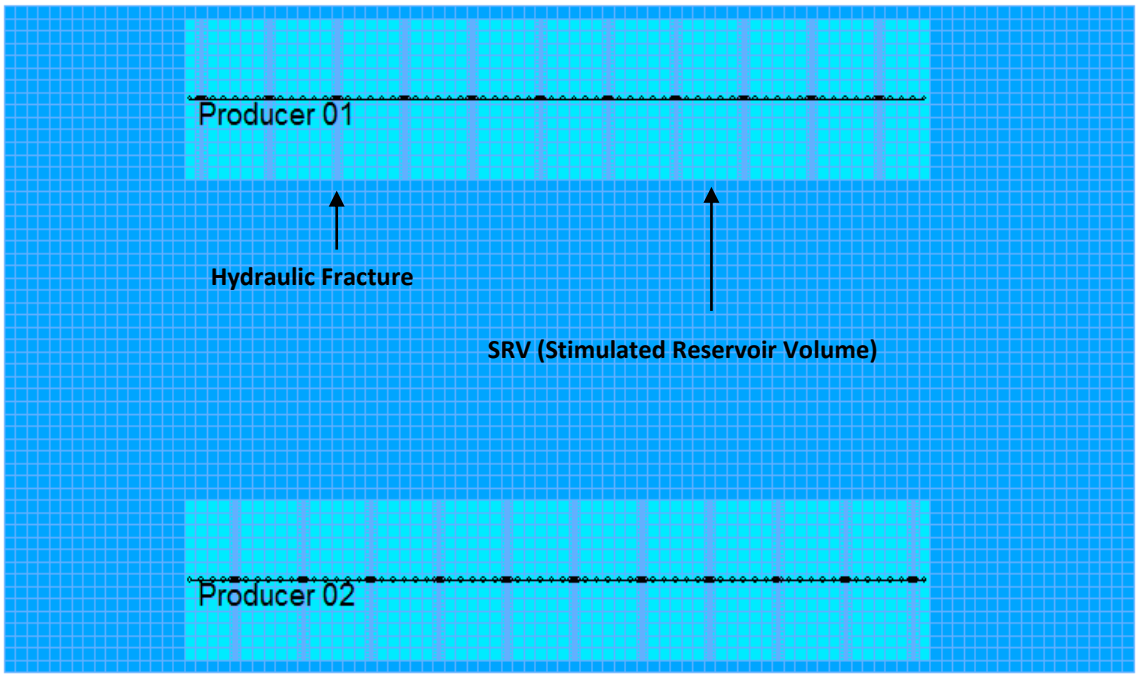

Figure 2.7 Hydraulic fractures and stimulated reservoir volume

As discussed previously, the major difference between the Bakken formation and the study area is the initial reservoir pressure. To investigate the effect of the initial reservoir pressure, the reservoir pressure of Model 1 is set to the same pressure of the study area, which is 16.5Mpa. The initial reservoir pressure of Model 2 is defined to be 36.5Mpa, which is close to the reservoir pressure of the Bakken formation.

Model 3 is built to study the effect of reservoir permeability. Compared with Model 1, the permeability of Model 3 is increased and is twice that of Model 1.

The general properties of the models and the hydraulic fractures are listed in Table 2.7. Summaries of thickness, porosity and permeability values, by layer, for the three models are shown in Table 2.8. Figures 2.8 and 2.9 show the water-oil and liquid-gas relative permeability used in this study, respectively.

Table 2.7 General properties of the models and the hydraulic fractures

Parameter	Value	Parameter	Value
Grid Number	100×54×9	Minimum Bottom Hole Pressure/Kpa	7650
Grid Size in I, J Direction/m	15	Hydraulic Fracture Width/m	0.5
Reservoir Depth/m	1970	Hydraulic Fracture Half Length/m	90
Reservoir Temperature/℃	64.75	Hydraulic Fracture Conductivity/md-m	10
Rock Compressibility/1/Kpa	7E-7	Distance between Hydraulic Fractures/m	90
Horizontal Well Length/m	990	Number of Hydraulic Fracture	11

Table 2.8 Summaries of the properties for all three models

			Model 1		Model 2		Model 3	
Reservoir Pressure/MPa			16.5		36.5		16.5	
	h/m	φ	Reservoir	SRV	Reservoir	SRV	Reservoir	SRV
			k/md	k/md	k/md	k/md	k/md	k/md
Layer 1	5.5	0.017	0.001		0.001		0.002	
Layer 2	4.5	0.12	0.022		0.022		0.044	
Layer 3	3.5	0.086	0.009		0.009		0.018	
Layer 4	5	0.124	0.019		0.019		0.038	
Layer 5	2	0.068	0.003		0.003		0.006	
Layer 6	6	0.124	0.022	0.044	0.022	0.044	0.044	0.088
Layer 7	6.5	0.124	0.022	0.044	0.022	0.044	0.044	0.088
Layer 8	4.5	0.017	0.001	0.002	0.001	0.001	0.002	0.004
Layer 9	4	0.017	0.001	0.002	0.001	0.001	0.002	0.004

*h stands for thickness, φ stands for porosity and k stands for permeability

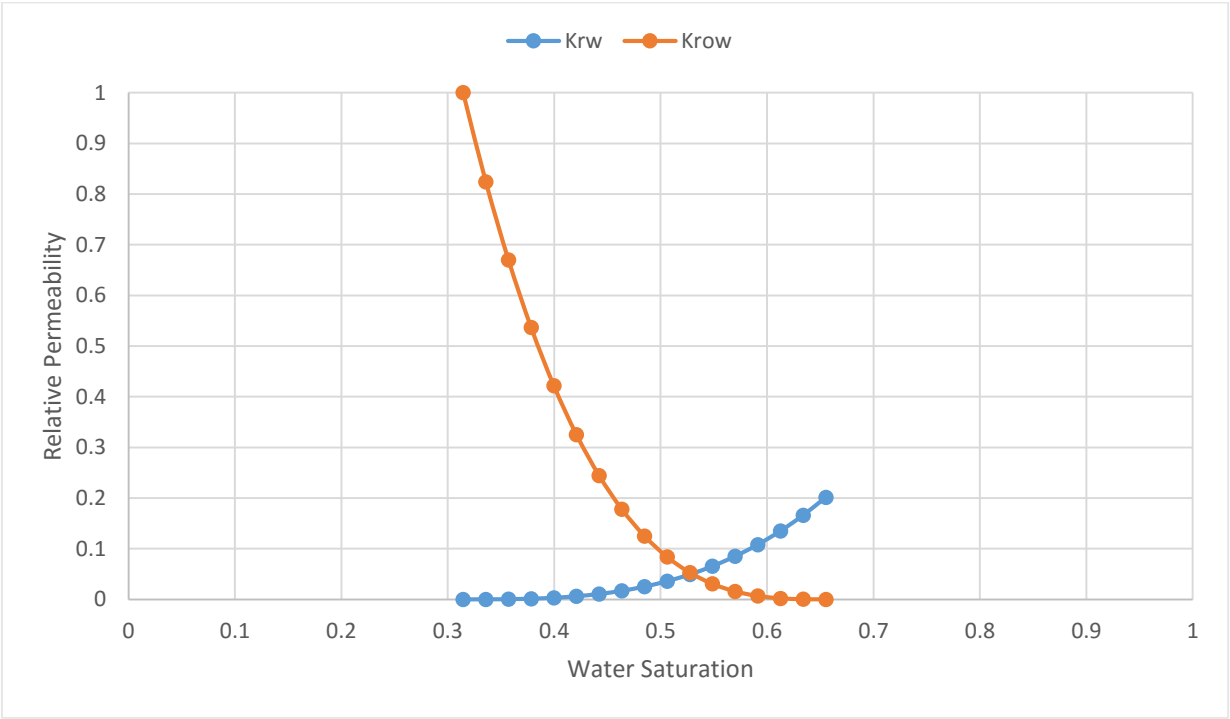

Figure 2.8 Water-oil relative permeability curve

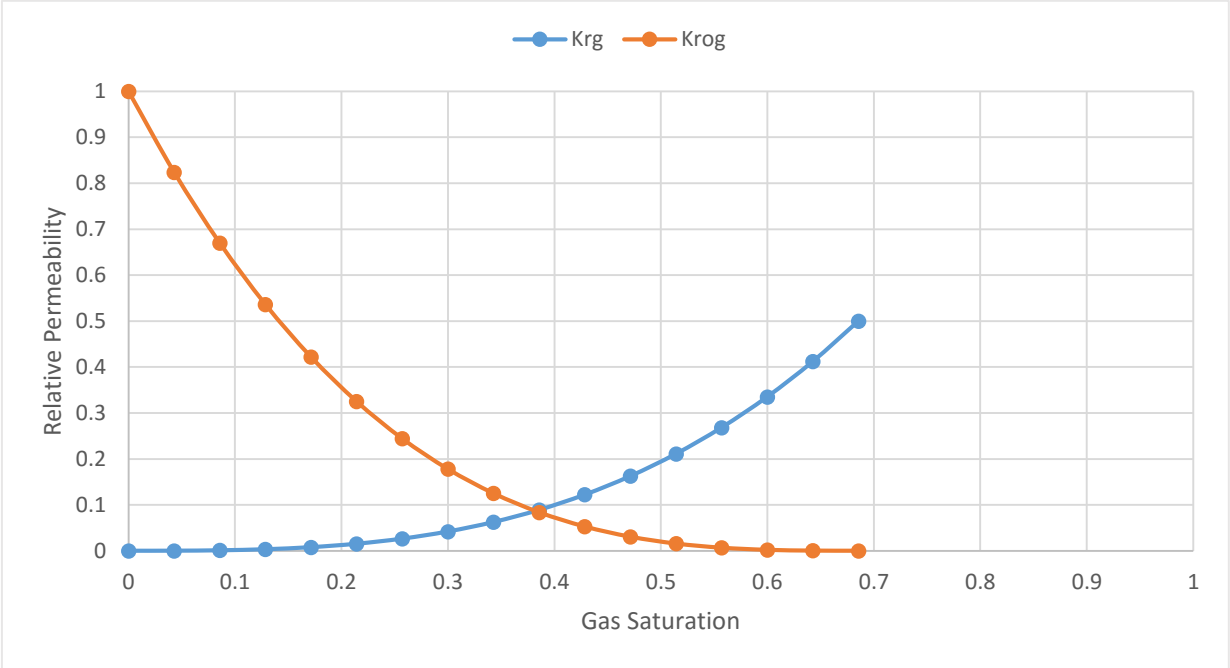

Figure 2.9 Liquid-gas relative permeability curve

2.2.2 Results and Discussion of Primary Recovery

2.2.2.1 Comparison of Pressure Variation

First, the pressure variation for all three models is compared. Before the reservoir is developed, its pressure system is balanced. The pressure is equivalent for the same depth. After the development of the reservoir, the balanced pressure system is broken. As the development continues, the pressure is decreased. The variation around a wellbore is most obvious and the pressure cone of depression is formed.

According to Table 2.9, comparisons of pressures variation around a wellbore after one month, three months, six months, one year, five years and ten years reveal that the pressure variation is significant at the initial stage of the production and the pressure decreases rapidly. After one year of production, the pressure tends to be stable. For Model 1, the initial reservoir pressure is 16.5Mpa; after one month of production, the pressure decreased to 10.316Mpa, a drop of 37.48%. Comparing reservoir pressures after six months of production and one year of production, the reservoir pressure only decreased 0.366Mpa, a decline of 4.1%. For Model 2, the initial reservoir pressure is 36.5Mpa; at the end of the first month of production, the pressure decreased to 15.855Mpa, a 56.56% decrease. Comparisons of reservoir pressure after six months of production and one year of production show that the reservoir pressure decreased 1.320Mpa, a 12.58% decline. After one year of production, the pressure tends to be stable. Comparing Model 1 and Model 2 shows that the higher the initial pressure is, the more rapidly the pressure decreases at the initial stage of production. After one year of production, the pressure around the wellbore is close for all three models.

Table 2.9 Pressure variation around the wellbore

		Pressure/Kpa							
	Initial Pressure/Kpa	1 month	3 months	6 months	1 year	5 years	10 years	15 years	20 years
Model 1	16500	10316	9360	8925	8559	8094	7958	7839	7788
Model 2	36500	15855	12468	10497	9177	9276	8044	7920	7844
Model 3	16500	9897	9110	8696	8433	8009	7856	7784	7745

Table 2.10 Pressure variation at center of models

		Pressure/Kpa							
	Initial Pressure/Kpa	1 month	3 months	6 months	1 year	5 years	10 years	15 years	20 years
Model 1	16500	16488	16488	16483	16397	13041	10645	9741	9545
Model 2	36500	36487	36487	36458	36055	23334	15040	11727	10310
Model 3	16500	16488	16485	16431	15959	11133	9609	9486	9412

Comparisons of the pressure variation at the center of the models (Table 2.10) show that the higher the initial pressure, the higher the drawdown pressure, which means the higher the driving energy. With a higher reservoir permeability, the pressure variation is more significant, which indicates higher displacement efficiency.

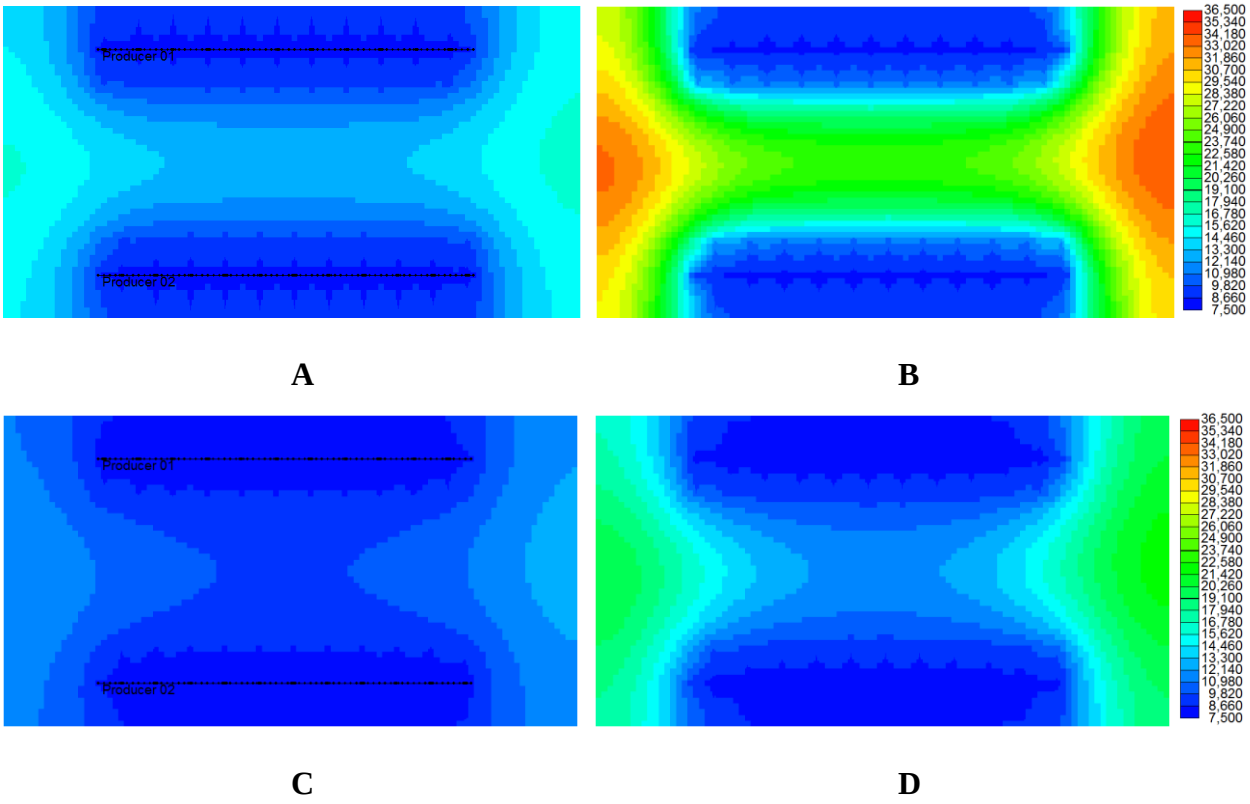

Figure 2.10 Pressure distribution (A: Model 1 after five years of production; B: Model 2 after five years of production; C: Model 1 after 15 years of production; D: Model 2 after 15 years of production)

Figure 2.10 shows the pressure distribution after five years and 15 years of production for Model 1 and Model 2. According to Figure 2.10, the pressure distribution of Model 2 after 15 years of production is similar to the pressure distribution of Model 1 after 5 years of production.

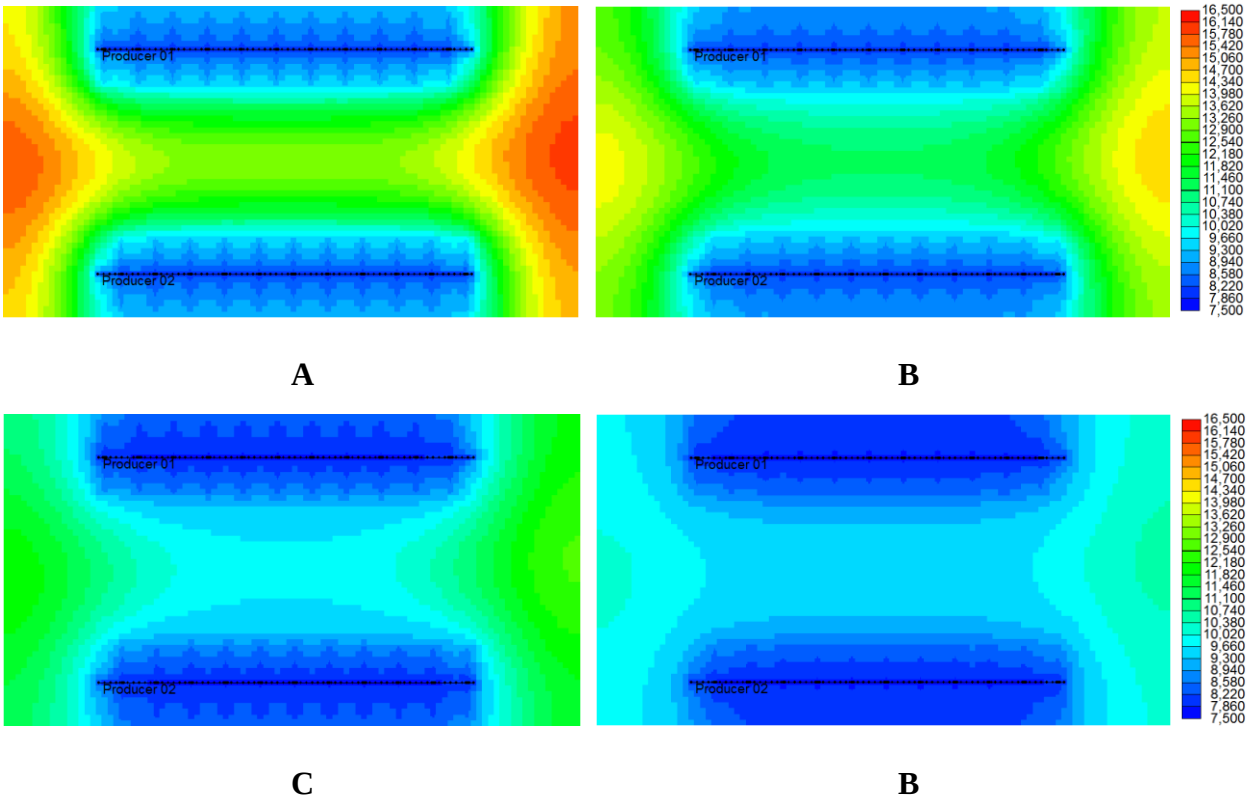

Figure 2.11 Pressure distribution (A: Model 1 after five years of production; B: Model 3 after five years of production; C: Model 1 after 15 years of production; D: Model 3 after 15 years of production)

Figure 2.11 shows the pressure distribution after five years and 15 years of production for Model 1 and Model 3. According to Figure 2.11, due to the higher permeability of Model 3, the pressure variation is more obvious, which means the driving energy will release more rapidly, resulting in higher oil production.

2.2.2.2 Comparison of Oil Rate and Oil Recovery Factor

As discussed previously, the initial reservoir pressure and permeability have significant effects on reservoir pressure distributions. The effect of the initial reservoir pressure is more profound. In this section, comparisons of oil production rates and oil recovery factors are discussed.

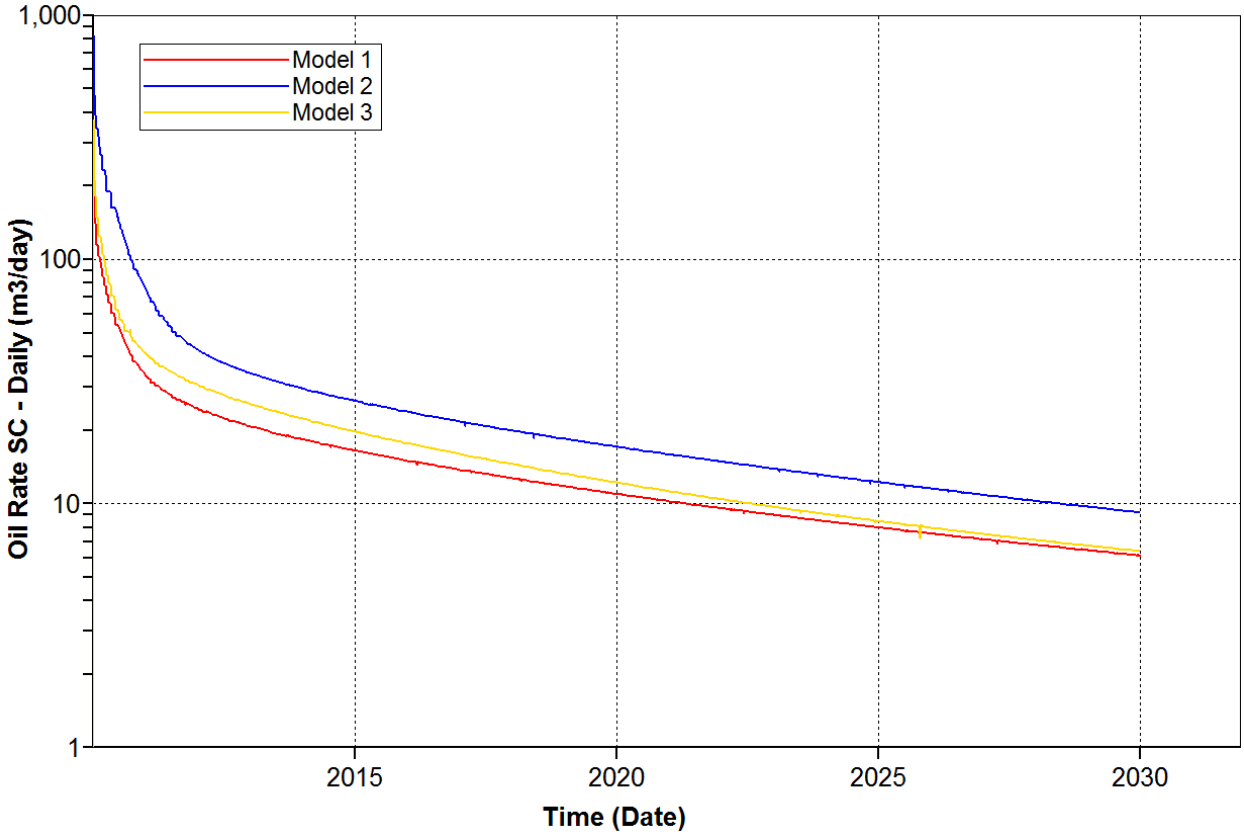

Figure 2.12 Oil production rate of primary recovery

Table 2.10 Oil production rate in the first year of production

	Oil Production Rate/m^3/day											
Time/month	01	02	03	04	05	06	07	08	09	10	11	12
Model 1	115	91	77	66	58	52	47	43	40	37	35	34
Model 2	336	266	221	189	163	142	124	110	99	90	82	75
Model 3	148	115	92	78	68	60	55	51	48	45	43	41

According to Figure 2.12 and Table 2.10, for all three models, the oil production is high at the initial stage of production and is declines rapidly in the first year of production. For instance, the

oil production of Model 1 in the first month is 115m^3/day. After three months of production, the oil rate declined to 77m^3/day, which is 66.96% of the first month. After one year of production, the oil rate declined to 34m^3/day, representing 29.56% of the first month.

High reservoir permeability also has positive effects on the oil production rate, especially at the initial stage of production. After 20 years of production, however, the oil production rate of Model 3 will be the same as that of Model 1. After 20 years of production, Model 2 still has the highest oil rate, at almost twice that of Model 1 and Model 3.

Even though the oil rate declines rapidly in the three models, the oil production rate of Model 2 remains the highest. Figure 2.13 and Table 2.11 show the oil recovery for the models. Based on Figure 2.13 and Table 2.11, the oil recovery factor of Model 2 after five years of production is equal to the oil recovery factor of Model 1 after 20 years of production. The oil recovery factor of Model 2 after 20 years of production is almost twice that of Model 1.

The variations of the oil production rate and oil recovery factor are consistent with the pressure changes.

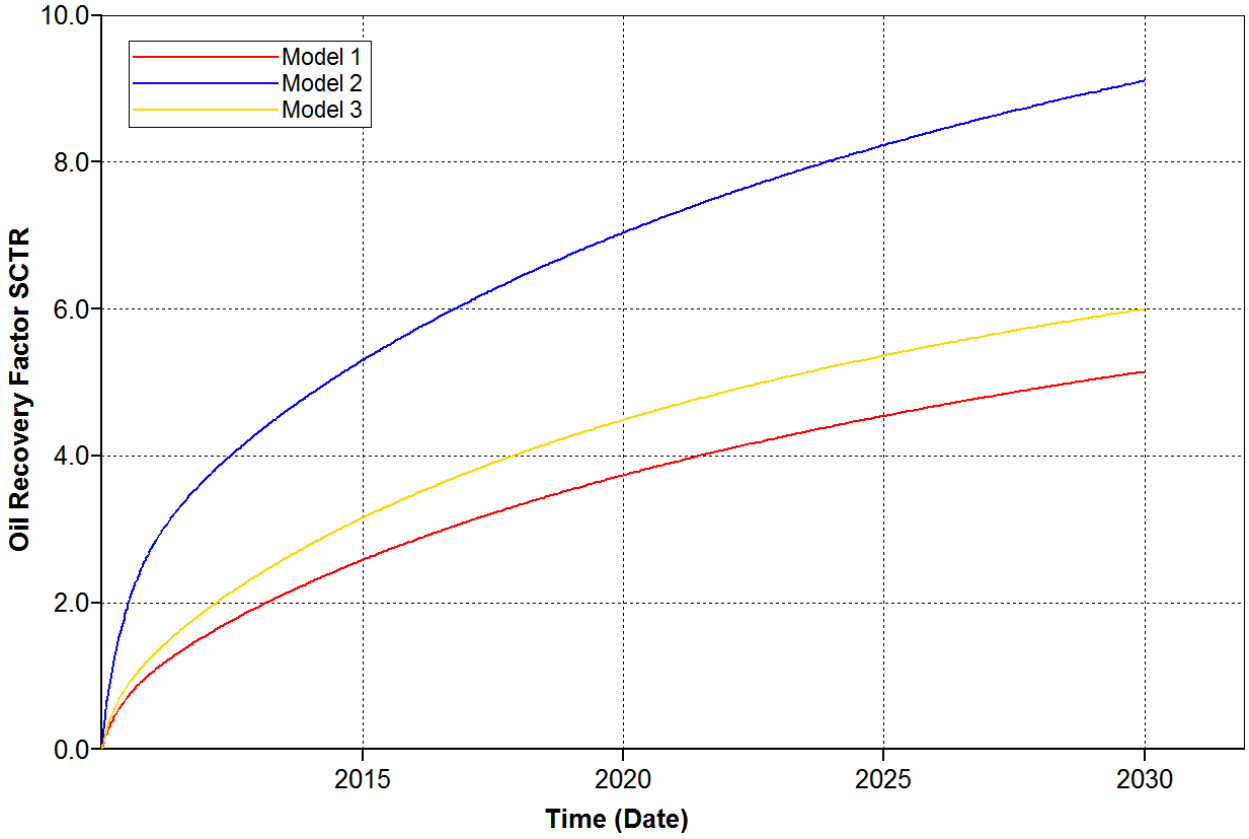

Figure 2.13 Oil recovery factor of primary recovery

Table 2.11 Oil recovery factor of primary recovery

	Oil Recovery Factor/%				
Time/year	01	05	10	15	20
Model 1	1.08	2.58	3.74	4.54	5.15
Model 2	2.81	3.50	7.04	8.23	9.11
Model 3	1.30	3.16	4.49	5.37	6.00

2.2.3 Necessity of Water and Gas Injection

As previously discussed, both high initial oil recovery and permeability can increase oil recovery. The effect of the initial reservoir pressure is more profound than is permeability, and is the main reason for the low oil recovery. Permeability can be increased through hydraulic fracturing and reservoir stimulation technologies, which is not the focus of this study.

Model 1 represents the reservoir properties of the study area in the Ordos basin. Based on Model 1, the initial pressure of Model 2 is increased to 36.5Mpa, which is similar to the pressure of the Bakken formation. Comparisons of Model 1 and Model 2 show that for reservoirs with high initial pressure, such as the Bakken formation, primary recovery is efficient. For low pressure reservoirs, like that in the study area, the primary recovery is quite low, at only 5.15%. Thus, water or gas injection is necessary to supplement driving energy and enhance oil recovery.

Chapter Three: WATER AND GAS INJECTION

As discussed in Chapter Two, the production rate of primary recovery is high at the initial stage of recovery and declines rapidly. Compared with the Bakken formation, the reservoir pressure of the study area is quite low and the primary recovery is inefficient. Consequently, water or gas should be injected to enhance the oil recovery. In this chapter, based on reservoir simulation, the performance of water and gas, including CH_4, CO_2 and the separator gas, is studied.

3.1 Simulation Model

Based on Model 1, as referenced in Chapter Two, one injector is added between the two producers (Figure 3.1). Because water or gas breakthrough will cause adverse effects on oil recovery, to avoid these situations from occurring, the injector is not hydraulically fractured in this study.

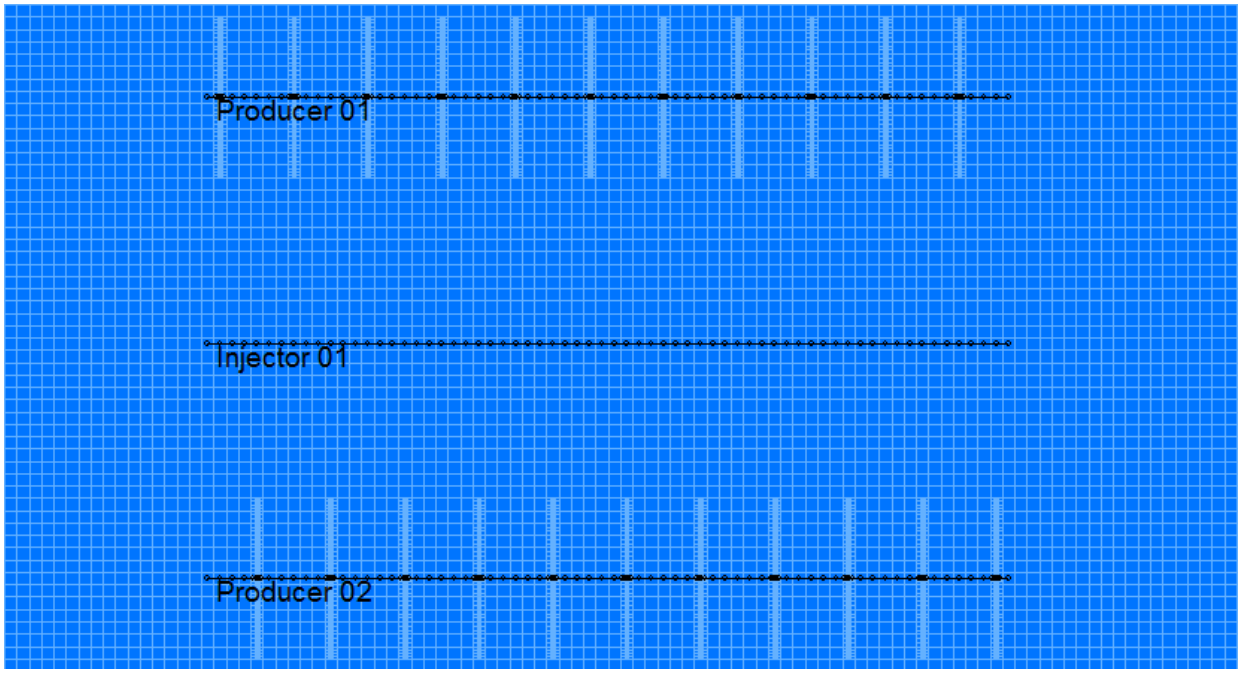

Figure 3.1 Well displacement for the simulation study of water and gas injection

The water and gas are continuously injected from the very onset of the simulation. The constraints for the water and gas injection are listed in Table 3.1.The maximum bottom hole pressure is defined as 42MPa, which is the rock fracturing pressure of the study area.

Table 3.1 Injector well constrains for water and gas injection

	Maximum Bottom Hole Pressure/Kpa	Surface fluid rate/m^3/day
Water	42000	100
Gas	42000	50000

3.2 Swept Area

The swept area can reflect the displacement efficiency of the injected fluid. The more area swept, the more oil displaced, resulting in an increase in oil recovery. In this study, the swept areas of water, CH_4, CO_2 and the separator gas are compared. Water saturation and gas molar fraction are used to indicate the swept areas.

Table 3.2 Swept area of water and gases

	Swept Area/m^2							
	1 year	2 years	3 years	4 years	5 years	10 years	15 years	20 years
Water	14850	14850	44550	44550	44550	75375	75375	105525
CH_4	44550	75375	77625	108675	110250	149850	210600	283050
CO_2	44550	63900	74250	74250	78750	119700	145800	178200
Hydrocarbon Gas	44550	75375	77625	86625	708675	143775	183150	228150

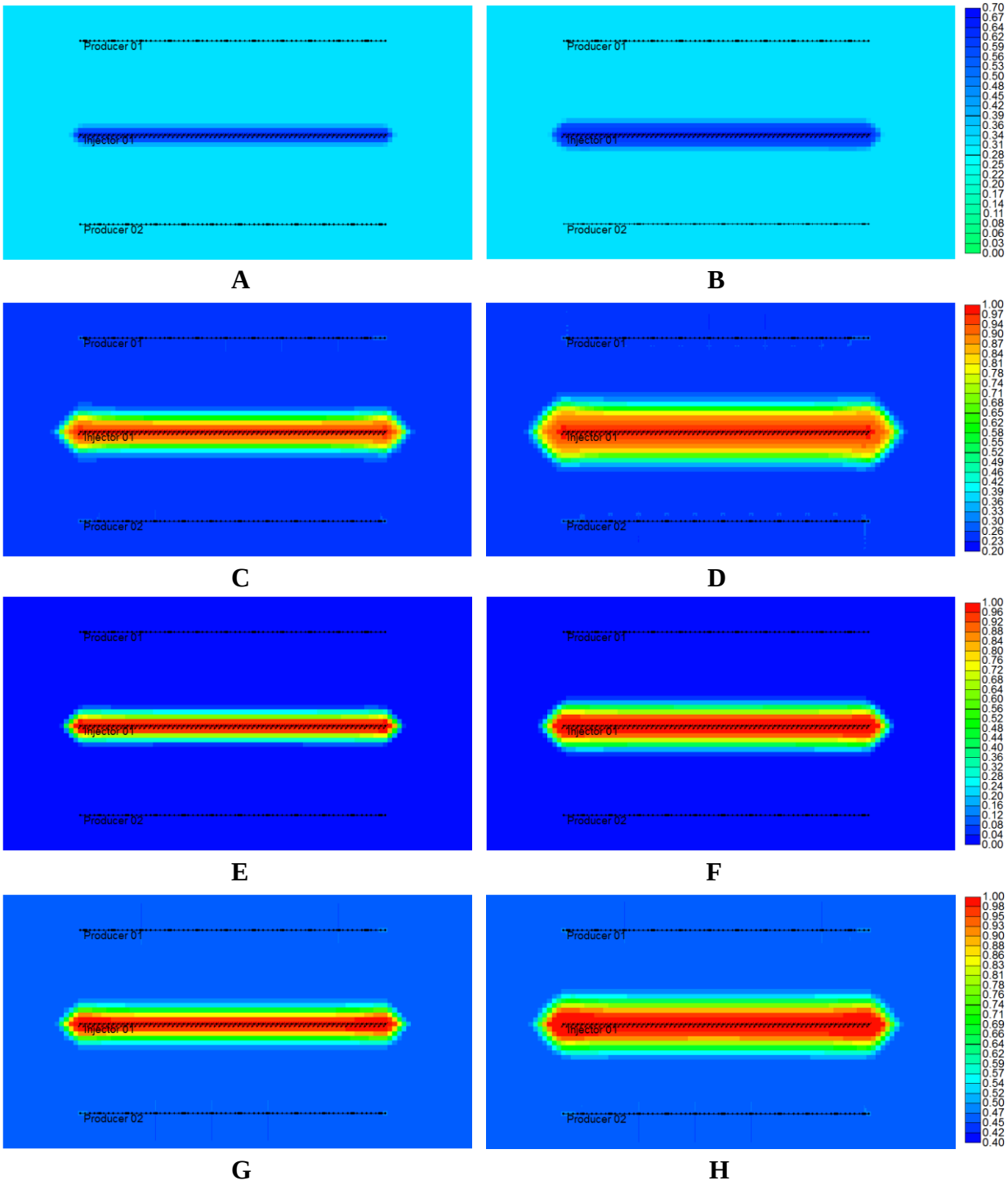

Figure 3.2 Swept area (A: water after 10 years of injection; B: water after 20 years of injection; C: CH_4 after 10 years of injection; D: CH_4 after 20 years of injection; E: CO_2 after 10 years of injection; F: CO_2 after 20 years of injection; G: separator gas after 10 years of injection; H: separator gas after 20 years of injection)

According to Table 3.2 and Figure 3.2, the swept area of water is much smaller than that of gas. The swept areas of water after 10 years and 20 years of injection are 75375m^2 and 105525m^2, respectively, while the swept areas of gas, such as CH_4, after 10 years and 20 years of injection are 149850m^2 and 283050m^2, respectively, which is more than twice that of the water. The swept area of CH_4 after 10 years of injection is already higher than that of water.

As mentioned in Chapter One, based on the study of Yang et al. (Yang, et al., 2012), in nanoscale pore throats of a tight oil reservoir, the water film adheres to the surface of a matrix, and the average thickness is 43nm, resulting in a low injectivity of water.

When the swept areas of gases are compared, CH_4 has the highest swept area, followed by the separator gas and then CO_2 as the lowest. The possible reason is that the diffusivity of CH_4 is higher than that of CO_2, meaning that CH_4 can move more easily than CO_2 in the reservoir. As almost 60% of composition of the separator gas is CH_4, the swept area of the separator gas is also higher than that of CO_2.

3.3 Pressure distribution

As the initial pressure of the study area is very low, water and gas should be injected to maintain and enhance reservoir pressure. In this study, the pressure distribution is divided into two areas, I and II. Area I, a high pressure zone, has a pressure higher than 105% of the initial pressure. Area II has a pressure lower than 95% of the initial pressure.

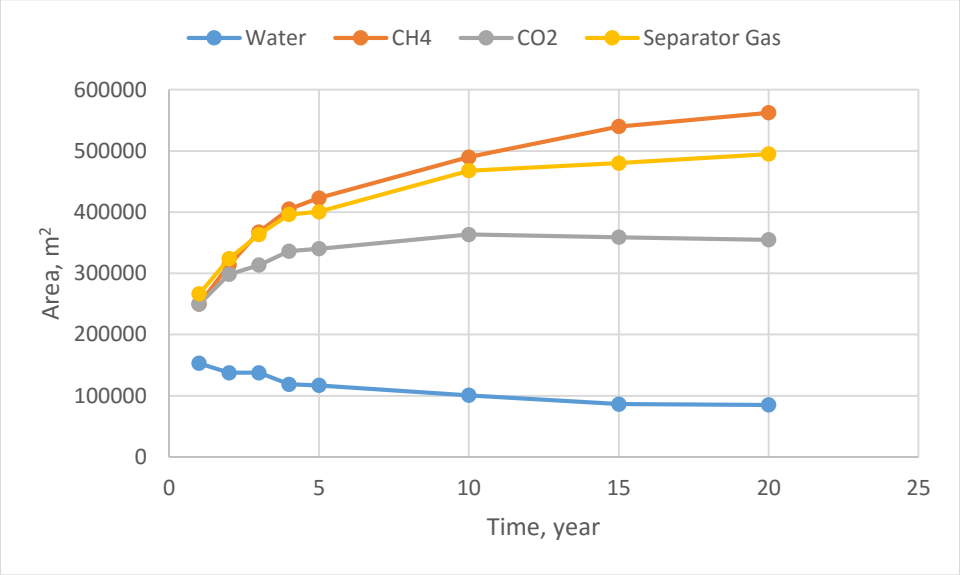

Figure 3.3 Pressure variation of Area I

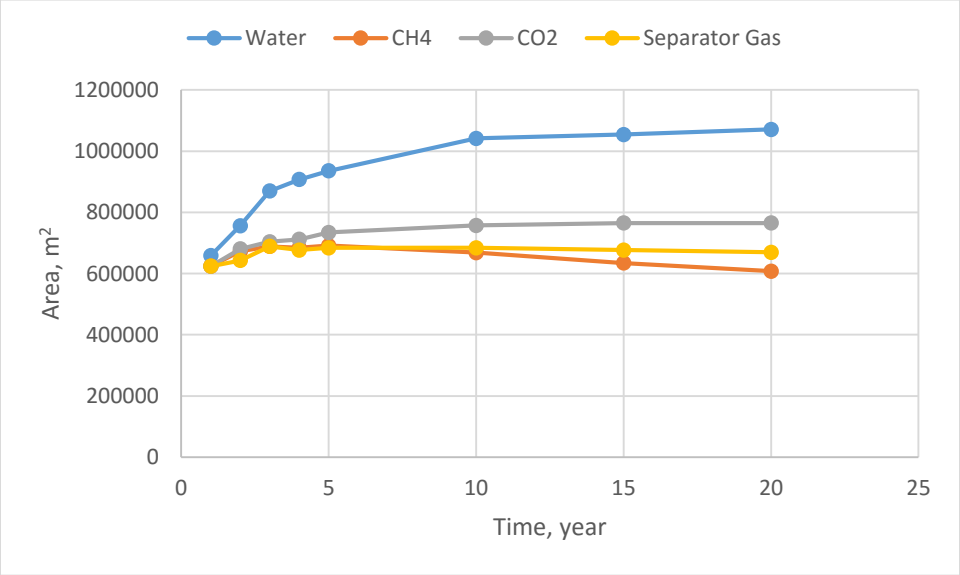

Figure 3.4 Pressure variation of Area Ⅱ

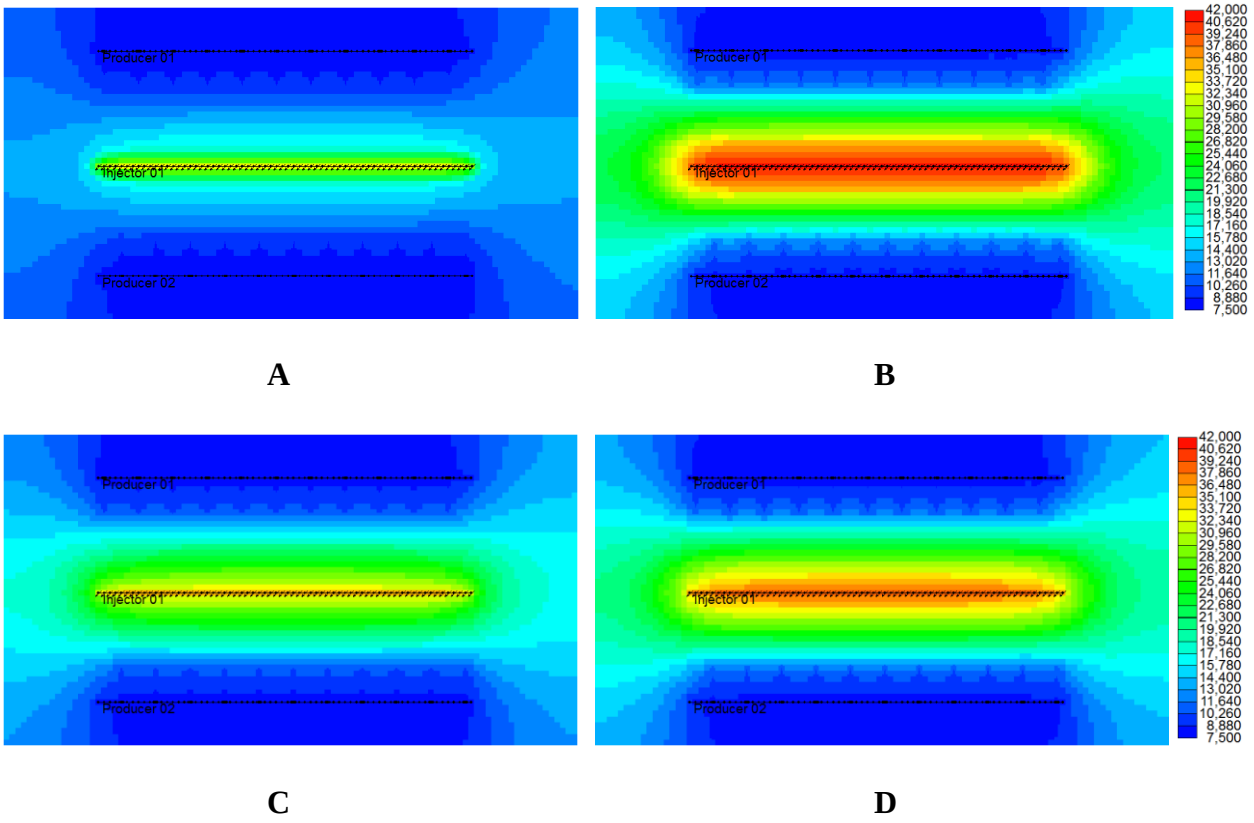

Figure 3.5 Pressure distribution (A: water injection after 20 years of production; B: CH_4 injection after 20 years of production; C: CO_2 injection after 20 years of production; D: separator gas injection after 20 years of production)

Figures 3.3 and 3.4 show the pressure variations of Areas I and II; Figure 3.5 is the pressure distribution of water, CH_4, CO_2 and separator gas injection after 20 years of production. Based on these figures, CH_4 performs best to enhance reservoir pressure, followed by the separator gas; the performance of CO_2 is moderate and the water is the worst. After 20 years of injection, Area I with CH_4 and the separator gas is significantly increased. For CO_2, Area I increased over the first five years and flattened in the following years, while Area I with water injection decreased after 20 years of production. For the purpose of increasing reservoir pressure, CH_4 is the best, followed by the separator gas.

3.4 Oil Viscosity and Oil Saturation

Figure 3.6 shows the viscosity variation of CH_4, CO_2 and separator gas injection after 5 years and 20 years of production. The white section in this figure means that the oil viscosity is lower than the values represented by the color scale, which is 0.3mPa·s. After gas injection, the injected gas contacts continuously with the reservoir oil and extracts the oil's light components. The order of gases based on their ability to extract light components from oil is CO_2＞separator gas＞CH_4. After the light components are extracted, the heavy components are left behind, increasing the oil viscosity. According to Figure 3.6, after 5 years of injection, the viscosity of the oil near the injector with CO_2 and separator gas injection is increased. As CH_4 can only extract small amounts of light components from oil, the viscosity variation of the CH_4 injection is not as obvious as CO_2 injection.

When gas is continuously injected into the reservoir, it moves forward and pushes oil to the producer. With a continuous gas injection, the reservoir pressure, near the injector, increases to the MMP, the miscible condition is gradually reached between the gas and oil, and oil viscosity is reduced, which is beneficial for enhancing oil recovery. The study of MMP for CH4, CO2 and separator gas can be found in Appendix A.

Figure 3.7 shows the oil saturation after 5 years and 20 years of injection for CH_4, CO_2 and the separator gas. According to Figure 3.7 at the area near the injector, the oil saturation is reduced below the critical water saturation, which indicates that as the pressure in this area increased, the miscible drive was reached.

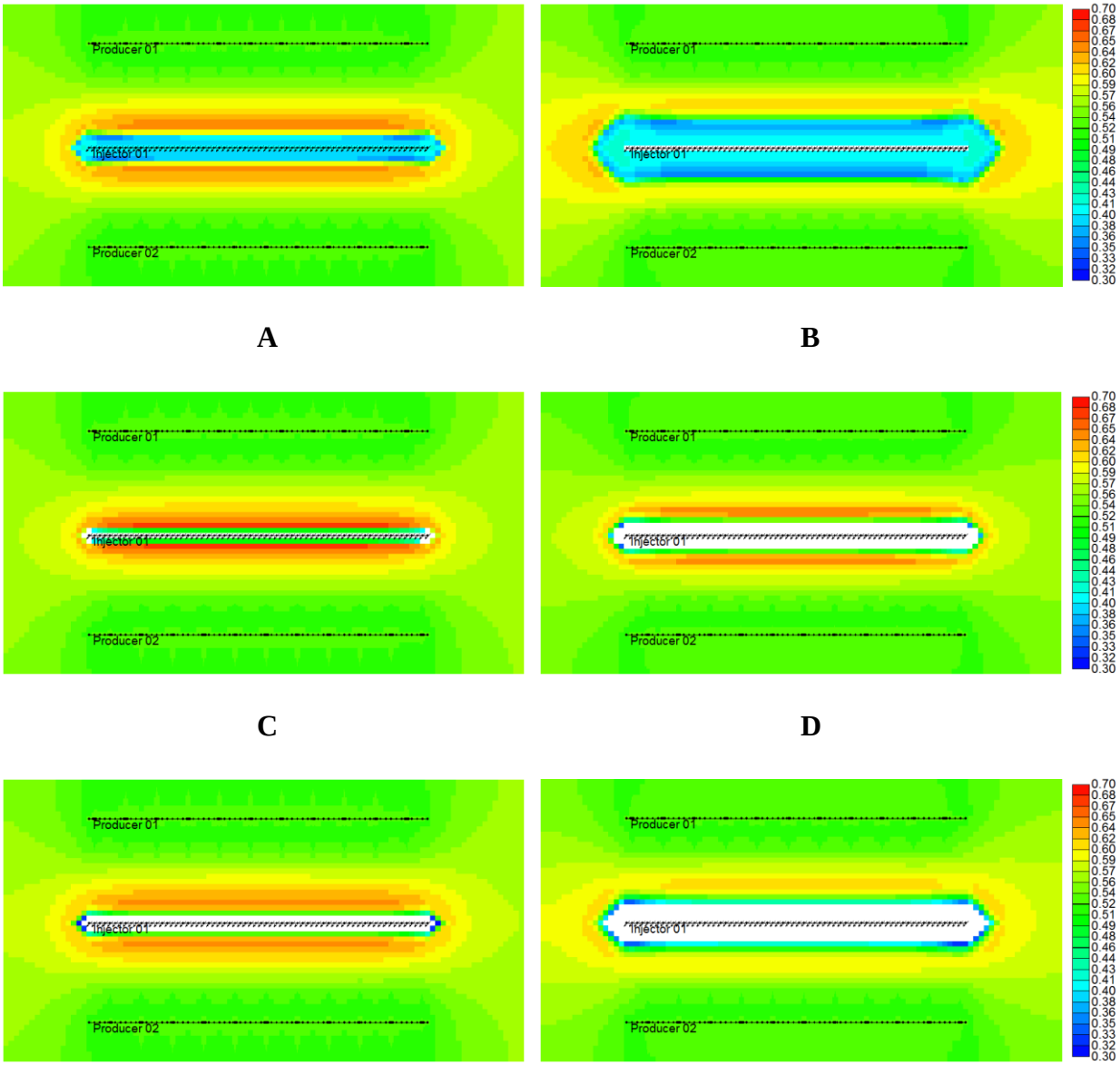

Figure 3.6 Oil viscosity (A: CH_4 after 5 years of injection; B: CH_4 after 20 years of injection; C: CO_2 after 5 years of injection; D: CO_2 after 20 years of injection; E: separator gas after 5 years of injection; F: separator gas after 20 years of injection)

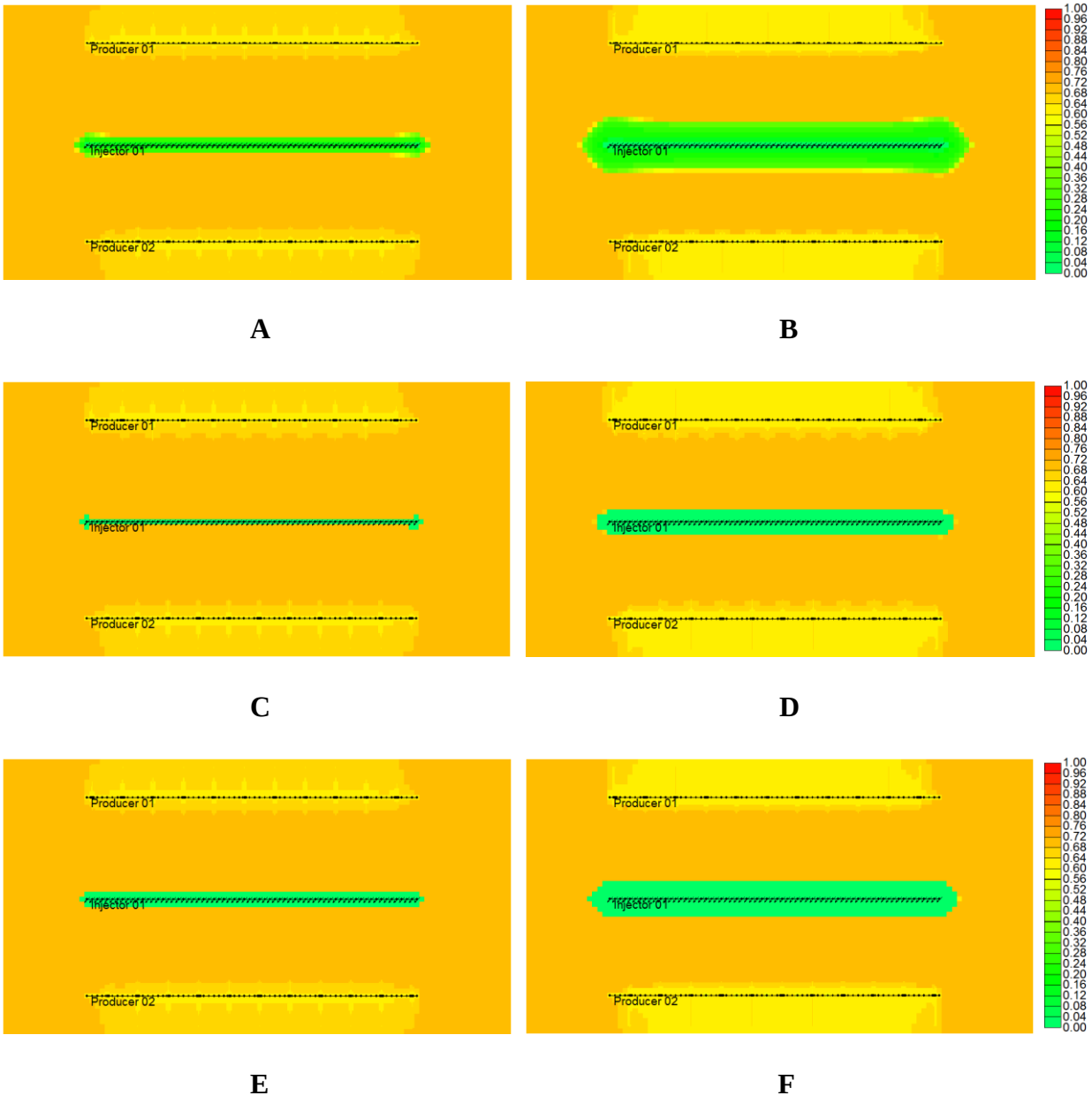

Figure 3.7 Oil Saturation (A: CH_4 after 5 years of injection; B: CH_4 after 20 years of injection; C: CO_2 after 5 years of injection; D: CO_2 after 20 years of injection; E: separator gas after 5 years of injection; F: separator gas after 20 years of injection)

3.5 Oil Rate and Oil Recovery factor

Table 3.3 and Figure 3.8 present the oil production rate of primary recovery, water injection and gas injection. Similar to the primary recovery, the oil rate of water and gas injection declined rapidly in the first year of production. Instead of continuous decline, however, the oil production rate tended to flatten in the following years of production. The underlying reason is that at the initial stage of the production, an effective displacement system is not established.

Table 3.3 Oil production rate of primary recovery and water and gas injection

		Primary	Water	CH_4	CO_2	Separator Gas
Oil Rate /m^3/day	1 month	115	115	115	115	115
	3 months	77	77	77	77	77
	6 months	52	52	52	52	52
	1 year	34	34	34	34	34
	5 years	17	17	21	20	21
	10 years	11	13	21	17	20
	15 years	8	11	21	16	19
	20 years	6	9	21	15	19

Compared with primary recovery, through water injection the oil production rate increased. Due to the low injectivity of water, the overall oil rate still declined. In comparing the three gases, the oil production with the CH_4 injection is the highest, followed by the separator gas injection. The results are consistent with the results of the swept area and pressure distribution.

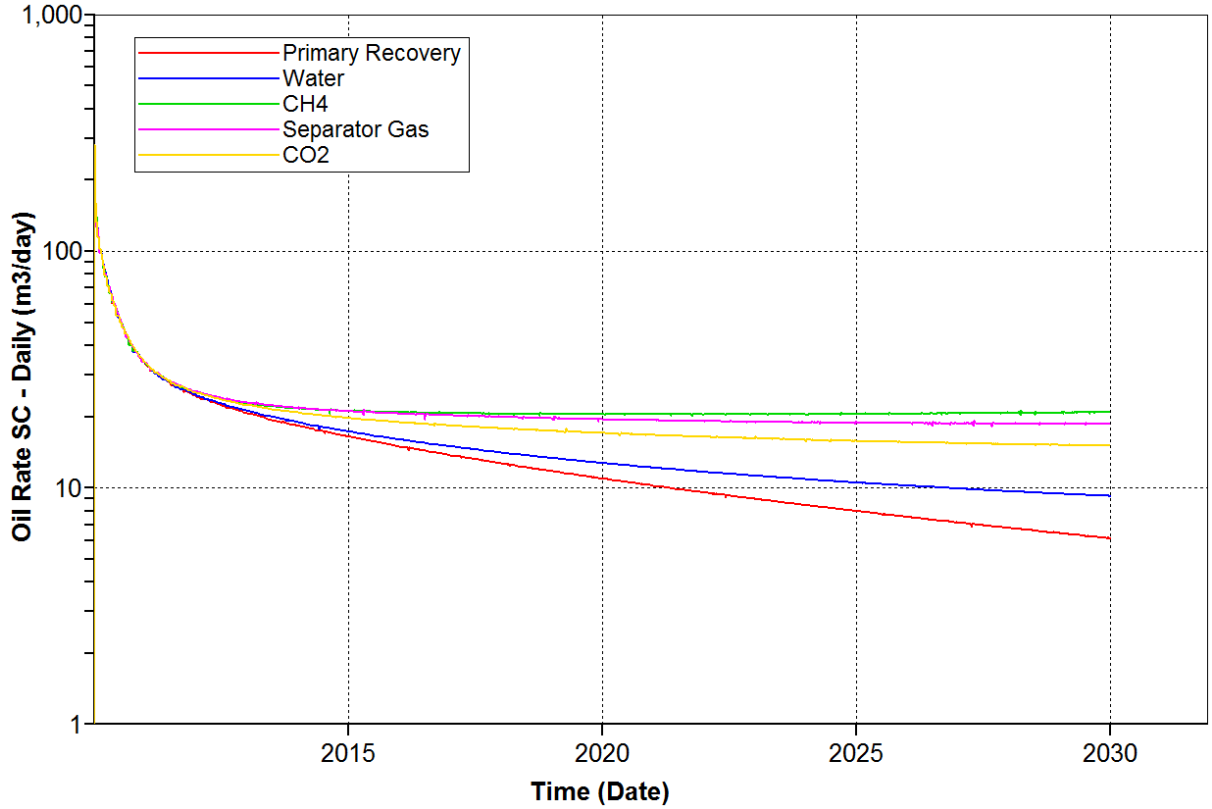

Figure 3.8 Oil production rate of primary recovery and water and gas injection

Table 3.4 and Figure 3.9 present the oil recovery factor of the primary recovery and water and gas injection. Similar to the oil production rate and compared with the primary recovery, the oil recovery factor of water after 20 years of production increased slightly from 5.15 to 5.73. The oil recovery factor of gas injection, such as CH_4, moved from 5.15 to 8.08, an increase of 57%.

Based on the above results, to enhance oil recovery from the low pressure reservoir in the study area, gas injection is much better than water injection, since the water injectivity in the tight oil reservoir is quite low. Among all gases investigated in this study, CH_4 and the separator gas are

better choices, not only because they can increase more oil recovery than CO_2, but they are also easily accessible.

Table 3.4 Oil recovery factor of primary recovery and water and gas injection

		Primary	Water	CH_4	CO_2	Separator Gas
Oil Recovery Factor/%	1 year	1.08	1.08	1.08	1.08	1.08
	5 years	2.58	2.62	2.73	2.7	2.74
	10 years	3.74	3.88	4.52	4.27	4.48
	15 years	4.54	4.88	6.29	5.69	6.14
	20 years	5.15	5.73	8.08	7.02	7.75

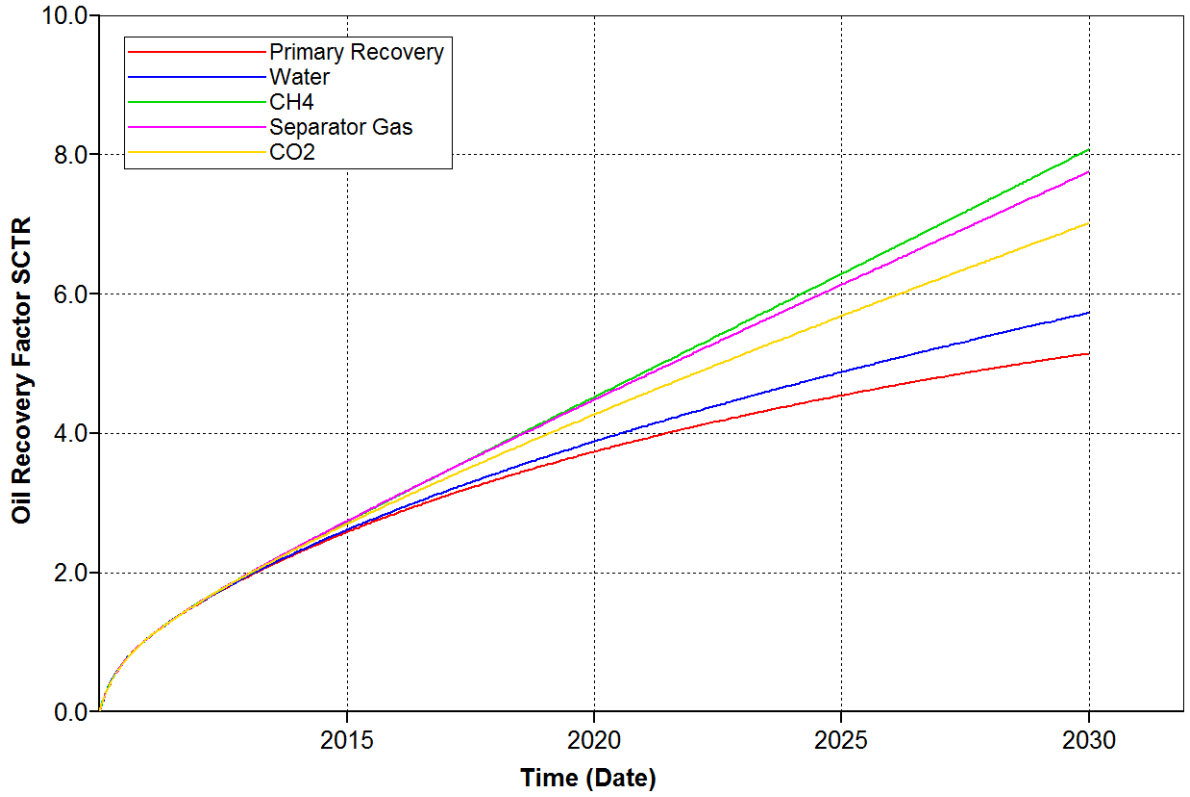

Figure 3.9 Oil recovery factor of primary recovery and water and gas injection

Chapter Four: Effect of Heterogeneity

The simulation model used in the above studies are homogeneous in the horizontal direction. In reality, a reservoir is heterogeneous. In this chapter, the effect of reservoir heterogeneity is investigated through a geostatistical approach.

4.1 Simulation model

A geostatistical approach is a commonly used method to describe spatial correlations between data points. In this study, to investigate the effect of heterogeneity, the geostatistical approach, based on Model 1 used in Chapter Three and the model used in Chapter Four is used to generate stochastically realizations of permeability. This approach is proposed by Wei et al. (Wei, et al., 2015) Geostatistical methods include the Ordinary Kriging Estimation, Gaussian Geostatistical Simulation and Unconditional Gaussian Geostatistical Simulation. In this study, the Unconditional Gaussian Geostatistical Simulation is employed since it does not need to define data points and is useful for testing assumptions when no sampling data is available (CMG Builder, 2013). A normal histogram is used to describe the distribution of permeability, and the mean and variance are set to 0.003 and 0.02, respectively. Spherical variograms are used to generate the heterogeneous models. The range is set to 200m and the sill is 1. The nugget effect is the apparent discontinuity, which can represent geological variability at small scales (Deutsch, 2014). With a higher nugget effect, the discontinuity is more obvious. In this study, three nuggets, which are 0.001, 0.2 and 0.5, are used to represent low heterogeneity, medium heterogeneity and high heterogeneity, respectively (Figure 4.1). As discussed in Chapter Four, gas injection can highly increase the oil recovery. In this chapter, CH_4 is injected to investigate the effect of reservoir heterogeneity.

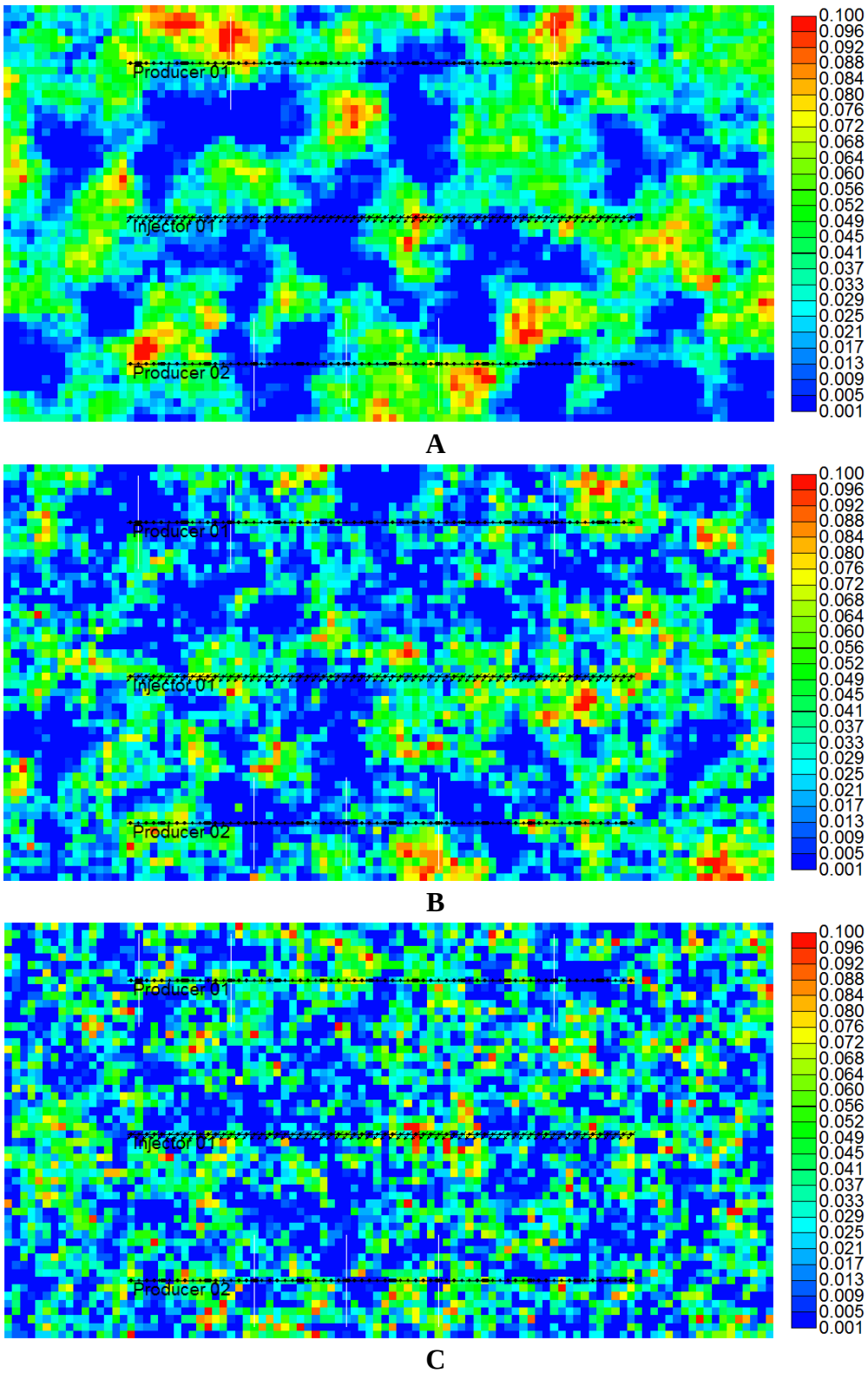

Figure 4.1 Permeability distribution (A: nugget=0.001; B: nugget=0.2; C: nugget=0.3)

4.2 Results and Discussion

Figure 4.2 shows the distribution of CH_4 after 20 years of injection. From this figure, it can be observed that reservoir heterogeneity has a significant effect on oil recovery and gas primarily moves forward along the area with high permeability. Compared with low heterogeneity and medium heterogeneity, the swept area of high heterogeneity is shrunk. In the cases of low heterogeneity and medium heterogeneity, the area with similar permeability is intensively distributed, which means the area with a similar size of pore throats is intensively distributed. In such conditions, CH_4 can easily move in the reservoir resulting in a large swept area. On the contrary, the permeability distribution of a high heterogeneity reservoir is scattered. Consequently, CH_4 can hardly move in the reservoir with high heterogeneity resulting in a small swept area.

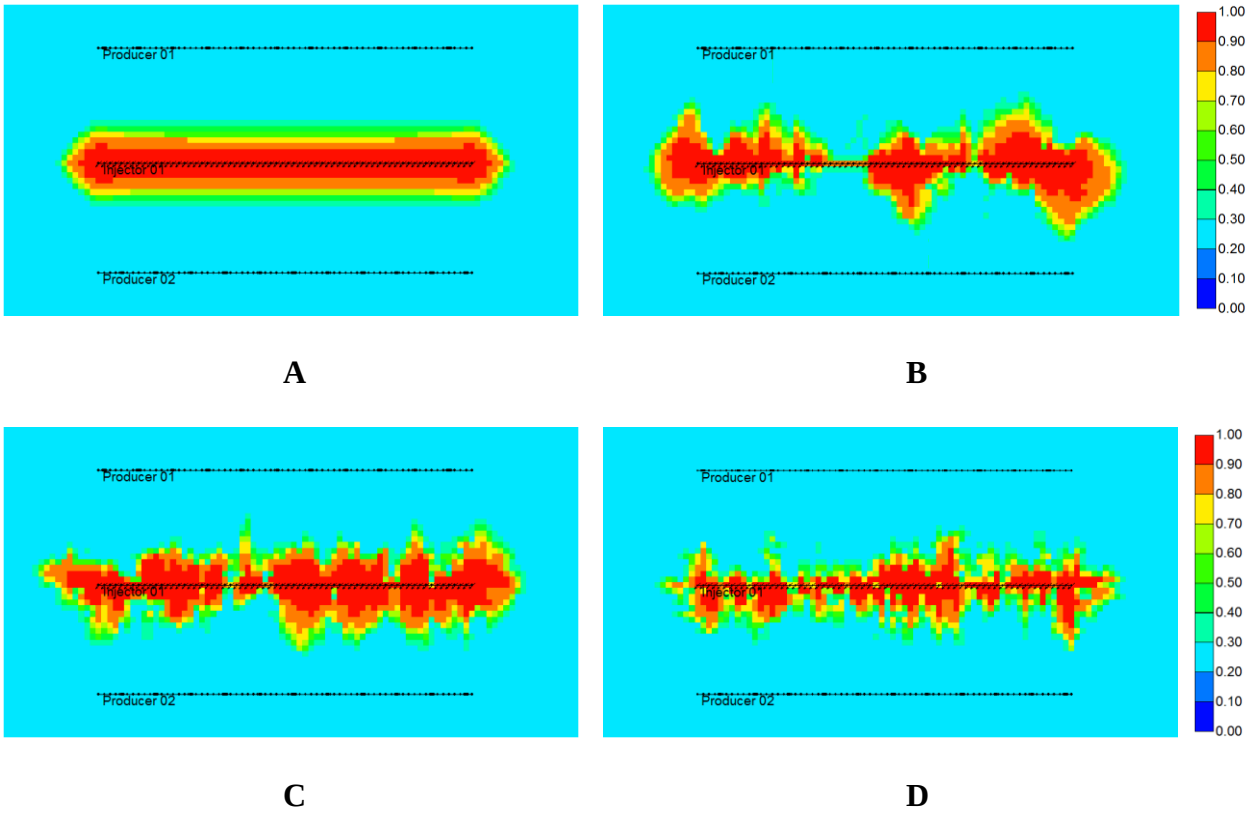

Figure 4.2 CH_4 distribution (A: homogeneous model; B: low heterogeneity model; C: medium heterogeneity model; D: high heterogeneity model)

Table 4.1 Comparison of oil recovery for homogeneous and heterogeneous cases

	Oil Recovery Factor/%		Incremental/%
	Primary	CH_4	
Homogeneous	5.15	8.08	56.89
Low Heterogeneous	4.60	8.04	76.96
Medium Heterogeneou	4.37	7.10	62.47
High Heterogeneous	4.35	6.32	45.29

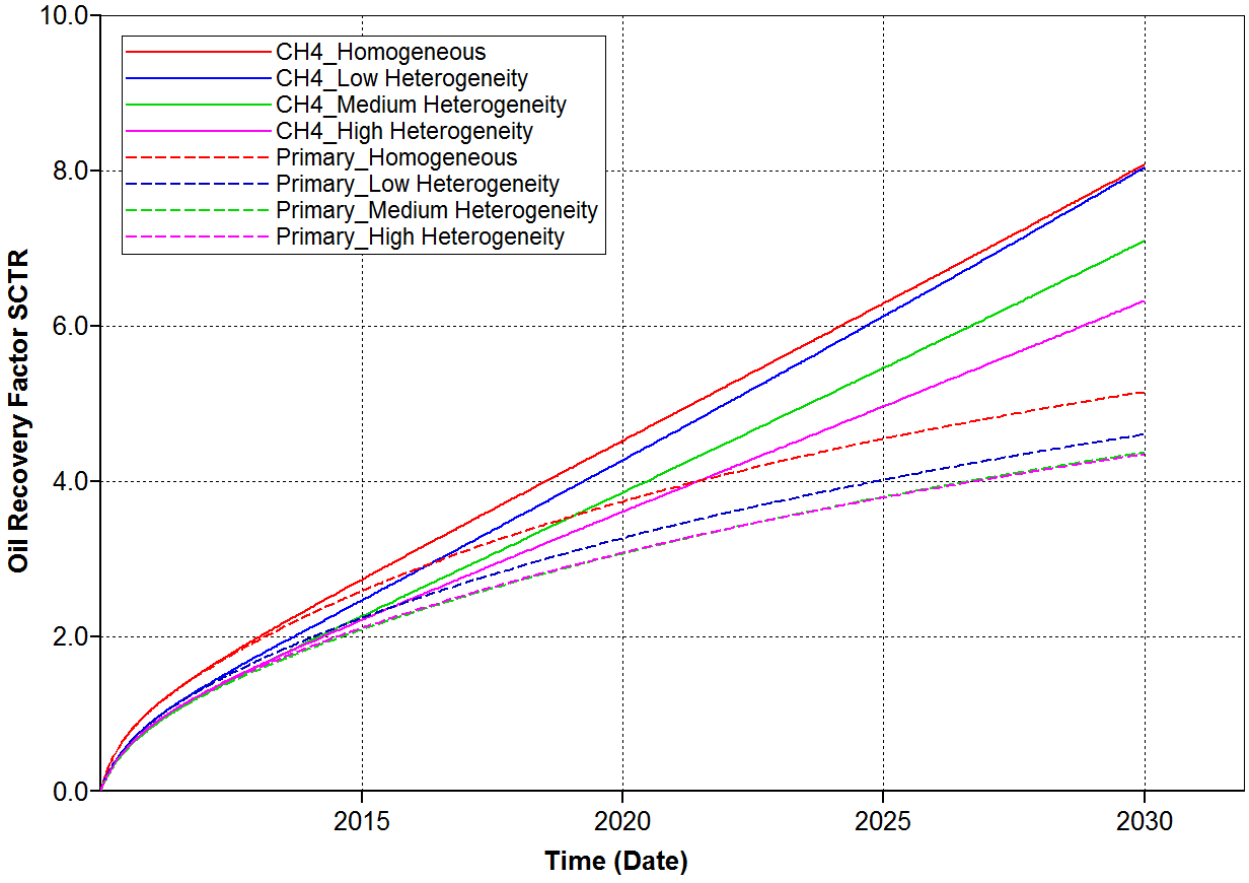

Figure 4.3 Comparison of oil recovery for homogeneous and heterogeneous cases

Table 4.1 and Figure 4.3 show the oil recovery for homogeneous and heterogeneous cases. According to Table 4.1 and Figure 4.3, reservoir heterogeneity has a significant effect on oil recovery. As the reservoir heterogeneity increased, the oil recovery decreased. Even so, gas injection can still highly improve the oil recovery. In the case of low heterogeneity, compared with primary recovery, the oil recovery with a CH_4 injection improved from 5.15 to 8.08, an increase of 76.96%. If homogeneous, low heterogeneity and medium heterogeneity cases, after 20 years of CH_4 injection, are compared, the incremental from the primary recovery is 56.89%, 76.96% and 62.47%, respectively. Such results indicate that gas injection is more beneficial for low heterogeneity and medium heterogeneity reservoirs. In the case of high heterogeneity, the distribution area of low permeability and small size pore throats is increased and scattered, which impedes the movement of CH_4 in the reservoir, diminishing oil recovery.

Chapter Five: Geological Modeling and Reservoir Simulation

Based on the core and log data of 16 observation wells, to further investigate the gas injection performance in the study area, a geological model is generated with Petrel and a sector of this model is intercepted for reservoir simulation. The oil recovery after 20 years of production is predicted.

5.1 Structural Modeling

In this study, individual layer data and well log data are collected from 16 observation wells. These wells are uniformly distributed and can satisfy the demand of accuracy. According to the individual layer data, four horizons, which are C72-1, C72-2, C72-3 and C73, are generated to define the boundary and carry out interpolation for the structural model. Figure 6.1 shows the structural map of C72-1, and the structural map of other horizons are shown in Appendix A. The generated geological model contains 413×472×36 grid blocks with blocks sized at 10m×10m×1m. From the structural model, it can be observed that the variations of reservoir depth and thickness in the study area are not obvious and the tectonic is flat.

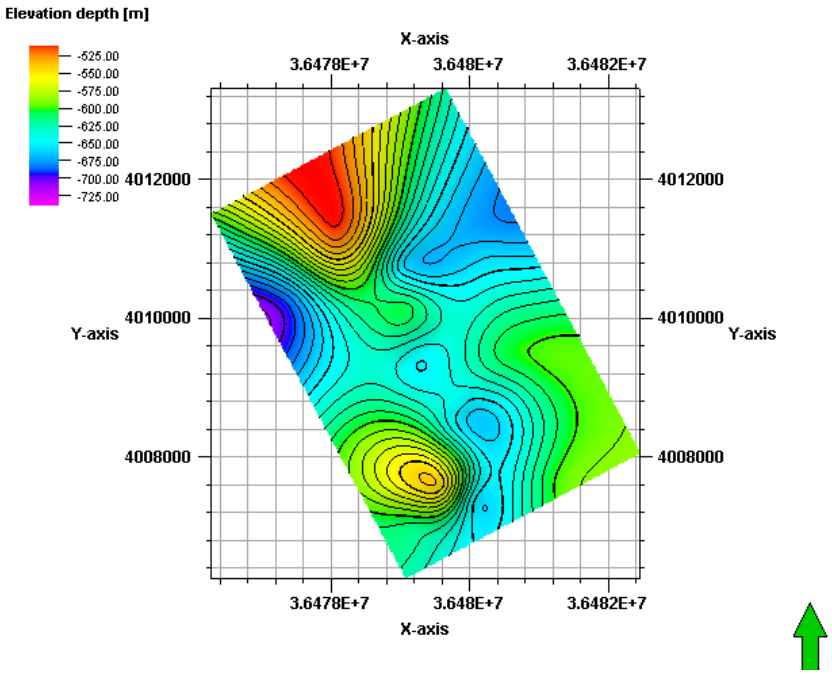

Figure 5.1 Structural map of C72-1

5.2 Facies Modeling

Facies modeling is the base of the geological modeling; it describes the sand body distribution characters, such as a shape and scale. Facies modeling includes deterministic and stochastic modeling methods. For the deterministic modeling method, as long as the input parameters are defined, only one result will be generated. In contrast, the stochastic method is able to generate multiple equi-probable realizations for different seed numbers. In this study, the stochastic Sequential Indicator Simulation (SIS) is used, along with spherical variograms, to describe the spatial continuality of the data. One realization is chosen from five runs. Figure 5.2 shows the facies for C72-1, and the facies for C72-2, C72-3 and C73 are shown in Appendix B. The facies in the study area is turbidite deposit, with shale mainly distributed at the bottom of the reservoir.

From the bottom to the top of the reservoir, the distribution of shale and sandstone exhibits directivity.

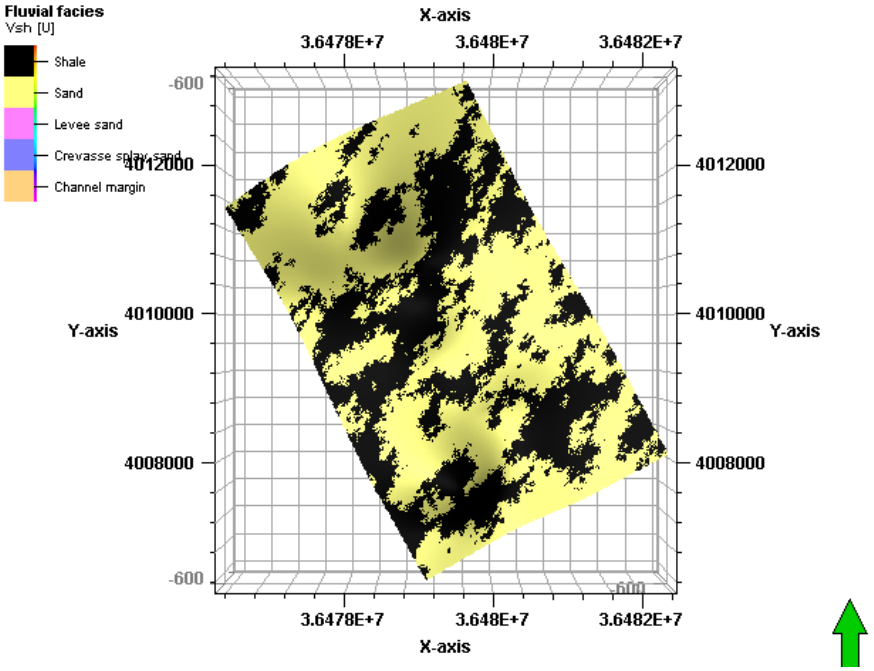

Figure 5.2 Shale and sandstone distribution of C72-1

5.3 Petrophysical Modeling

Petrophysical modeling is the interpretation of reservoir properties including porosity, permeability and oil saturation. Similar to facies modeling, petrophysical modeling can also be divided into the deterministic and stochastic methods. As one of the stochastic methods, in this study, Sequential Gaussian Simulation (SGS) is used. The SGS is steady, in addition to the original input data, simulated data is included in the simulation. Since the distribution of the reservoir properties is also controlled by facies, the facies model is used to constrain the petrophysical modeling. One realization is chosen from five runs. The distributions of porosity, permeability and

oil saturation for C72-1 are shown in Figure 5.3, Figure 5.4 and Figure 5.5, respectively. The reservoir properties for C72-2, C72-3 and C73 are shown in Appendix A.

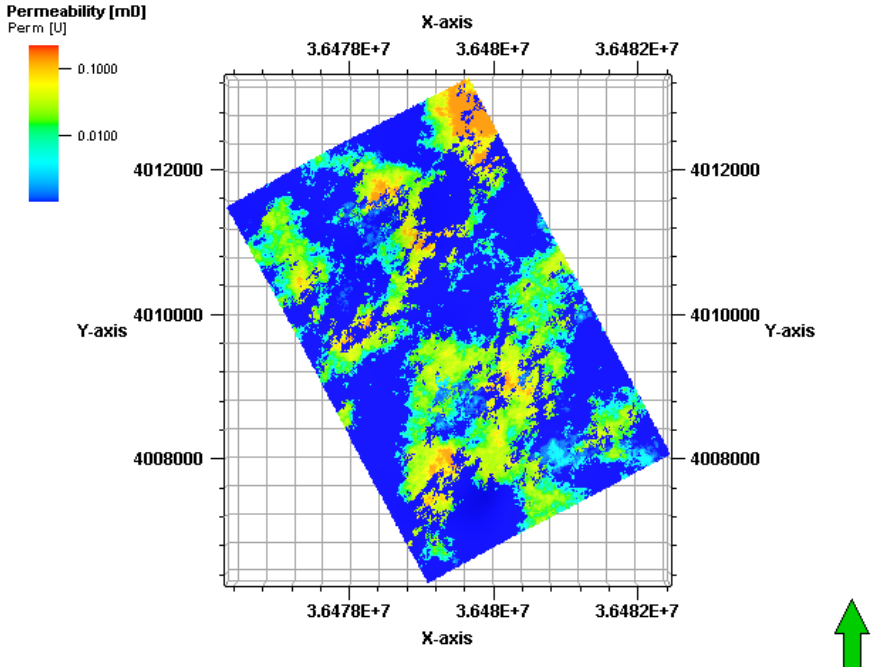

Figure 6.3 Permeability distribution of C72-1

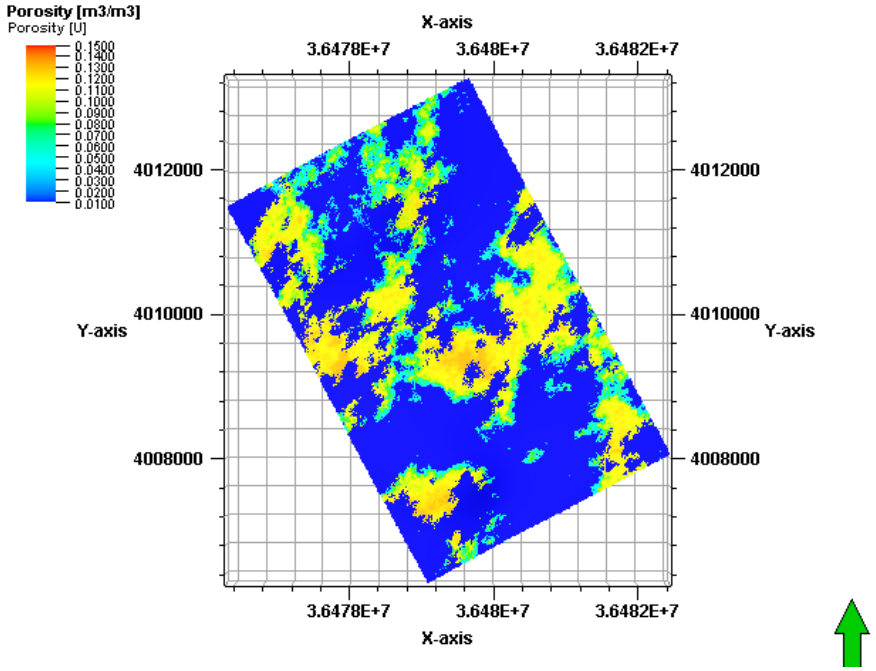

Figure 6.4 Porosity distribution of C72-1

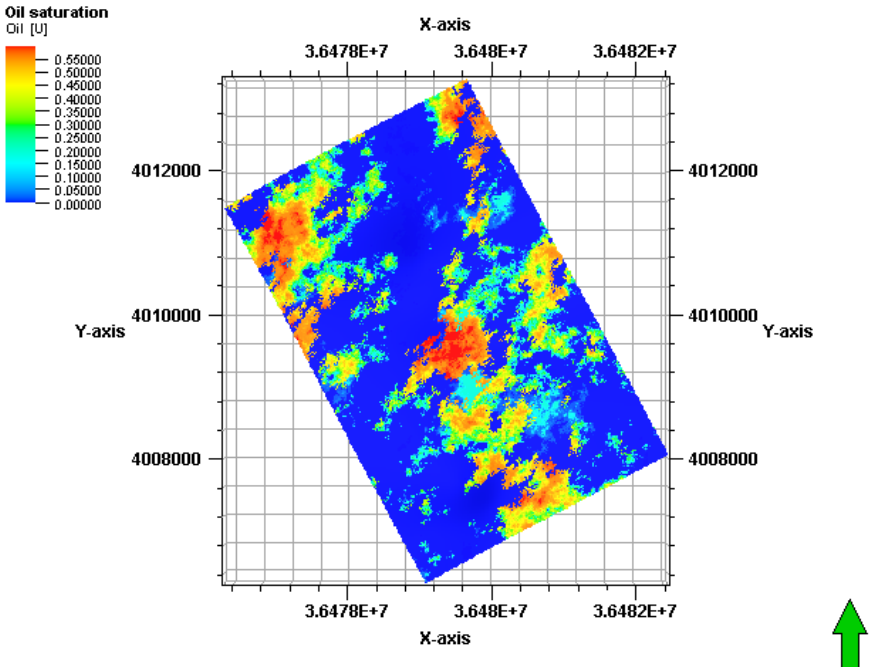

Figure 6.5 Oil saturation of C72-1

5.4 Simulation Model

The geological model is upscaled from 10m×10m×1m to 15m×15m×4m and is input into the CMG GEM. For the simulation study, a sub-model with 100×54×9 grid blocks is intercepted. Figures 5.6-5.8 show the distribution of permeability, porosity and oil saturation, respectively. Results from Figures 5.6 and 5.7 reveal that the study area has low to medium heterogeneity.

In this study, CH_4, CO_2 and the separator gas are injected, and the reservoir produces for 20 years.

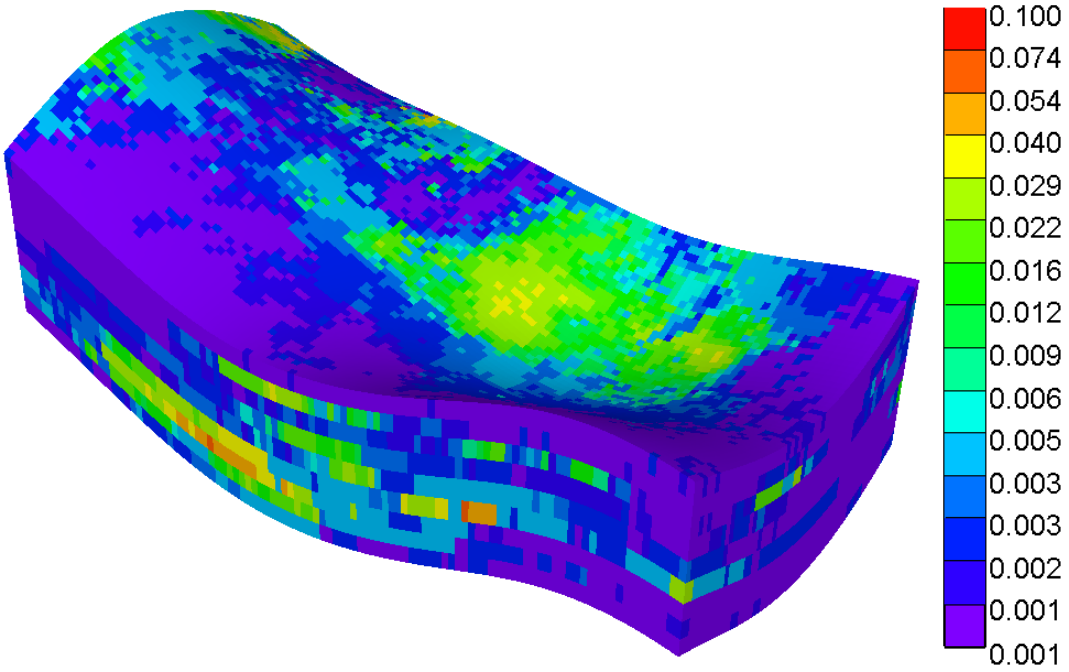

Figure 5.6 Distribution of permeability

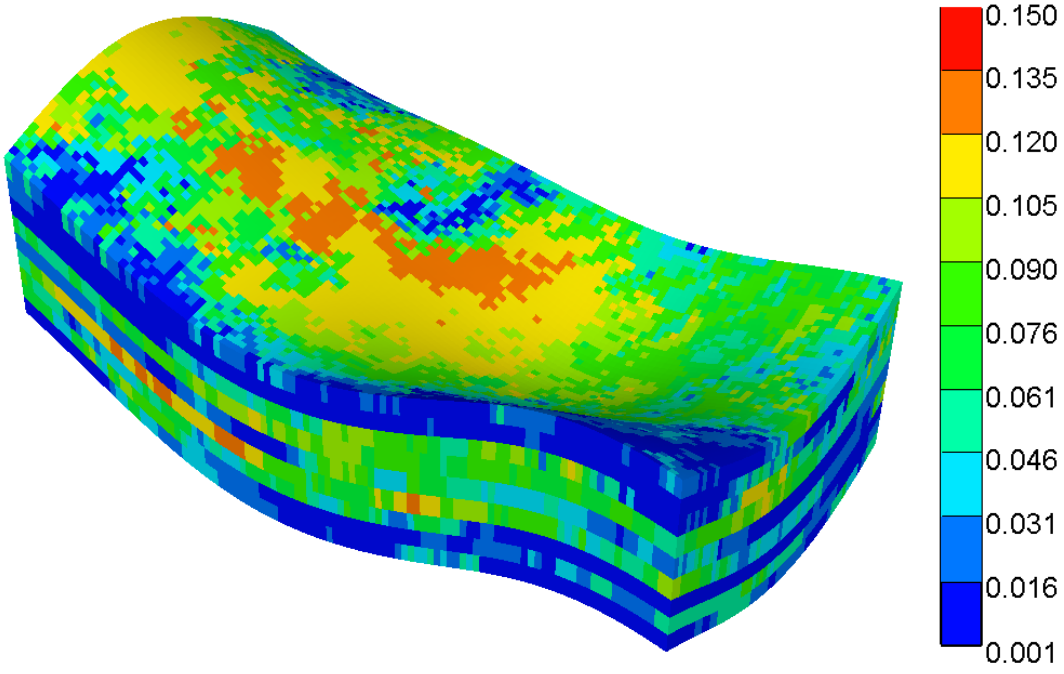

Figure 5.7 Distribution of porosity

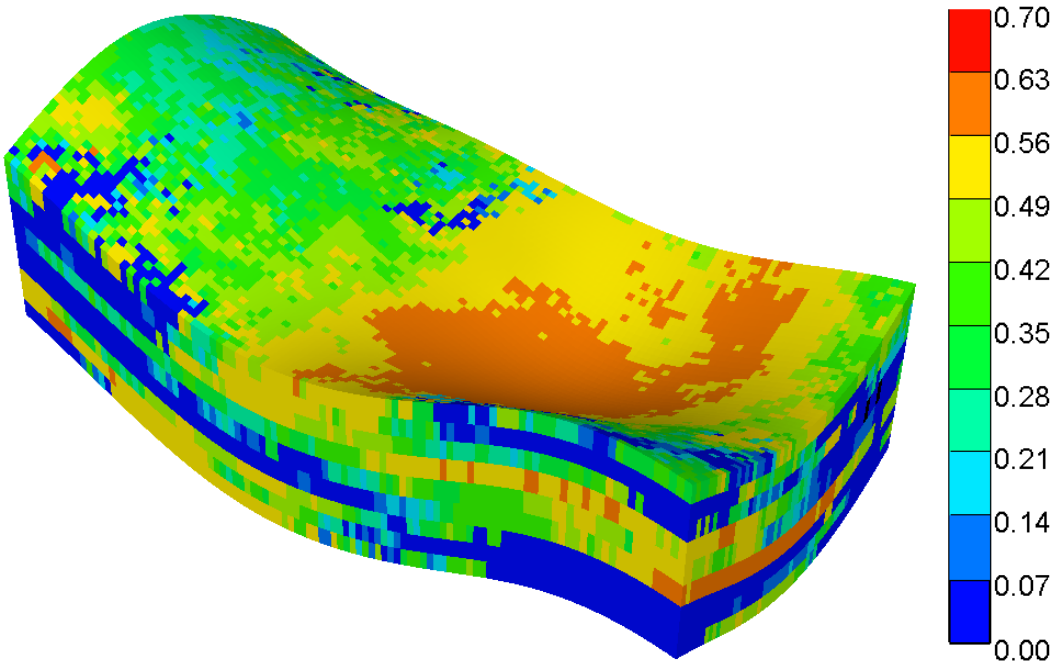

Figure 5.8 Distribution of oil saturation

5.5 Oil Recovery

The reservoir exhibits low to medium heterogeneity. As discussed in Chapter Five, gas injection is beneficial for these types of reservoirs as it can highly improve the oil recovery.

Figure 5.9 shows the distribution of CH_4. The permeability and porosity at the right side of the injector are high, while the permeability and porosity at the left side are quite low. Although gas is suitable for improving oil recovery from such a low pressure tight reservoir, due to the differences of permeability, part of the reservoir still cannot be displaced. In this study, the area with permeability greater than 0.003md is effectively displaced, while gas can hardly displace in an area where permeability is lower than 0.003md.

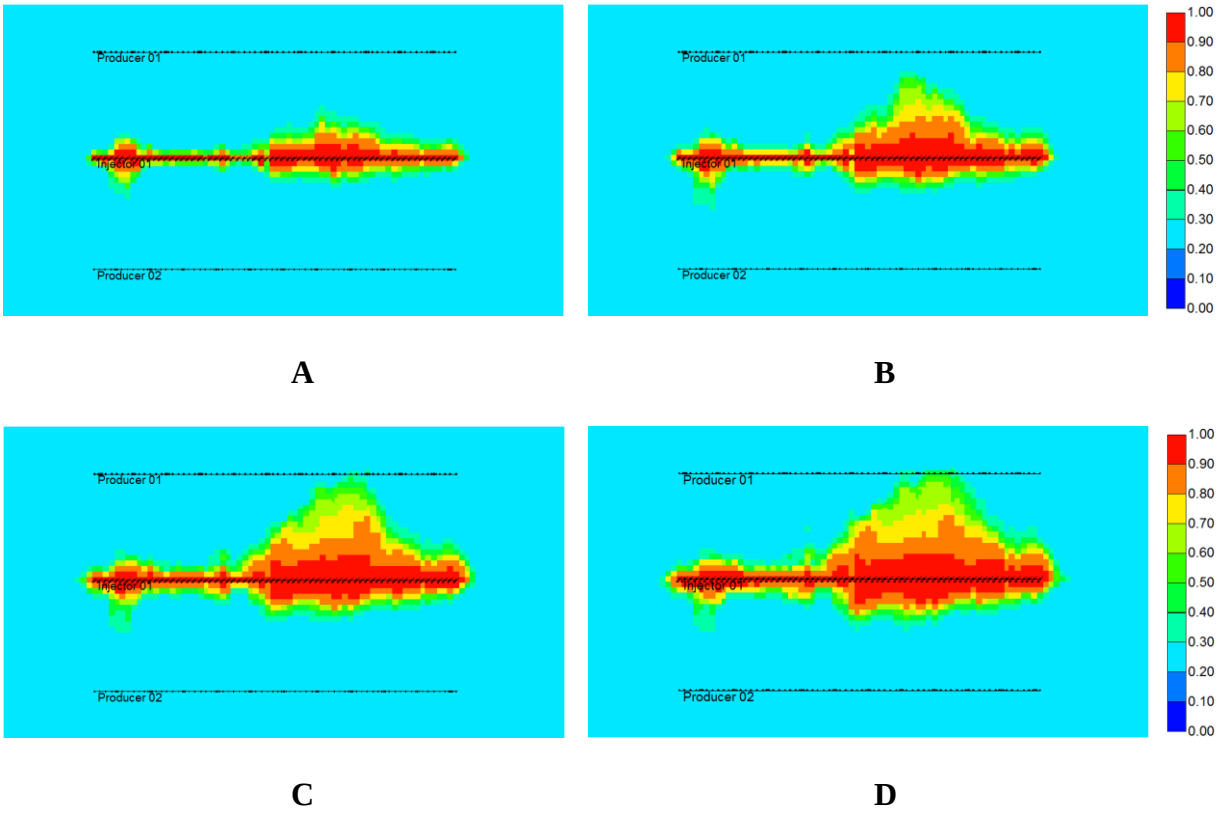

Figure 5.9 Mole Fraction of CH4 (A: after 5 years of injection; B: after 10 years of injection; C: after 15 years of injection; D: after 20 years of injection)

Table 5.1 and Figure 5.26 show the oil recovery of primary recovery and oil recovery after CH_4, CO_2 and separator gas injection. The results are constant with the results of the homogeneous model. Gas can highly improve oil recovery. Compared with primary recovery, the oil recovery of CH_4, CO_2 and separator gas injection increased 52.57%, 32.24% and 46.82%, respectively. The displacement effectiveness of CH_4 and the separator gas is better than that of CO_2.

Table 5.1 Oil Recovery of primary recovery, CH_4, CO_2 and separator gas injection for geological model

	Primary	CH_4	CO_2	Separator Gas
Oil Recovery Factor/%	4.87	7.43	6.44	7.15
Incremental/%		52.57	32.24	46.82

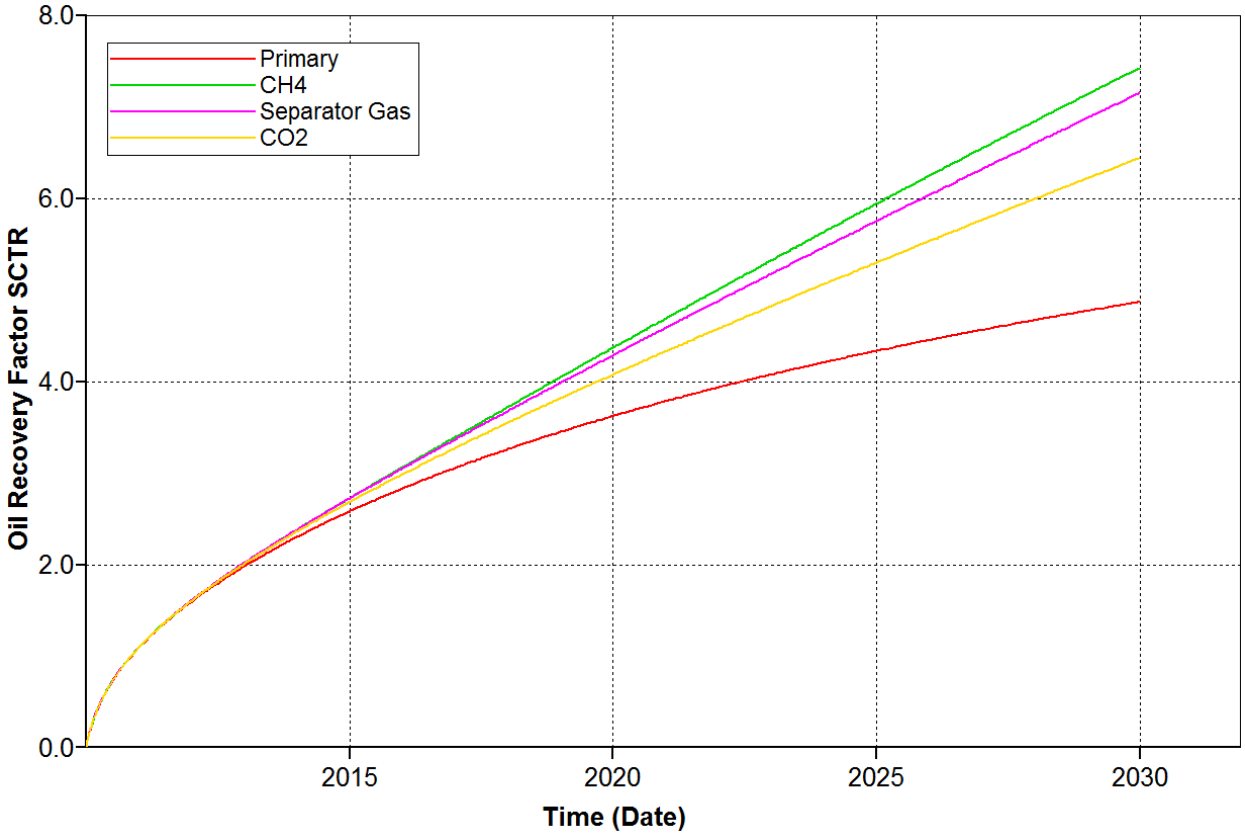

Figure 5.26 Oil Recovery of primary recovery, CH_4, CO_2 and separator gas injection for geological model

Chapter Six: CONCLUSIONS AND FUTURE WORKS

6.1 Conclusions

Compared with the Bakken formation, the main differences of the study area in the Ordos basin are low pressure gradient and low pressure. In this study, the way of effective production of such a low-pressure reservoir is investigated and the following conclusions are drawn:

1. The primary recovery of the Bakken formation and the study area are investigated and compared through reservoir simulation. For both the Bakken formation and the study area, the oil production is relatively high at the initial stage of the production and declined rapidly in the first two years. After one year of production, the oil rate is 10% of the original oil rate.

2. Based on the reservoir simulation study, the primary recovery of the Bakken formation is 9.11%, while the primary recovery of the study area is only 5.15% - almost half of the Bakken formation - which means that the primary recovery is inefficient for oil recovery from the study area.

3. Due to a water film attached on the surface of a matrix, water can hardly be injected into tight oil reservoirs. Water injection is inefficient for enhancing oil recovery. Due to its high diffusivity, gas can easily move in reservoirs and push oil to producers. Moreover, reservoir pressure is increased and oil viscosity is decreased through gas injection, which is beneficial for oil recovery. Although the overall reservoir pressure does not fulfill the requirement of miscible flooding, the pressure near an injector is higher than the MMP of

gases and a miscible condition can be reached in this area. Compared with primary recovery, the incremental after CH_4, CO_2 and separator gas injections are 56.89%, 36.31% and 50.49%, respectively. CH_4 and the separator gas are more suitable than CO_2 for enhancing oil recovery in the study area.

4. Reservoir heterogeneity has a significant effect on oil recovery. As reservoir heterogeneity increased, oil recovery decreased. Compared with the primary recovery, gas injection can still increase oil recovery. The incremental for homogeneous, low heterogeneous, medium heterogeneous and highly heterogeneous cases are 56.89%, 76.96%, 62.47% and 45.29%, respectively. Gas injection is beneficial for production in low and medium heterogeneous reservoirs.

5. A geological model is built to further investigate the performance of gas injection in the study area. The area with permeability greater than 0.003md is effectively displaced, while gas hardly displaces in the area where permeability is lower than 0.003md. The oil recovery factors are 7.43%, 6.44% and 7.15% for CH_4, CO_2 and the separator gas, respectively. Consistent with the results of the homogeneous model, CH_4 and separator gas are more suitable than CO_2 for enhancing oil recovery in the study area.

6.2 Future Work

In this study, oil recovery is improved with gas injection, but it is still lower than 10%. To further improve oil recovery, the following studies should be carried out in the future:

1. Well patterns may have significant effects on oil recovery so optimization of well patterns should be studied.

2. Hydraulic fracturing is a key parameter for the successful recovery of tight oil reservoirs. Thus, a sensitivity analysis and optimization of hydraulic fracturing parameters, such as fracture conductivity, fracture half-length and the distance between hydraulic fractures should be studied.

3. Validity of economic feasibility is important for a project to be a success so evaluation of economics should be investigated.

REFERENCES

Chen, Quanhong, Wenhou Li, Yanqin Guo, Jiwei Liang, Junping Cui, and Daofeng Zhang. "Turbidite systems and the significance of petroleum exploration of Yanchang Formation in the southern Ordos Basin." *Acta Geologica Sinica* 80, no. 5 (2006): 663-672.

Christiansen, Richard L., and Hiemi Kim. "Apparatus and method for determining the minimum miscibility pressure of a gas in a liquid." U.S. Patent 4,627,273, issued December 9, 1986.

Clarkson, Christopher R., and Per Kent Pedersen. "Production analysis of Western Canadian unconventional light oil plays." In *Canadian Unconventional Resources Conference*. Society of Petroleum Engineers, 2011.

CMG Builder User's Guide (2013). Computer Modeling Group Ltd.

CMG WINPROP User's Guide (2013). Computer Modeling Group Ltd.

CMG GEM User's Guide (2013). Computer Modeling Group Ltd.

CSUR. Understanding Tight Oil. Internet (2014) www.csur.com

Dou, Hongen, and Ma Shiying. "Lessons learned from oil production of tight oil reservoirs in Bakken play." *Oil Drilling & Production Technology* 34, no. 2 (2012): 120-124.

Du Jinhu, He Haiqing, and Yang Tao. "Progress in China's tight oil exploration and challenges." *China Petroleum Exploration* 19, no. 1 (2014): 1-9.

Gao, Gang, Xianyang Liu, and Yinhui Wang. "Characteristics and resource potential of the oil shale of Chang 7 Layer in Longdong Area, Ordos Basin."*Earth Science Frontiers* 20, no. 2 (2013): 140-146.

Green, Don W., and G. Paul Willhite. *Enhanced oil recovery*. Richardson, Tex.: Henry L. Doherty Memorial Fund of AIME, Society of Petroleum Engineers, 1998.

Hutchinson, C. A., and Philip H. Braun. "Phase relations of miscible displacement in oil recovery." *AIChE Journal* 7, no. 1 (1961): 64-72.

Jia, Chengzao, Caineng Zou, Jianzhong Li, D. H. Li, and M. Zheng. "Assessment criteria, main types, basic features and resource prospects of the tight oil in China." *Acta Petrolei Sinica* 33, no. 3 (2012): 343-350.

Li, Shilun, and Zhou Shouxin. "Review and prospects for the development of EOR by gas injection at home and abroad.[J]." *Oil & Gas Recovery Techinology* 2 (2002).

Lin, Senhu, Zou Caineng, Yuan Xuanjun, and Y. A. N. G. Zhi. "Status quo of tight oil exploitation in the United States and its implication." *Lithologic Reservoirs* 23, no. 4 (2011): 25-30.

Meissner, Fred F. "Petroleum Geology of the Bakken Formation Williston Basin, North Dakota and Montana*." (1991): 19-42.

Pramudito, A. "Depositional facies, diagenesis, and petrophysical analysis of the Bakken Formation." *Elm Coulee field, Williston Basin, Montana: Master of science thesis, Colorado School of Mines* (2008).

Pyrcz, Michael J., and Clayton V. Deutsch. *Geostatistical reservoir modeling*. Oxford university press, 2014.

Sieminski, Adam. "Outlook for shale gas and tight oil development in the US." *US Energy Information Administration* (2013).

Taber, Joseph John, F. D. Martin, and R. S. Seright. "EOR screening criteria revisited-Part 1: Introduction to screening criteria and enhanced recovery field projects." *SPE Reservoir Engineering* 12, no. 03 (1997): 189-198.

Teklu, Tadesse Weldu, Najeeb Alharthy, Hossein Kazemi, Xiaolong Yin, Ramona M. Graves, and Ali M. AlSumaiti. "Phase behavior and minimum miscibility pressure in nanopores." *SPE Reservoir Evaluation & Engineering*17, no. 03 (2014): 396-403.

Thomas, F. B., X. L. Zhou, D. B. Bennion, and D. W. Bennion. "A comparative study of RBA, Px, multicontact and slim tube results." *Journal of Canadian Petroleum Technology* 33, no. 02 (1994).

Wu, Qi, Yun Xu, Yuzhang Liu, Yunhong Ding, Xiaoquan Wang, and Tengfei Wang. "The current situation of stimulated reservoir volume for shale in US and its inspiration to China." *Oil drilling & production technology* 32, no. 2 (2011): 1-7.

Yang, Hua, S. X. Li, and X. Y. Liu. "Characteristics and resource prospects of tight oil and shale oil in Ordos Basin." *Acta Pet Sin* 34, no. 1 (2013): 1-6.

Yao, Jingli, Deng Xiuqin, Zhao Yande, H. A. N. Tianyou, C. H. U. Meijuan, and P. A. N. G. Jinlian. "Characteristics of tight oil in Triassic Yanchang Formation, Ordos Basin." *Petroleum Exploration and Development* 40, no. 2 (2013): 161-169.

Zhenglian, Pang, Zou Caineng, Tao Shizhen, Yang Zhi, and Wu Songtao. "Formation, distribution and resource evaluation of tight oil in China [J]."*Engineering Sciences* 7 (2012): 60-67

Zhao, Jiyong, Liu Zhenwang, and Xie Qichao. "Micro pore throat structural classification of Chang 7 tight oil reservoir of Jiyuan oilfield in Ordos Basin."*China Petroleum Exploration* 19, no. 5 (2014): 73-80.

Zick, A. A. "A combined condensing/vaporizing mechanism in the displacement of oil by enriched gases." In *SPE annual technical conference and exhibition*. Society of Petroleum Engineers, 1986.

Zou, Caineng, Yang Zhi, Tao Shizhen, Li Wei, Wu Songtao, Hou Lianhua, Zhu Rukai et al. "Nano-hydrocarbon and the accumulation in coexisting source and reservoir." *Petroleum Exploration and Development* 39, no. 1 (2012): 15-32.

Zou, Caineng. *Unconventional petroleum geology*. Newnes, 2012.

Zou, Caineng, R. K. Zhu, S. T. Wu, Zhi Yang, S. Z. Tao, X. J. Yuan, L. H. Hou et al. "Types, characteristics, genesis and prospects of conventional and unconventional hydrocarbon accumulations: taking tight oil and tight gas in China as an instance." *Acta Petrolei Sinica* 33, no. 2 (2012): 173-187.

APPENDIX A Determination of MMP

Gas injection can be divided into miscible and immiscible gas-driven. In this study, before comparisons of the performance of water and gas injection are made, slim tube experiments are performed to determine if miscible gas injection can be reached.

A.1 Experimental Methods for MMP determination

Theoretically speaking, MMP is the minimum pressure whereupon multiple contact miscible is established between the injection gas and reservoir oil under reservoir temperature. In practice, MMP is determined through experiments.

A.1.1 Slim tube Experiment

Slim tube experiments are a commonly used method to determine MMP. They can reflect the fluid flow in porous media and can maximally eliminate the effects of an unfavorable mobility ratio, viscous fingering, gravity segregation and rock heterogeneity. Although the sweep efficiency of a slim tube experiment cannot represent the practical sweep efficiency in real reservoirs, the MMP determined by this experiment is reliable. Slim tube experiments, however, are expensive and time consuming.

A.1.2 Rising-Bubble Experiment

The rising-bubble experiments were proposed by Christiansen and Kim in 1986 (Christiansen and Kim, 1986). Their merit is that their time period is short (usually can be finished in one day). In the experiment, the determination of the MMP is not based on whether the bubbles vanish; rather,

determining the MMP is based on the way the bubbles disappear. The accuracy of the result is highly dependent on the experience of an experimenter.

A.2 Slim tube Experiment

As slim tube experiments are reliable, in this study, we used these experiments to determine the MMP of CH_4 and CO_2.

A.2.1 Experimental Device

Figure 3.1 is the schematic of the experimental device. The experimental device is comprised of an injection pump, a slim tube, pressure gages, observation windows, a pressure regulator, a liquid meter, a gas meter and a temperature control system.

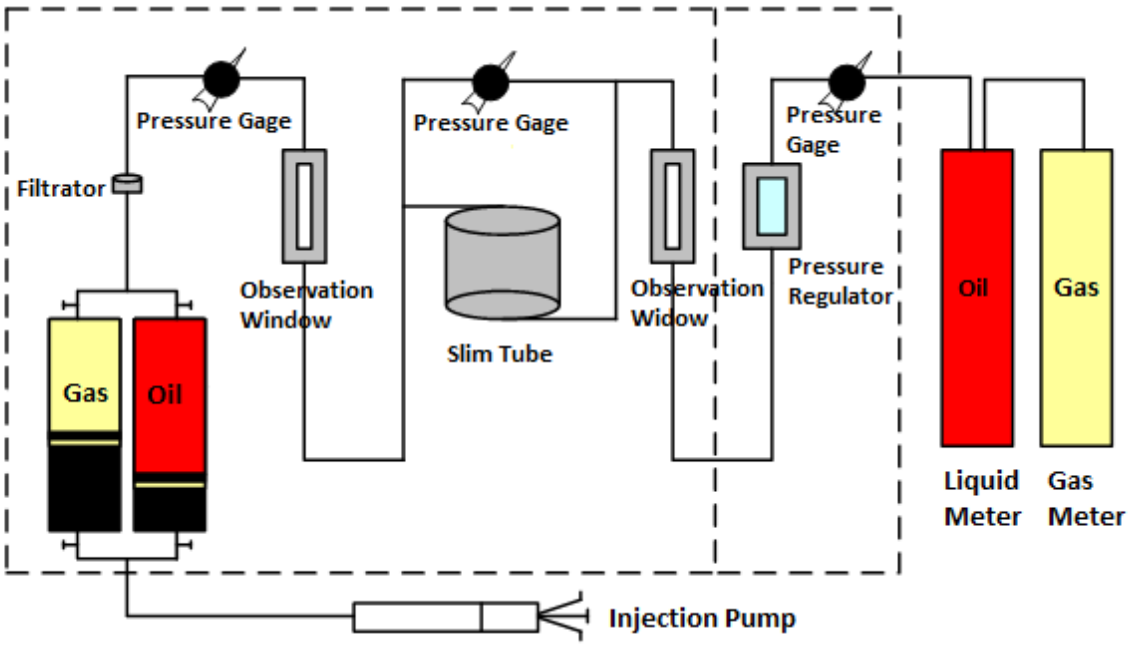

Figure A.1 Experimental device of slim tube experiment

The slim tube is the key apparatus of the experiment; its length is usually 10m to 30m, it is typically filled with fine sand to mimic a porous medium, and it provides a place for gas and oil to flow and make contact with each other.

A.2.1.1 Design of Slim tube

As a miscible condition is achieved through multiple contacts between gas and oil, the transition zone will be formed before the miscible condition is reached. The slim tube should be long enough to ensure that the miscible condition can be reached. In this experiment, the displacing fluid is gas, which has a low density and viscosity, and the displaced fluid is oil, which has a relatively high density and viscosity. The diameter of the slim tube and sand grain should be appropriate to eliminate the effect of viscous fingering and gravity segregation. If not, after injecting 1.2 PV of gas, the sweep efficiency will be much lower, yielding unfavourable results.

Based on the *Chinese Standard for Petroleum and Gas Industry SY/T6573-2003*, in this study, the length of the slim tube is 12m and the diameter is 5mm. The slim tube is filled with fine sand, which has a diameter of 40μm. The total volume of the slim tube is 235.5cm^3, with a porosity of 18.54%.

A.2.1.2 Design of Flow Rate

Viscous fingering will result if the flow rate of injected gas is too quick; on the contrary, gravity segregation occurs if the flow rate is too slow. In this study, gas is injected from the top of the slim tube and drives oil vertically. According to *Chinese Standard for Petroleum and Gas Industry SY/T6573-2003*, the critical flow rate can be calculated from Equation (3-1).

$$u_c = 0.0438 \frac{(\rho_0 - \rho_g)K}{\mu_0 - \mu_g} \quad (3\text{-}1)$$

where u_c is the critical flow rate, ml/min; ρ_0 is the oil density, lb/ft^3; ρ_g is the gas density, lb/ft^3; K is the rock permeability, md; μ_0 is the oil viscosity, mPa·s; μ_g is the gas viscosity, mPa·s. Any flow rate lower than the critical flow rate is appropriate; in this study, the gas flow rate is 0.125ml/min.

A.2.2 Experimental Procedure

The oil sample used in this study was collected from the field. The experimental temperature is 64.75℃. Five experiments were conducted for both CH_4 and CO_2 under pressures of 16MPa, 25MPa, 30 MPa, 32 MPa, and 36MPa.

Before the experiment begins, the slim tube is cleaned with petroleum ether. The cleaning process is finished when the same color is observed from the entrance and exit. After cleaning, the slim tube is blow-dried with nitrogen and put into a drying box for six hours. The slim tube is then saturated with oil and injected with gas under constant pressure and temperature. After each 0.1PV gas injection, the recovered oil and gas are recorded. After 1.2PV gas is injected, one displacement is finished and results are recorded. Changes are made to the pressure and the former steps are repeated.

A.2.3 MMP Determination

As pressure increased, the oil recovery after injecting 1.2 PV gas increased. The oil recovery at different pressures are recorded on the pressure-oil recovery plot. The pressure at the inflection point is the MMP between the injected gas and reservoir oil.

A.3 Results of CH_4

The first slim-tube experiment is conducted under 64.75℃ and 16Mpa. During the experiment, the efflux is initially black. After 0.7PV of injection, CH_4 breaks through, and the oil recovery reaches 57.91% at this time. After 1.2 PV of injection, the oil recovery is 62.23% (Figure A.2). The results indicate that this displacement is immiscible.

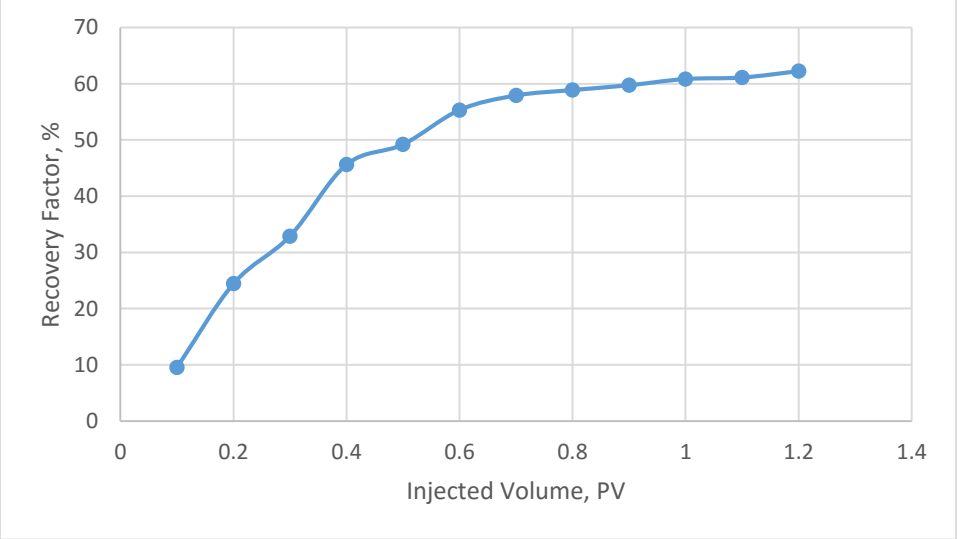

Figure A.2 Oil recovery factor of CH_4 injection at 16Mpa

The second experiment is under 64.75℃ and 25Mpa. After 0.9PV of gas is injected, gas breakthrough occurs, resulting in an oil recovery factor of 68.89%. After injecting 1.2PV of gas, the oil recovery factor is 76.83% (Figure A.3). This displacement is immiscible.

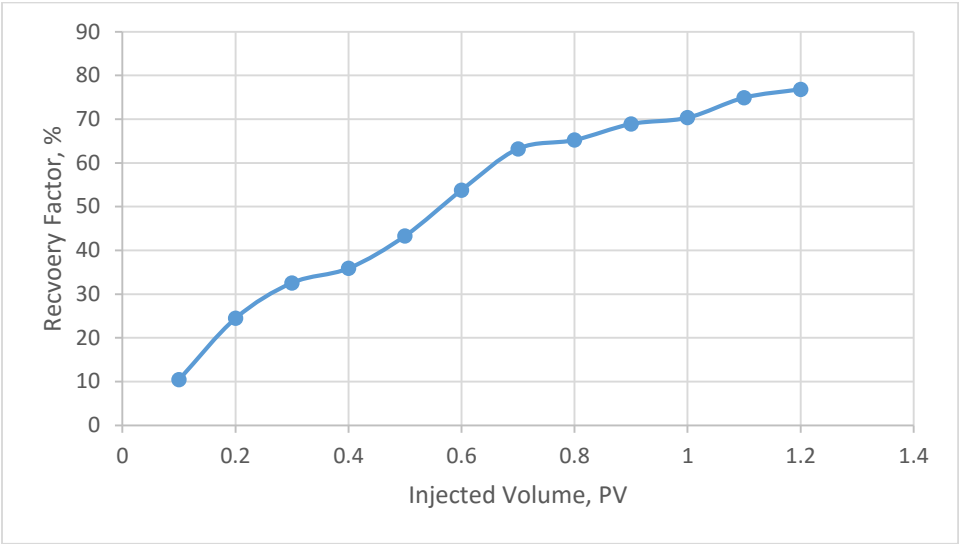

Figure A.3 Oil recovery factor of CH_4 injection at 25Mpa

The third experiment is under 64.75℃ and 30Mpa. After injecting 0.8 PV of gas, gas breakthrough is achieved, resulting in a 75.21% oil recovery factor. After injecting 1.2PV of gas, the oil recovery factor is 84.6% (Figure A.4). This displacement is immiscible.

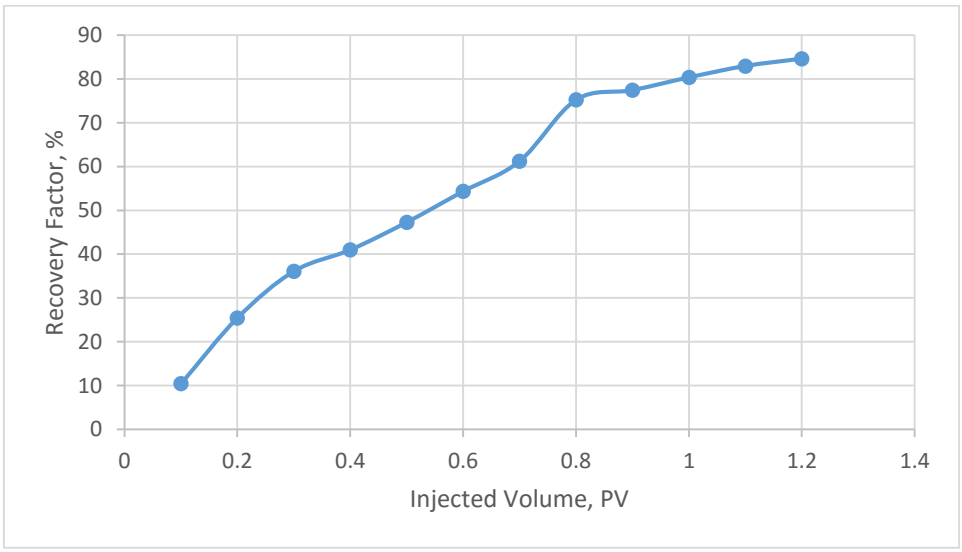

Figure A.4 Oil recovery factor of CH_4 injection at 30Mpa

As with the former experiments, the fourth is under 64.75℃, and according to the results of the previous experiment, the pressure is increased to 32Mpa. From the observation window it can be seen that the efflux is black initially, and then changes to dark red, which indicates that the gas is miscible with oil. After injecting 1.2PV of gas, the oil recovery is 92.38% (Figure A.5). This displacement is miscible.

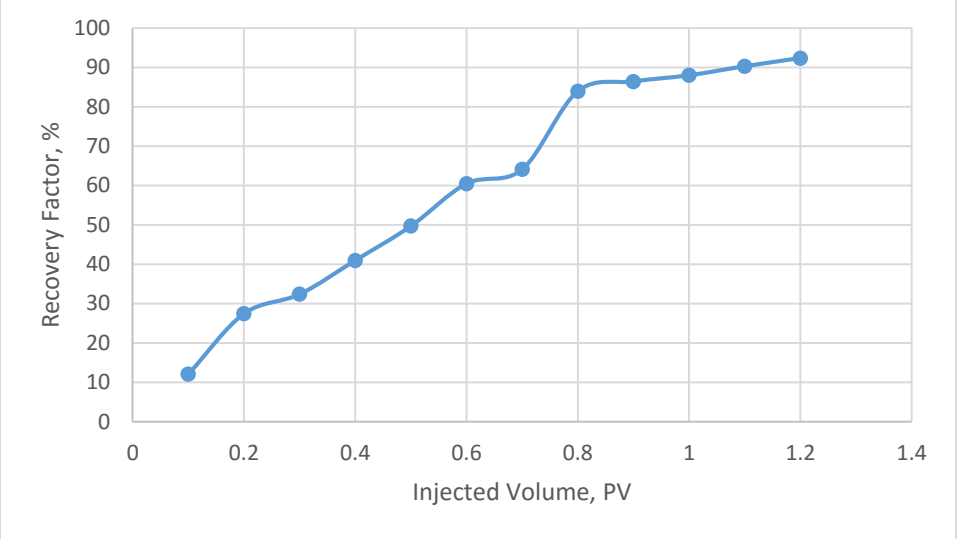

Figure A.5 Oil recovery factor of CH_4 injection at 32Mpa

To further study the miscibility between injected gas and oil, the fifth experiment's pressure is increased to 36Mpa and the temperature remains at 64.75℃. The gas breakthrough occurs earlier than in the previous experiment. Rather than an interface between gas and oil, only a continuous variation of fluid color is observed from the observation window. After injecting 1.2PV of gas, the oil recovery factor is 93.75% (Figure A.6). This displacement is miscible.

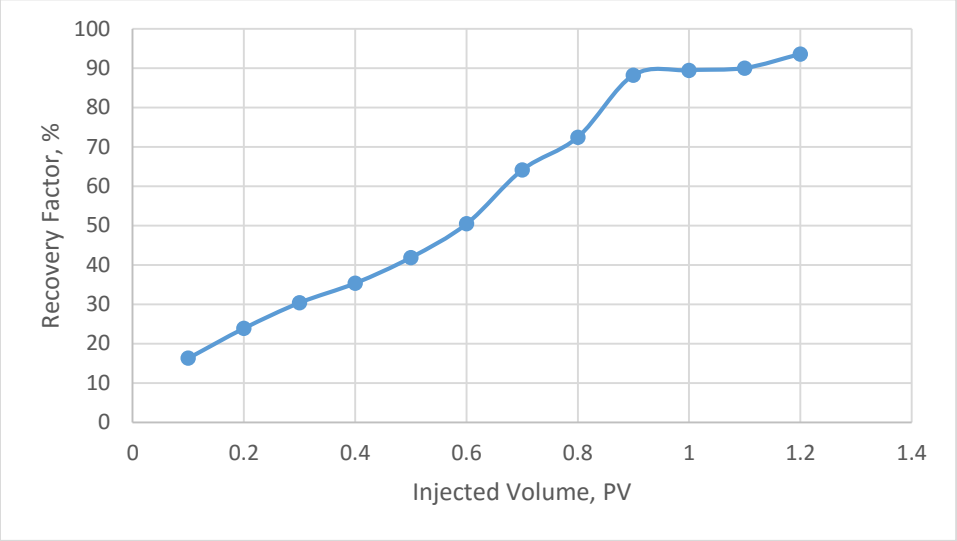

Figure A.6 Oil recovery factor of CH_4 injection at 36Mpa

Table A.1 summarises the experimental results of the CH_4 injection. The oil recovery factor is plotted with the corresponding pressure on the pressure-oil recovery plot (Figure A.7). The MMP of CH_4 for the oil in the study area is 33Mpa, which means that the CH_4 injection is an immiscible gas injection process in this study area.

Table A.1 Summary of the experimental results of CH_4

	Pressure/MPa	Injected PV at Breakthrough/PV	Oil recovery Factor/%	Miscibility
Experiment 1	16	0.7	62.23	Immiscible
Experiment 2	25	0.7	76.83	Immiscible
Experiment 3	30	0.8	84.60	Immiscible
Experiment 4	32	0.9	92.38	Miscible
Experiment 5	36	0.8	93.57	Miscible

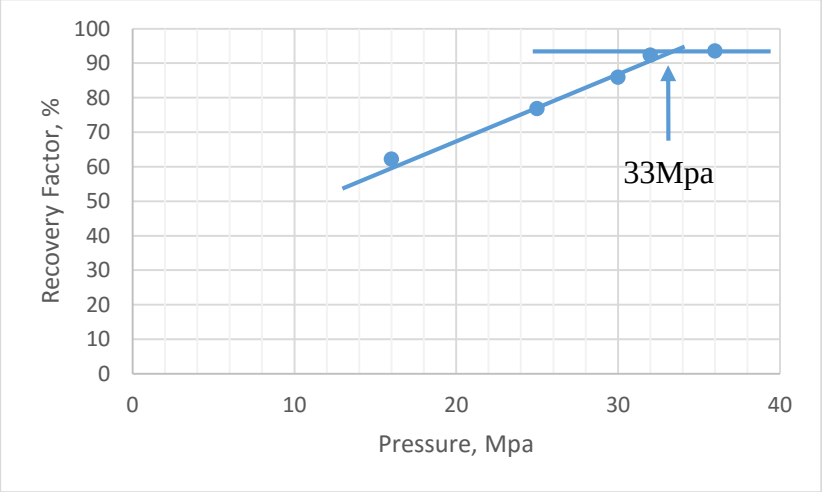

Figure A.7 Results of CH_4 slim-tube experiment

A.4 Results of CO_2

Similar to the experiments using CH_4, five experiments for CO_2 were conducted under five pressures (16MPa, 25MPa, 30MPa, 32MPa and 36MPa). The results are listed in Table.A.2. The oil recovery factors are plotted with the corresponding pressure on the pressure-oil recovery plot (Figure A.8). The MMP of CO_2 for the oil in the study area is 26Mpa, which means the CO_2 injection in the study area is immiscible.

Table A.2 Summary of the experimental results of CO_2

	Pressure/Mpa	Injected PV at Breakthrough/PV	Oil recovery Factor/%	Miscibility
Experiment 1	16	0.8	73.16	Immiscible
Experiment 2	25	0.8	90.45	Near-miscible
Experiment 3	30	0.8	92.09	Miscible
Experiment 4	32	0.9	92.72	Miscible
Experiment 5	36	0.8	93.44	Miscible

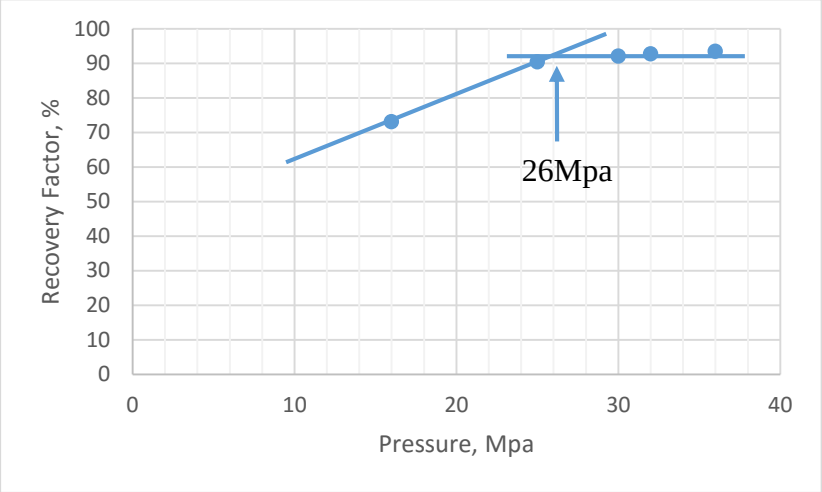

Figure A.8 Results of CO_2 slim-tube experiment

A.5 MMP of Separator Gas

An abundance of solution gas exists in the reservoirs in the study area. Due to transportation difficulties, this gas is usually flared, which is both wasteful and contaminating to the environment. After a simple separation of the solution gas, the separator gas can be reinjected into the reservoir to supplement the driving energy and enhance the oil recovery. The components of the separator gas are listed in Table A.3.

Table A.3 Composition of Separator Gas

	CH_4	C_2H_6	C_3H_8
Molar Fraction/%	59.65	18.66	21.69

Even though the slim tube experiment is expensive and time consuming, ascertaining the MMP of the separator gas is important. In this study, the MMP of the separator gas is calculated with CMG WINPROP. Table A.4 shows the calculated results. The MMP of CH_4 is also calculated with CMG WINPROP (Table A.4). The calculated results of CH_4 by the semi-analytical (key tie lines) method

are very close to the experiment results, while the difference between the experimental results and the calculated results by cell to cell simulation is relatively large. The possible reason is that the cell to cell simulation considers the vaporizing and condensing drive mechanisms separately, rather than in combination, which overestimates the MMP. The semi-analytical method considers all three drive mechanisms (CMG WINPROP, 2013). In this study, the calculated results from the semi-analytical method is considered reliable; the MMP of the separator gas in the study area is 25.125Mpa. The same with the application of CH_4 and CO_2, the separator gas injection is also immiscible.

Table A.4 MMP calculation from CMG WINPROP

	MMP/Mpa	
	Cell to Cell Simulation	Semi-analytical (Key Tie Lines) Method
CH_4	37.25	33.313
Separator Gas	27.813	25.125

APPENDIX B

B.1 Structural Modeling

Figure B.1, Figure B.2 and Figure B.3 show the structural map of C72-2, C72-3 and C73, respectively

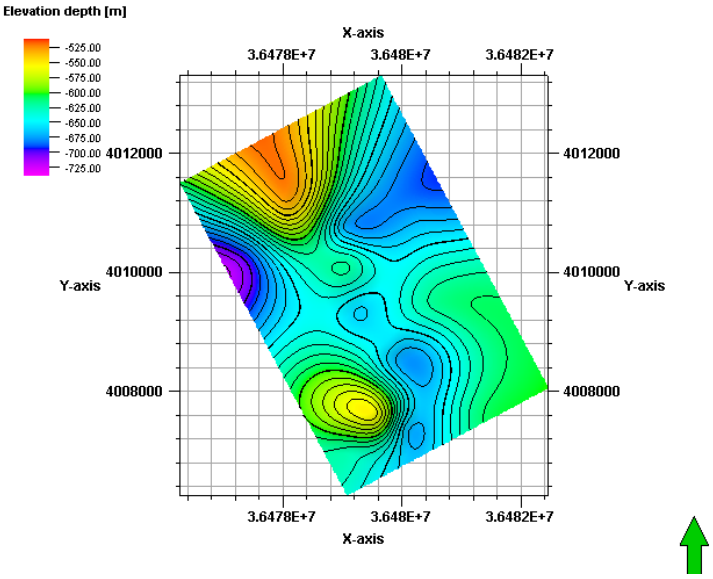

Figure B.1 Structural map of C72-2

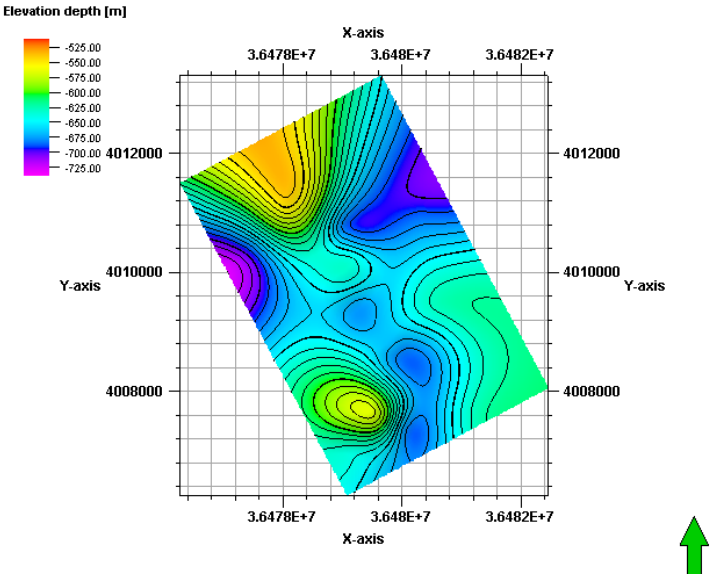

Figure B.2 Structural map of C72-3

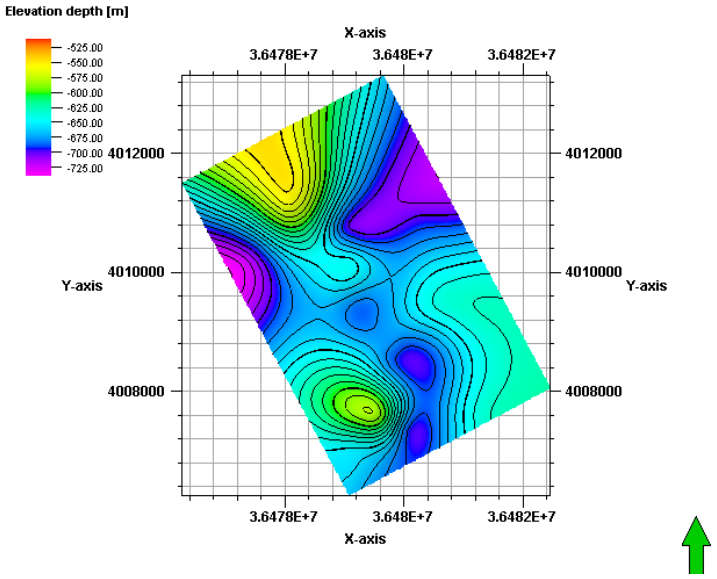

Figure B.3 Structural map of C73

B.2 Facies Modeling

Figure B.4, Figure B.5 and Figure B.6 show the distribution of sand and shale for C72-2, C72-3 and C73, respectively.

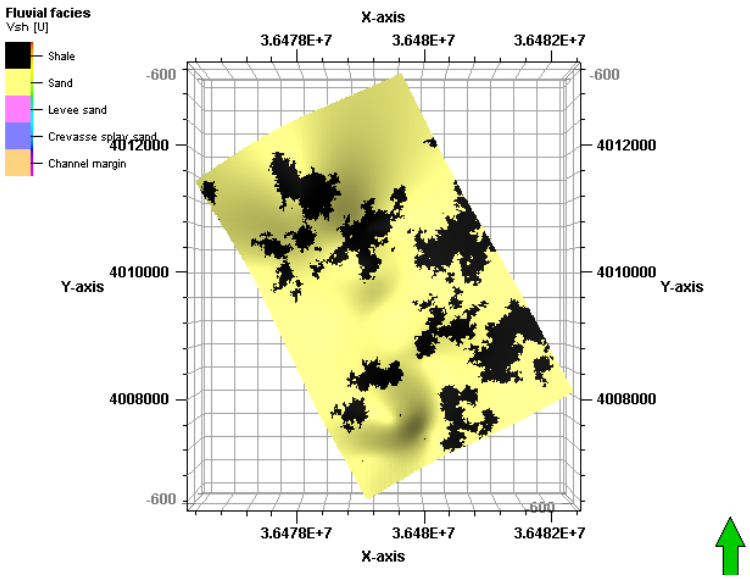

Figure B.4 Shale and sandstone distribution of C72-2

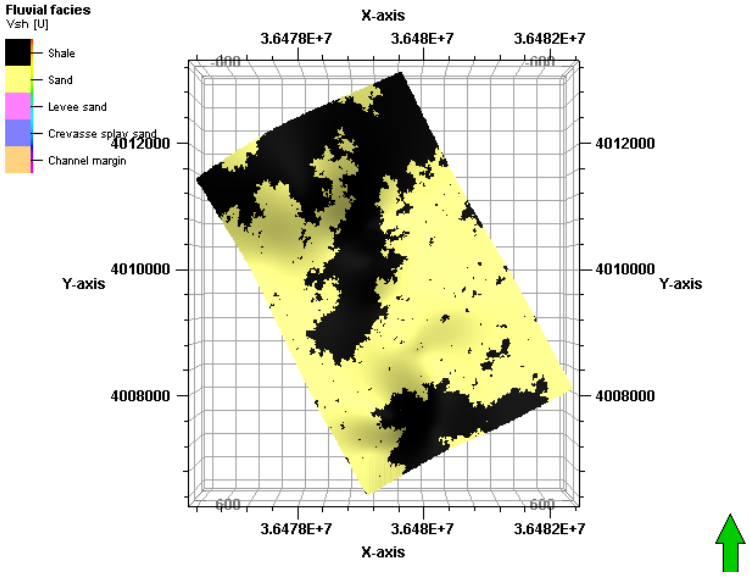

Figure B.5 Shale and sandstone distribution of C72-3

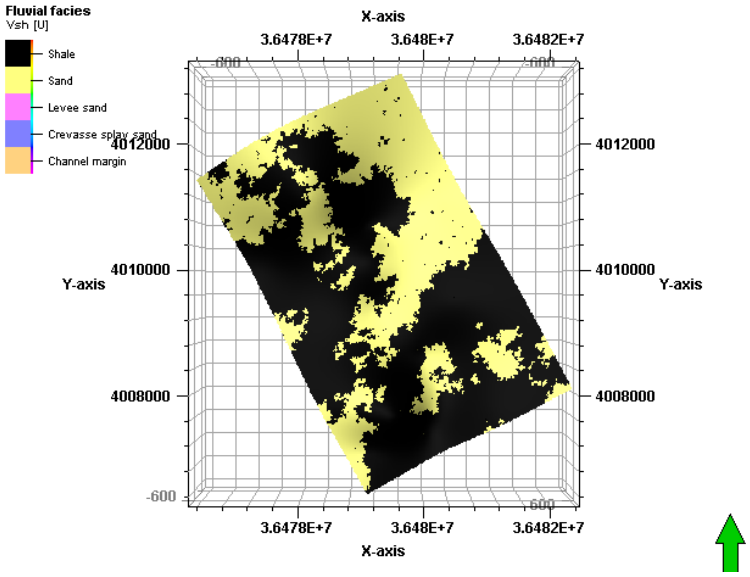

Figure B.6 Shale and sandstone distribution of C73

B.3 Petrophysical Medling

Figure B.7, Figure B.8 and Figure B.9 show the permeability distribution of C72-2, C72-3 and C73, respectively.

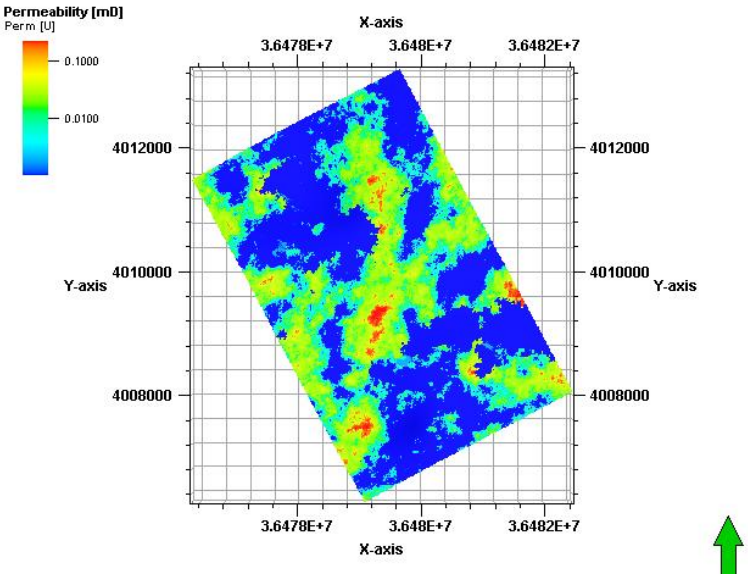

Figure B.7 Permeability distribution of C72-2

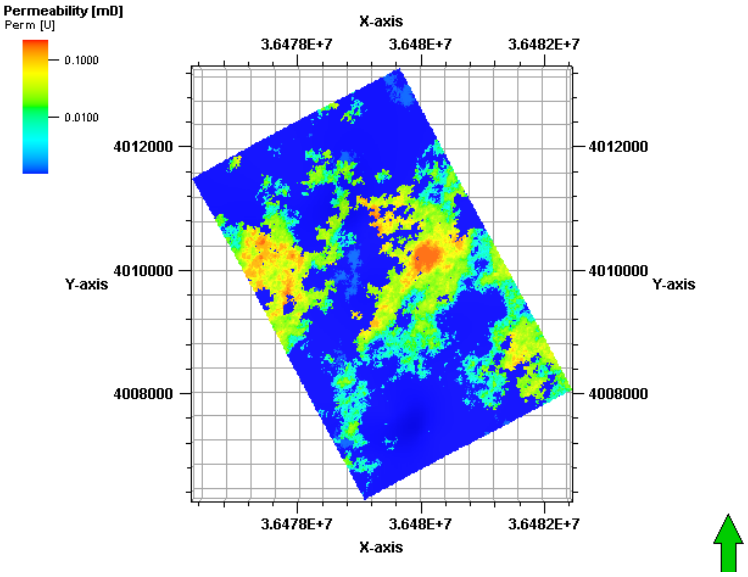

Figure B.8 Permeability distribution of C72-3

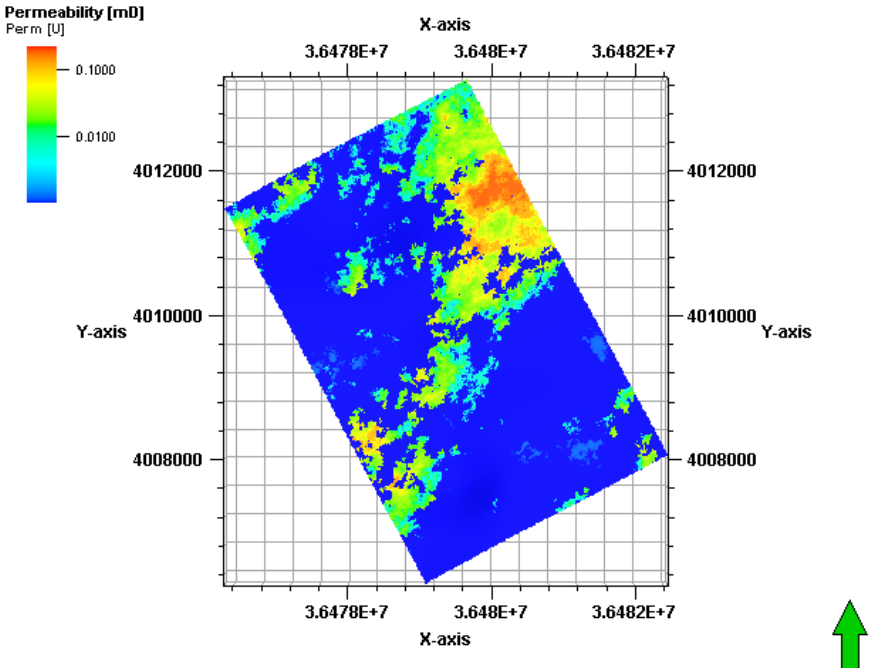

Figure B.9 Permeability distribution of C73

Figure B.10, Figure B.11 and Figure B.12 show the porosity distribution of C72-2, C72-3 and C73, respectively.

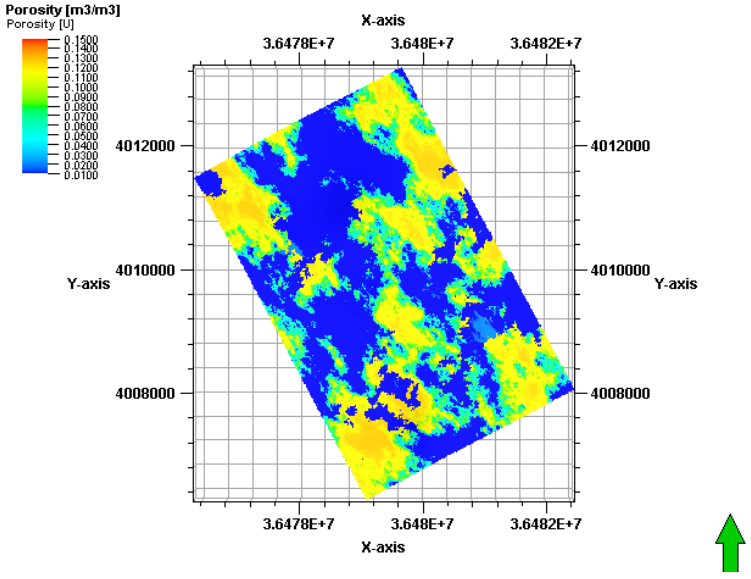

Figure B.10 Porosity distribution of C72-2

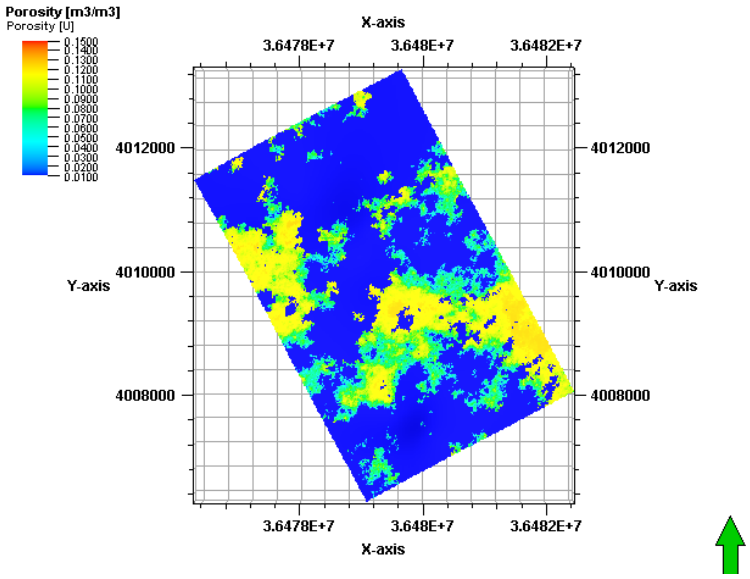

Figure B.11 Porosity distribution of C72-3

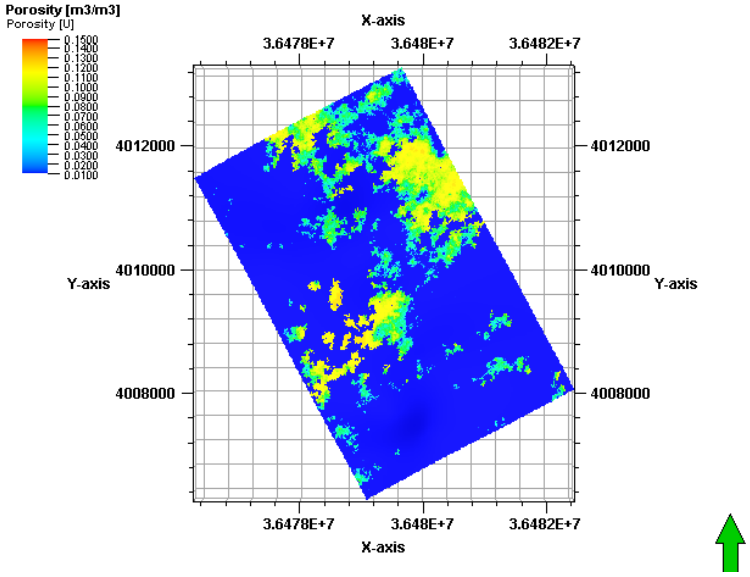

Figure B.12 Porosity distribution of C73

Figure B.13, Figure B.14 and Figure B.15 show the oil saturation distribution of C72-2, C72-3 and C73, respectively.

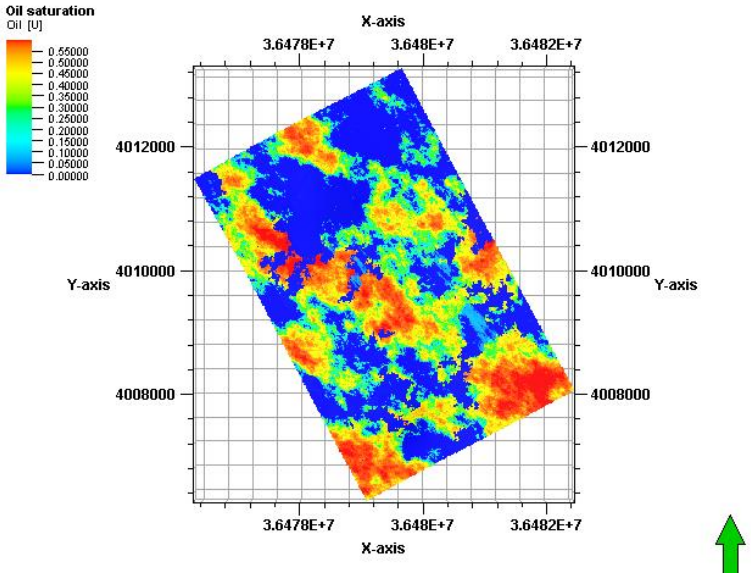

Figure B.13 Oil saturation of C72-2

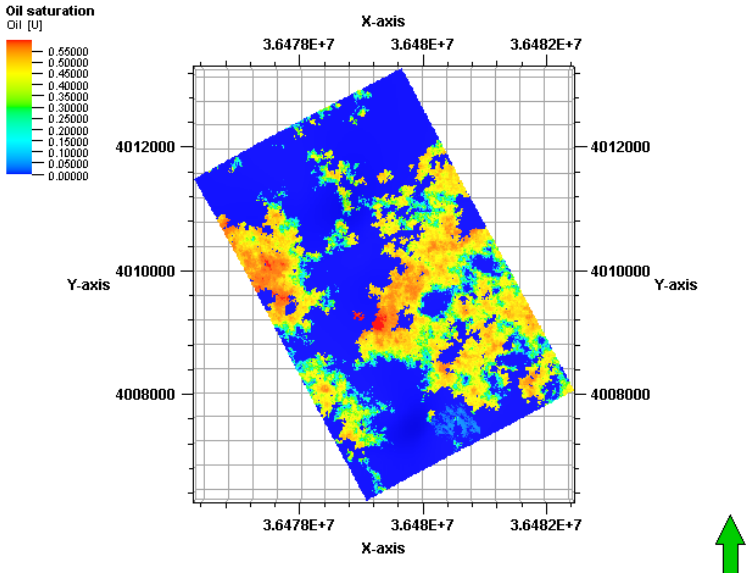

Figure B.14 Oil saturation of C72-3

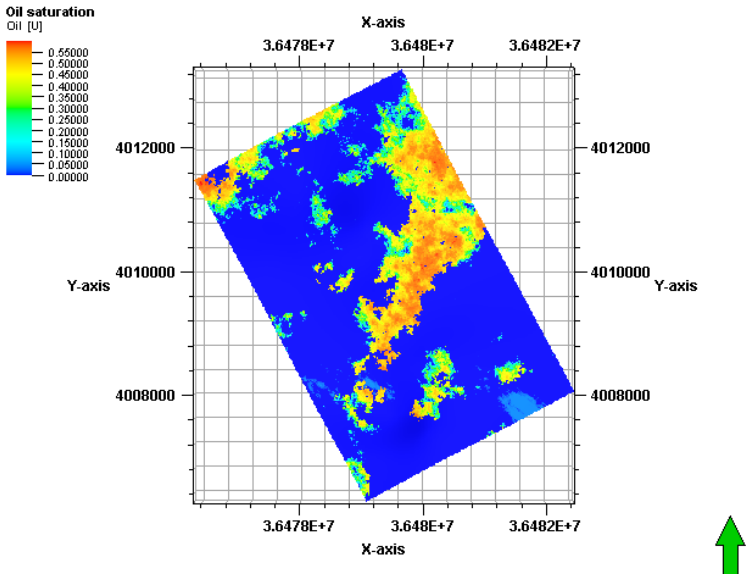

Figure B.15 Oil saturation of C73